NTNU
Innovation and Creativity

Stability Analysis of Nonlinear Attitude Determination and Control Systems

Ivar-Kristian Waarum

Master of Science in Engineering Cybernetics
Submission date: June 2007
Supervisor: Jan Tommy Gravdahl, ITK

Norwegian University of Science and Technology
Department of Engineering Cybernetics

Problem Description

Master Thesis Assignment

Name of the candidate: Ivar-Kristian Waarum

Subject: Teknisk Kybernetikk (Engineering Cybernetics)

Title (Norwegian): Stabilitetsanalyse av ulineære estimering- og reguleringssystemer for orientering
Title (English): Stability analysis of nonlinear attitude determination and control systems

The thesis covers the topics of attitude determination and control for the planned ESMO spacecraft. A nonlinear observer is to be used for attitude determination.

Assignments:

- Investigate the concept of nonlinear separation principles
- Design a nonlinear observer for the attitude determination system for ESMO
- Analyze the stability properties of attitude controllers for ESMO
- Analyze the stability of the combined attitude control/determination system
- Simulate the attitude control/determination system

Assignment given: 8/1-2007

To be handed in by: 5/6-2007

Assignment handed in:

The work is to be carried out at the Department of Engineering Cybernetics, NTNU

Trondheim, 8/1-07

Jan Tommy Gravdahl

Stability Analysis of Nonlinear Attitude Determination and Control Systems

Ivar-Kristian Waarum

June 4, 2007

Preface

This report is the written result of the subject ”TTK4920 - Teknisk Kybernetikk, masteroppgave”. The subject is a 30 study point effort compulsory for graduate students at the Department of Engineering Cybernetics at NTNU. The project report at hand is written as a part of the Student Space Engineering Technology Initiative hosted by the European Space Association on the topic of attitude determination of a small satellite. The satellite in question is named European Student Moon Orbiter, and is planned for launch in 2011. It is currently undergoing a Phase A feasibility study, in which this report tries to play a part as background research for the design of the control system.

One of the fascinating aspects with cybernetics as a field of study is the variety of situations and environments where it can be applied. The author has appreciated the opportunity to work in the borderline between more familiar subjects and that of spacecraft design. Satellite control is somewhat related to marine vessel control, which is the main area of application in the master program, but the environment is different to the degree that it seems at first a new direction of study. The heart of the work did evolve around the study of separation principles, which is in its basic form purely abstract mathematics. Taking this highly theoretical approach to cybernetics turned out to be very rewarding, at least on a personal level, as it showed how many of the techniques and concepts of control engineering thaught in earlier courses have a sound foundation in mathematics.

Well-earned thanks go to supervisor J. Tommy Gravdahl for being the ESA contact at NTNU and thus providing interesting projects, and to the master students at GG48 for a good and productive atmosphere during our final six months as students.

Ivar-Kristian Waarum, Trondheim, June 4, 2007

Contents

Abstract

This report describes the modelling and performance of an attitude determination and control system (ADCS) for a small satellite in lunar orbit. The focus is on stability analyses of each of the components in the system, and of the system as a whole. In connection to this, the separation principle for nonlinear systems is investigated.

Central background information is presented, covering necessary rigid body dynamics and stability properties. Three different controller types are analysed and compared herein, namely a model-dependent linearizing controller, a robust controller and a standard PD-controller. An observer is chosen based on earlier work, but some detail modifications are made to its structure. A state-space model of the satellite and environment is derived and implemented in Matlab, along with the observer and controllers. The observer and all three controllers are shown to be stable with Lyapunov analysis. The total ADCS including the observer is shown to have a cascaded structure, on which theory of nonlinear separation principles is used to establish stability properties of the total system. Finally, the ADCS is put to simulation tests imitating real-life scenarios and the performance of the different controllers are compared.

The PD-controller shows the best performance, both in speed of convergence and robustness to model errors. While not completely satisfactory, the results give a basis on which to perform further work.

Chapter 1

Introduction

1.1 ESA and SSETI

As a mean to step out of its American and Russian competitors' shadows, the European collaborative space programme efforts were in 1973 gathered under one organization, named the European Space Agency (ESA). This establishment made European countries able to expand their frontiers in space and develop independent communication, infrastructure and surveillance capabilities. ESA was originally constituted by eleven member countries, and the association now has near to twenty countries as full time members and even more as associated members. Its record of space missions consists of over seventy successful and independent missions, in addition to over fifty done in collaboration with NASA or the Russian Space Agency. Of the most significant milestones are the first Ariane launch in 1979, the Mars Express orbiter in 2003 and the landing of the Huygens probe on Saturn's moon Titan in 2005.

ESA's Education Office started the Student Space Exploration and Technology Initiative (SSETI) in 2000 to stimulate the future generation of scientists and engineers to pursue a career in space-related fields. SSETI connects students from over fifteen universities in European countries and provides resources and an environment allowing them to cooperate and learn from each other during projects. The Norwegian participants have formed the Attitude Determination and Control Systems (ADCS) group, consisting of students from NTNU and Narvik University College.

1.2 ESMO

This section is based on information on the SSETI Homepage (2007). From the start SSETI had a list of goals, successive space missions where the large part of the work should be done by students from the member countries:

- Mission 0: SSETI Express - launched in 2005

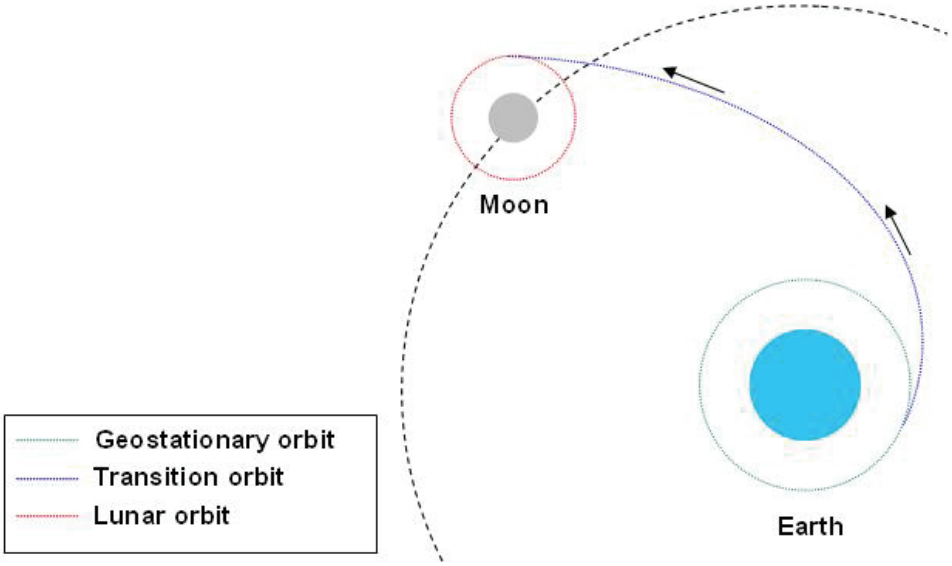

Figure 1.1: Simple overview of the ESMO trajectories

- Mission 1: ESEO - Earth Orbiter - planned for launch in 2008
- Mission 2: ESMO - Moon Orbiter - possible launch in 2011
- Mission 3: Moon Rover - no date fixed

This thesis is a part of the European Student Moon Orbiter project, which started in March 2006. The ”Phase A” feasibility study of the project will be carried out until July 2007 after which the project will receive a go/no-go decision. The ADCS group has handed in a ’Call for Proposals’ paper (ADCS group Narvik 2006) as a tentative outline of the work to be done during Phase A.

The ESMO mission objectives are summarised as follows:

Education: *Prepare students for careers in future projects of the European space exploration and space science programmes by providing valuable hands-on experience on a relevant and demanding project.*

Outreach: *Acquire images of the Moon and transmit them back to Earth for public relations and education outreach purposes.*

Science: *Perform new scientific measurements relevant to lunar science and the future human exploration of the Moon, in complement with past, present and future lunar missions.*

Engineering: *Provide flight demonstration of innovative space technologies developed under university research activities.*

The ESMO benefits from the research done on the ESEO project, and is a natural step towards a Moon Rover expedition. From a piggy-back launch in a geostationary orbit, the satellite will make a self-propelled lunar transfer before adjusting to a low altitude orbit around the moon, see Figure 1.1. As of May 1st 2006 the core payload is meant to be a high-resolution CCD camera, and possibly infra-red imaging devices, radars and equipment for gravity field measurements. The satellite propulsion system is to be decided. Options include a solid/liquid "conventional" thruster system and a solar powered electric system. Dependant on the choice, the lunar transfer can be performed in respectively a few days or almost a year. This project is concerned with the part of the mission where the satellite is already in lunar orbit.

1.3 ADCS design outline

The attitude of a body, it being a robot, boat or satellite, can be as important to control as its position. At any time during space flight, transfer or orbit, one must be able to orientate the satellite body exactly to take advantage of its cameras and instruments, solar panels etc. As the accuracy of such instruments have increased over the years, so has the demand of more precise positioning systems. A satellite needs a motion control system to position and orientate itself correctly. The work in this project focuses primarily on attitude control, leaving the integration of a position controller for future work. The attitude determination and control system consists of two parts; The attitude determination system includes sensors and noise filters for acquiring the orientation of the satellite, whereas the control system is made up by a control algorithm, actuators and thrusters. The term *attitude* of a satellite refers to the angular deviation between reference frames, usually the body deviation from the orbit frame. Chapter 2 introduces the reference frames used in the project, along with some mathematical definitions and techniques used in modelling and stability analysis.

The basis for the ADCS is the model of the ESMO satellite attitude, which is worked out in Chapter 3.

An important factor in the attitude determination system is the measurement hardware. Acquisition of orientation and angular velocity data can be done with various sensor configurations. During simulations and analysis the hardware must be modelled and integrated with the total system to clarify how different configurations and changes in sensor parameters will impact performance. The 'Call for proposals' paper from the ADCS group suggested a configuration of star trackers, sun sensors and inertia sensors. As a pre-study for this thesis, different sensors were modelled and a configuration was suggested in Waarum (2006).

Sensor measurements will often suffer from noise pollution, drift errors and slow sample rates. Some systems may have states impossible to measure. Numerical differentiation can not be used to compute missing states, since the differentiation will add noise to a signal. To obtain signals that are of sufficient quality to

be fed to a controller, filtering techniques have been developed that removes noise. One of the tools that can be used is an *observer*, which will also estimate states that can not be measured. The observer is a mathematical model of the system, which based on input of some system states can estimate the overall system behaviour. The most important pre-study results on observers are included and elaborated in Chapter 4.

Various control algorithms are discussed in Chapter 5. Different approaches are taken. Some algorithms are model dependant, while some are more robust. All are analysed with regards to stability as if they had direct access to the necessary system states.

In a controller/observer system the control law is based on state estimates, i.e. the output from the observer instead of the true states. This may alter the stability properties so that the properties of the total system are not the sum of the properties of the stand-alone controller and observer. To establish stability for the controller/observer system, a *separation principle* must be present. Chapter 6 tries to explain what the presence of a separation principle actually means, starting with a set of generally interdependent differential equations and ending with a controller/observer configuration. The main contribution of the thesis can be found in Chapter 7, where the presence of such a separation principle is proven for a chosen observer and control law.

The performance of the different controllers are presented in Chapter 8. The methods of testing are chosen based on possible real-life scenarios. Finally, some conclusions are made along with a few proposals for further work.

1.4 Previous work

Former NTNU students have written diplomas which has been information resources for this project. Kyrkjebø (2000) wrote on satellite attitude determination using a magnetometer/star tracker sensor configuration, and has been extensively referenced in other diplomas. Sunde (2005) modelled sensors and made both an Extended Kalman filter and an observer for a micro-satellite. The observer used for analysis in this project is based on the work of Salcudean (1990). The model has later been extended with sensor error models by Vik (2000) and Thienel & Sanner (2001).

A huge amount of work exists on attitude controllers for satellites, boats and robot manipulators. The most obvious to mention are the works of Egeland & Godhavn (1994) and Josh et al. (1995) which is treated in detail in the chapter on controllers. Other notable works used as background are Wen & Kreutz-Delgado (1991), which considers the attitude control problem thoroughly and compares the performance of different controller types. Adaptive controllers similar to that of Egeland & Godhavn (1994) can be found in Slotine & Li (1988) and Thienel & Sanner (2001).

The presentation of the separation principle herein is based on works by Michel

et al. (1978), Vidyasagar (1980*a*), Vidyasagar (1980*b*) and Panteley & Loria (1997). Other good sources to understand what a separation principle means are Jankovic et al. (1996), Saberi et al. (1989) and Atassi & Khalil (1999). Related areas include theory of complete systems and input-to-state stability, of which Angeli & Sontag (1999) and Sontag (1989) are good readings.

An example of showing the cascaded form of an observer/controller system and then proving stability can be found in Loria et al. (2000). More general background on the same topic are the lecture notes of Loria (2004).

These and other authors are referenced throughout the report.

1.5 Contributions of this thesis

The work presented in this thesis leans heavily on the earlier mentioned books and articles. However, some new results are made. The observer from Vik (2000) was simplified and the stability proof was done with basis in the original proof. The linearizing controller was derived from the adaptive controller of Egeland & Godhavn (1994), and the stability proof was done based on the original proof and the one found in Thienel & Sanner (2001). Both the control law and the stability proof of the PD-controller is based on the work of Wen & Kreutz-Delgado (1991).

The presentation of the nonlinear separation principle is solely based on previous works of distinguished authors, but the presentation herein tries to show how the problem arises in the first place by starting with a general set of differential equations and then gradually transforming the problem to a set of equations corresponding to a cascaded controller/observer system. The most original work of the thesis is, along with the linearizing controller, the proofs of total stability and the existence of separation principles for the cascaded system. This is, however, based on the theorems of Panteley & Loria (1997) and the method in Loria et al. (2000).

Chapter 2

Mathematical Background

The attitude motion of a satellite can be described as a set of differential equations. The motion is given by the satellite body rotation with respect to different frames of motion. Which frames of motion that are practical depends on the satellite's area of use. Body rotation is usually presented with vector notation. The first part of this chapter presents some useful theory and properties of vectors and rotation matrices as well as the convenient frames of motion for a moon orbiting satellite. To signify vectors and matrices, non-scalar attributes are written in bold letters throughout the report. The second part presents stability theory, in particular the direct method of Lyapunov.

2.1 Vectors

Fjellstad (1994) stated how a rigid body in n-dimensional space has $n(n+1)/2$ degrees of freedom (DOF). A satellite in $\mathcal{R}^3$ has six DOF, which can be described with a position vector $\boldsymbol{\eta} = [\ x \quad y \quad z \quad \varphi \quad \theta \quad \psi\ ]^T$, where $[\ x \quad y \quad z\ ]^T$ are the positions in the orthogonal Euler space $\mathcal{R}^3$ and $[\ \varphi \quad \theta \quad \psi\ ]^T$ are the Euler angles of the satellite body relative to the xyz reference frame. The satellite velocities in the respective directions are then given by the vector $\boldsymbol{\nu} = \dot{\eta} = [\ v_1 \quad v_2 \quad v_3 \quad w_1 \quad w_2 \quad w_3\ ]^T$. The following theory is based on Egeland & Gravdahl (2002), in which more detailed explanations can be found.

If $\boldsymbol{r}$ is a general vector in reference frame $\mathcal{F}_\sigma$, it can be written on component form as

$$\boldsymbol{r}^\sigma = \begin{bmatrix} r_1 & r_2 & r_3 \end{bmatrix}^T,$$

where $\boldsymbol{r}^\sigma = r_1\sigma_1 + r_2\sigma_2 + r_3\sigma_3$ and σ_i are the unit vectors of the orthogonal system $\mathcal{F}_\sigma$. The cross product $\boldsymbol{t}$ of two vectors $\boldsymbol{r}$ and $\boldsymbol{s}$ in the frame $\mathcal{F}_\sigma$ can be found from

$$\boldsymbol{t} = \boldsymbol{r}\times\boldsymbol{s} = \begin{vmatrix} \sigma_1 & \sigma_2 & \sigma_3 \\ r_1 & r_2 & r_3 \\ s_1 & s_2 & s_3 \end{vmatrix} = (r_2s_3 - r_3s_2)\sigma_1 - (r_1s_3 - r_3s_1)\sigma_2 + (r_1s_2 - r_2s_1)\sigma_3,$$

which corresponds to the vector

$$\begin{bmatrix} r_2 s_3 - r_3 s_2 \\ r_3 s_1 - r_1 s_3 \\ r_1 s_2 - r_2 s_1 \end{bmatrix}. \tag{2.1}$$

To easily compute the cross product, the *skew-symmetric* form of a vector is introduced as

$$\boldsymbol{S}(\boldsymbol{r}) = \begin{bmatrix} 0 & -r_3 & r_2 \\ r_3 & 0 & -r_1 \\ -r_2 & r_1 & 0 \end{bmatrix}$$

such that

$$\boldsymbol{S}(\boldsymbol{r})\boldsymbol{s} = \begin{bmatrix} 0 & -r_3 & r_2 \\ r_3 & 0 & -r_1 \\ -r_2 & r_1 & 0 \end{bmatrix} \begin{bmatrix} s_1 \\ s_2 \\ s_3 \end{bmatrix} = \boldsymbol{r} \times \boldsymbol{s}$$

which computes to the same result as in Equation 2.1. Some useful properties of the skew-symmetric matrix which will be used in this report:

$$\boldsymbol{S}(-\boldsymbol{r}) = -\boldsymbol{S}(\boldsymbol{r}) = \boldsymbol{S}(\boldsymbol{r})^T \tag{2.2}$$

$$\boldsymbol{r}\boldsymbol{S}(\boldsymbol{r}) = 0 \tag{2.3}$$

2.2 Rotation matrices

To transform a vector between reference frames, some information regarding the relative orientation of the frames is necessary. Unless otherwise stated, the following theory is based on Sciavicco & Siciliano (1996) in which a more detailed explanation can be found. A matrix $\boldsymbol{R}$ is a rotation matrix if and only if $\boldsymbol{R} \in \mathcal{R}^{3\times3}$, $\boldsymbol{R}^T\boldsymbol{R} = \boldsymbol{I}$ and $\det(\boldsymbol{R}) = 1$ (Egeland & Gravdahl 2002). $\boldsymbol{R}$ has two interpretations;

1. It rotates a vector inside a reference frame: $\boldsymbol{x}' = \boldsymbol{R}\boldsymbol{x}$.

2. It gives the rotation between two reference frames: $\boldsymbol{r}^\rho = \boldsymbol{R}^\rho_\sigma \boldsymbol{r}^\sigma$.

A rotation between two reference frames in $\mathcal{R}^3$ is given by the composite rotation $\boldsymbol{R}^\rho_\sigma = \boldsymbol{R}_{z,\psi}\boldsymbol{R}_{y,\theta}\boldsymbol{R}_{x,\phi}$ where xyz are the orthogonal axes, $\psi\theta\phi$ are the corresponding Euler angles and the matrices $\boldsymbol{R}_{r,\vartheta}$ are shown in 2.4.

$$
\begin{aligned}
\boldsymbol{R}_{x,\phi} &= \begin{bmatrix} 1 & 0 & 0 \\ 0 & \cos\phi & -\sin\phi \\ 0 & \sin\phi & \cos\phi \end{bmatrix} \\
\boldsymbol{R}_{y,\phi} &= \begin{bmatrix} \cos\theta & 0 & \sin\theta \\ 0 & 1 & 0 \\ -\sin\theta & 0 & \cos\theta \end{bmatrix} \\
\boldsymbol{R}_{z,\psi} &= \begin{bmatrix} \cos\psi & -\sin\psi & 0 \\ \sin\psi & \cos\psi & 0 \\ 0 & 0 & 1 \end{bmatrix} \\
\boldsymbol{R}_{\sigma}^{\rho} &= \begin{bmatrix} c(\phi)c(\theta) & c(\phi)s(\theta)s(\psi) - s(\phi)c(\psi) & c(\phi)s(\theta)c(\psi) + s(\phi)s(\psi) \\ s(\phi)c(\theta) & s(\phi)s(\theta)s(\psi) + c(\phi)c(\psi) & s(\phi)s(\theta)c(\psi) - c(\phi)s(\psi) \\ -s(\theta) & c(\theta)s(\psi) & c(\theta)c(\psi) \end{bmatrix}
\end{aligned}
\tag{2.4}
$$

The general rotation matrix for a rotation ϑ about a vector $\boldsymbol{r} = [\ r_x \quad r_y \quad r_z\ ]$ can be written as 2.5, from which one finds R_1, R_2 and R_3 by inserting respectively $\boldsymbol{r} = [\ r_1 \quad 0 \quad 0\ ]$, $\boldsymbol{r} = [\ 0 \quad r_2 \quad 0\ ]$ and $\boldsymbol{r} = [\ 0 \quad 0 \quad r_3\ ]$. Sciavicco & Siciliano (1996) gives the general rotation matrix as

$$
\boldsymbol{R}_{r,\vartheta} = \begin{bmatrix} r_x^2 d + c\vartheta & r_x r_y d - r_z s_\vartheta & r_x r_z d + r_y s_\vartheta \\ r_x r_y d + r_z s_\vartheta & r_y^2 d + c\vartheta & r_y r_z d - r_x s_\vartheta \\ r_x r_z d - r_y s_\vartheta & r_y r_z d + r_x s_\vartheta & r_z^2 d + c\vartheta \end{bmatrix}, \tag{2.5}
$$

where $d = (1 - \cos\vartheta)$.

Due attention must be paid to the order of multiplication. Postmultiplication corresponds to rotation around the rotated system, i.e. the current frame, whereas premultiplication implies rotation around a fixed system. The different approaches are shown in Equations 2.6 (postmultiplication) and 2.7 (premultiplication).

$$
\begin{aligned}
\boldsymbol{r}^1 &= \boldsymbol{R}_2^1 \boldsymbol{r}^2 \\
\boldsymbol{r}^0 &= \boldsymbol{R}_1^0 \boldsymbol{r}^1 \\
\boldsymbol{r}^0 &= \boldsymbol{R}_1^0 \boldsymbol{R}_2^1 \boldsymbol{r}^2
\end{aligned}
\tag{2.6}
$$

$$
\begin{aligned}
\boldsymbol{r}^0 &= \boldsymbol{R}_1^0 \boldsymbol{r}^1 \\
\boldsymbol{r}^1 &= \boldsymbol{R}_0^1 \boldsymbol{R}_2^1 \boldsymbol{R}_1^0 \boldsymbol{r}^2 \\
\boldsymbol{r}^0 &= \boldsymbol{R}_1^0 \boldsymbol{R}_0^1 \boldsymbol{R}_2^1 \boldsymbol{R}_1^0 \boldsymbol{r}^2 = \boldsymbol{R}_2^1 \boldsymbol{R}_1^0 \boldsymbol{r}^2
\end{aligned}
\tag{2.7}
$$

The first approach is common in robot technique, where joints rotate relative to each other, while the fixed frame method is standard in navigation.

Rotation matrices using Euler angles is a well-known tool in robot technique, vessel control and navigation. The technique does, however, have a problem with singularities. For instance, Equation 2.5 is singular for $\vartheta = \pm\pi/2$, and is therefore impractical when modelling a satellite that can make 360° rotations.

2.3 Euler parameters

As a solution to the singularity problems with Euler angle rotation matrices, Euler presented the Euler parameters in 1770. Combined, they consitute the unit quaternion $\boldsymbol{q} = [\ \eta \quad \epsilon_1 \quad \epsilon_2 \quad \epsilon_3\ ]^T$. This presentation of Euler parameters is based on Egeland & Gravdahl (2002), where their definition is given as

$$\eta = \cos\frac{\vartheta}{2}\ \boldsymbol{\epsilon} = \boldsymbol{k}\sin\frac{\vartheta}{2} \tag{2.8}$$

$$\eta^2 + \boldsymbol{\epsilon}^T\boldsymbol{\epsilon} = \cos^2\frac{\vartheta}{2} + \sin^2\frac{\vartheta}{2} = 1, \tag{2.9}$$

which proves boundedness and the unit property. A rotation of 0° corresponds to the identity quaternion $\boldsymbol{q}_{id} = [\ 1 \quad 0 \quad 0 \quad 0\ ]^T$. The inverse of a quaternion is $q^{-1} = [\ \eta \quad -\boldsymbol{\epsilon}\ ]^T$. The general rotation matrix corresponding to Equation 2.5 is given by:

$$\begin{aligned}\boldsymbol{R}_{\eta,\epsilon} =& \boldsymbol{I} + 2\eta\boldsymbol{S}(\boldsymbol{\epsilon}) + 2\boldsymbol{S}(\boldsymbol{\epsilon})\boldsymbol{S}(\boldsymbol{\epsilon}) \\ =& \begin{bmatrix} \eta^2+\epsilon_1^2-\epsilon_2^2-\epsilon_3^2 & 2(\epsilon_1\epsilon_2-\eta\epsilon_3) & 2(\epsilon_1\epsilon_3+\eta\epsilon_2) \\ 2(\epsilon_1\epsilon_2+\eta\epsilon_3) & \eta^2-\epsilon_1^2+\epsilon_2^2-\epsilon_3^2 & 2(\epsilon_2\epsilon_3-\eta\epsilon_1) \\ 2(\epsilon_1\epsilon_3-\eta\epsilon_2) & 2(\epsilon_2\epsilon_3+\eta\epsilon_1) & \eta^2-\epsilon_1^2-\epsilon_2^2+\epsilon_3^2 \end{bmatrix}\end{aligned} \tag{2.10}$$

Rotating a vector with quaternion rotation matrices is written as

$$\boldsymbol{r}' = \begin{bmatrix} 0 \\ \boldsymbol{R}_{\eta,\epsilon}\boldsymbol{r} \end{bmatrix} = \boldsymbol{q}\begin{bmatrix} 0 \\ \boldsymbol{r} \end{bmatrix}\boldsymbol{q}^{-1}.$$

A successive rotation by $\boldsymbol{R}_{\eta 1,\epsilon 1}$ and $\boldsymbol{R}_{\eta 2,\epsilon 2}$ is thus written as:

$$\boldsymbol{r}'' = \boldsymbol{q}_2 \otimes \boldsymbol{q}_1 \begin{bmatrix} 0 \\ \boldsymbol{r} \end{bmatrix} \boldsymbol{q}_1^{-1} \otimes \boldsymbol{q}_2^{-1}$$

The introduced operator denotes the *quaternion product*:

$$\boldsymbol{q}_2 \otimes \boldsymbol{q}_1 = \begin{bmatrix} \eta_2\eta_1 - \boldsymbol{\epsilon}_2^T\boldsymbol{\epsilon}_1 \\ \eta_2\boldsymbol{\epsilon}_1 + \eta_1\boldsymbol{\epsilon}_2 + \boldsymbol{S}(\boldsymbol{\epsilon}_2)\boldsymbol{\epsilon}_1 \end{bmatrix} \tag{2.11}$$

From Equation 2.11 it can be seen that $\boldsymbol{q} \otimes \boldsymbol{q}^{-1} = \boldsymbol{q}_{id}$, which in turn gives $\boldsymbol{q} = \boldsymbol{q}_{id} \otimes \boldsymbol{q}$.

The use of four parameters instead of three avoids singularities. However, it also introduces some redundancy in the attitude representation. As stated, the vector $\boldsymbol{q} = [\ 1 \quad 0 \quad 0 \quad 0\ ]^T$ correspons to a rotation of 0°. But the vector $\boldsymbol{q} = [\ -1 \quad 0 \quad 0 \quad 0\ ]^T$ corresponds to a rotation of 360°, i.e. the same physical attitude.

2.4 Kinematics

Fundamental to the construction of a differential kinematic model is differentiation of vectors, matrices and Euler parameters. Regular vectors and matrices are differentiated by the basic rules where for instance acceleration is computed from a velocity vector as $\boldsymbol{a} = \dot{\boldsymbol{v}} = \begin{bmatrix} \dot{v}_1 & \dot{v}_2 & \dot{v}_3 \end{bmatrix}^T$. Kinematics for the rotation matrix $\boldsymbol{R} = \boldsymbol{R}^{\rho}_{\sigma}$ is given by

$$\frac{d}{dt}\boldsymbol{R} = \lim_{\triangle t \to 0} \frac{\boldsymbol{R}(t + \triangle t) - \boldsymbol{R}(t)}{\triangle t}, \tag{2.12}$$

where $\boldsymbol{R}(t + \triangle t)$ can be written as the composite rotation between the general rotation $\boldsymbol{R}_{\triangle\theta,r}$ and $\boldsymbol{R}$(t) such that

$$\frac{d}{dt}\boldsymbol{R} = \lim_{\triangle t \to 0} \frac{(\boldsymbol{R}_{\triangle\vartheta,r} - I_{3\times 3})\boldsymbol{R}(t)}{\triangle t}.$$

Inserting $\triangle\vartheta$ and r into Equation 2.5 and using $\sin\triangle\vartheta = \triangle\vartheta$ and $\cos\triangle\vartheta = 1$ gives

$$\boldsymbol{R}_{\triangle\vartheta,r} = \begin{bmatrix} 1 & -r_z\triangle\vartheta & r_y\triangle\vartheta \\ r_z\triangle\vartheta & 1 & -r_x\triangle\vartheta \\ -r_y\triangle\vartheta & r_x\triangle\vartheta & 1 \end{bmatrix},$$

from which it can be seen that

$$\frac{d}{dt}\boldsymbol{R} = \begin{bmatrix} 0 & -r_z\dot{\vartheta} & r_y\dot{\vartheta} \\ r_z\dot{\vartheta} & 0 & -r_x\dot{\vartheta} \\ -r_y\dot{\vartheta} & r_x\dot{\vartheta} & 0 \end{bmatrix}.$$

Since $r_i\dot{\vartheta}$ denotes the angular velocity $\boldsymbol{\omega}^{\sigma}_{\sigma\rho}$ between $\mathcal{F}_\sigma$ and $\mathcal{F}_\rho$, Equation 2.12 may be written as

$$\dot{\boldsymbol{R}}^{\rho}_{\sigma} = \boldsymbol{S}(\boldsymbol{\omega}^{\sigma}_{\sigma\rho})\boldsymbol{R}^{\rho}_{\sigma} = \boldsymbol{R}^{\rho}_{\sigma}\boldsymbol{S}(\boldsymbol{\omega}^{\rho}_{\sigma\rho}).$$

Derivation of the differentiated Euler parameters is somewhat lengthy, a detailed explanation can be found in Egeland & Gravdahl (2002). The resulting equations are given as:

$$\begin{aligned} \dot{\boldsymbol{q}} &= \frac{1}{2}\boldsymbol{q} \otimes \begin{bmatrix} 0 \\ \boldsymbol{\omega}^{\sigma} \end{bmatrix} \\ \begin{bmatrix} \dot{\eta} \\ \dot{\boldsymbol{\epsilon}} \end{bmatrix} &= \begin{bmatrix} -\frac{1}{2}\boldsymbol{\epsilon}^T\boldsymbol{\omega}^{\sigma} \\ \frac{1}{2}\left(\eta\boldsymbol{I}_{\mathbf{3}\times\mathbf{3}} - \boldsymbol{S}(\boldsymbol{\epsilon})\right)\boldsymbol{\omega}^{\sigma} \end{bmatrix} = \frac{1}{2}\boldsymbol{Q}(\boldsymbol{q})\boldsymbol{\omega}^{\sigma} \end{aligned} \tag{2.13}$$

2.5 Frames of motion

Newton's laws are only applicable when all motion is described in a common frame. For all practical purpose most systems can be described in the Earth-Centered Inertial frame. When treating the entire ESMO mission, including the

Index	Frame of motion
e	Earth Centered Inertial
m	Moon Centered
o	Orbit Centered
b	Body

Table 2.1: Indexed frames of motion

lunar transfer, the sun might suit better as inertial frame. In lunar orbit, the moon may be regarded as the inertial frame. Motion relative to other frames has to be translated to the inertial frame. Using different frames is practical in describing the relative motion of objects, and considering a satellite system the different frames of motion are listed in Table 2.1. Common for these frames is that they are right-handed and that their axes are orthogonal, both properties simplifying the translation between the frames.

Earth-Centered Inertial frame

The ECI frame has its origo at the center of the Earth, its z-axis pointing upwards through the North Pole. The x-axis points in the vernal equinox direction, which is the direction of the vector from the center of the Sun to the center of the Earth during spring equinox on the northern hemisphere. The direction of the y-axis then follows from the frame being an orthogonal right-hand frame. So the ECI frame does not follow Earth's rotation. Whenever something is described relative to the ECI-frame it is in this report indicated by the subscript e.

Moon-fixed reference frame

Treating satellites in lunar orbit is somewhat complicated by the introduction of a new reference frame. However, it simplifies the description of the relative motion of the moon and the satellite. As for the earth frame, the z-axis points from the origo in the moon centre and upwards through the north pole. The x-axis is parallel with the vector between the origo of the moon-fixed and the the earth-fixed frame. The moon-fixed reference frame is denoted by the subscript m.

Orbit-fixed reference frame

This frame has its origin in a mean orbit trajectory. The origin moves along this trajectory as the satellite travels in orbit. The z-axis points toward the mass centre of the encircled object, the x-axis points in the direction of motion, tangentially to the orbit. When the orbit is around Earth, it is denoted by the subscript t, around the Moon the subscript is o.

Body-fixed reference frame

With origin in the satellite's centre of mass, it coincides with the origin of the orbit frame whenever the satellite orbit coincides with the mean (non-perturbed) orbit. The two frames are aligned if the satellite has an attitude of 0° in roll, pitch and yaw. Whenever satellite attitude is mentioned in this report, it is meant the deviation between the body frame and the orbit frame. The body frame is denoted b.

Frame translation

With the reference frames defined, Equation 2.13 can be used to describe the satellite body attitude relative to the orbit frame:

$$\dot{q} = \begin{bmatrix} \dot{\eta} \\ \dot{\epsilon} \end{bmatrix} = \frac{1}{2} \begin{bmatrix} -\epsilon^T \\ \eta \mathbf{I} + \mathbf{S}(\epsilon) \end{bmatrix} \omega_{ob}^b$$

However, the internal gyros and sensors of the satellite measures motion relative to the inertial frame. Translating between frames of motion, ω_{ob}^b can be found from Equation 2.14 which will be used in the satellite model.

$$\omega_{ob}^b = \omega_{eb}^b - \omega_{eo}^b = \omega_{eb}^b - (\omega_{em}^b + \omega_{mo}^b) \tag{2.14}$$

2.6 Stability preliminaries

Some concepts used extensively throughout the thesis are norms and $\mathcal{L}_p$ spaces. They are introduced here, along with some function properties that applies to the Lyapunov function theorems in the next subchapter. $|r|$ denotes the absolute value of a scalar r. $||\boldsymbol{r}||$ denotes the norm of a vector $\boldsymbol{r}$.

2.6.1 Norms and $\mathcal{L}_p$-spaces

Definition 2.1 (Ioannou & Sun 1996) pp 68. *The norm $||\boldsymbol{r}||$ of a vector $\boldsymbol{r}$ is a real valued function with the following properties:*

i) $||\boldsymbol{r}|| \geq 0$ *with* $||\boldsymbol{r}|| = 0$ *if and only if* $\boldsymbol{r} = 0$

ii) $||\alpha \boldsymbol{r}|| = |\alpha| ||\boldsymbol{r}||$ *for any scalar* α

iii) $||\boldsymbol{r} + \boldsymbol{s}|| \leq ||\boldsymbol{r}|| + ||\boldsymbol{s}||$ *(triangle inequality)*

Inequality $iii)$ above is a special case of the Cauchy-Schwarz inequality, which treats the relationship between two vectors in the same real or complex inner product space[1]:

$$| < \boldsymbol{r}, \boldsymbol{s} > | \ \leq < \boldsymbol{r}, \boldsymbol{r} > \cdot < \boldsymbol{s}, \boldsymbol{s} > . \tag{2.15}$$

[1]For more theory on inner product spaces, consult e.g. Young (1988)

The two sides of Equation 2.15 are equal only if the vectors r and s are linearly independent, or if one or both vectors are equal to zero. The triangle inequality is a consequence of the Cauchy-Schwarz inequality. Consider

$$\begin{aligned}||\boldsymbol{r}+\boldsymbol{s}||^2 &= <\boldsymbol{r}+\boldsymbol{s},\boldsymbol{r}+\boldsymbol{s}> \\ &= ||\boldsymbol{r}||^2 + <r,s> + <\boldsymbol{s},\boldsymbol{r}> + ||\boldsymbol{s}||^2 \\ &\leq ||\boldsymbol{r}^2+2|<\boldsymbol{r},\boldsymbol{s}>| + ||\boldsymbol{s}||^2 \\ &\leq ||\boldsymbol{r}^2+2||\boldsymbol{r}||||\boldsymbol{s}|| + ||\boldsymbol{s}||^2 \\ &= (||\boldsymbol{r}|| + ||\boldsymbol{s}||)^2,\end{aligned}$$

which gives $||\boldsymbol{r}+\boldsymbol{s}|| \leq (||\boldsymbol{r}|| + ||\boldsymbol{s}||)$.

A matrix $\boldsymbol{A}^{m\times n}$ represents a mapping from the space $\mathcal{R}^n$ to the space $\mathcal{R}^m$. The induced norm of a matrix is defined as:

Definition 2.2 (Ioannou & Sun 1996) pp 68. *Let $||\cdot||$ be a given vector norm. Then for each matrix $\boldsymbol{A} \in \mathcal{R}^{m\times n}$, the quantity $||\boldsymbol{A}||$ defined by*

$$||\boldsymbol{A}|| \triangleq \sup_{\boldsymbol{x}\neq 0, \boldsymbol{x}\in\mathcal{R}^n} \frac{||\boldsymbol{A}\boldsymbol{x}||}{||\boldsymbol{x}||} = \sup_{||\boldsymbol{x}||\leq 1} ||\boldsymbol{A}\boldsymbol{x}|| = \sup_{||\boldsymbol{x}||=1} ||\boldsymbol{A}\boldsymbol{x}||$$

is called the induced (matrix) norm of $\boldsymbol{A}$ corresponding to the vector norm $||\cdot||$.

Some properties of the induced norm:

i) $||\boldsymbol{A}\boldsymbol{x}|| \leq ||\boldsymbol{A}||||\boldsymbol{x}||, \qquad \forall \boldsymbol{x} \in \mathcal{R}$

ii) $||\boldsymbol{A}+\boldsymbol{B}|| \leq ||\boldsymbol{A}|| + ||\boldsymbol{B}||$

iii) $||\boldsymbol{A}\boldsymbol{B}|| \leq ||\boldsymbol{A}||||\boldsymbol{B}||$.

The induced matrix norm also satisfies properties $i)$ through $iii)$ of Definition 2.1.

The $\mathcal{L}_p$ norm is defined as

Definition 2.3 (Ioannou & Sun 1996) pp. 69.

$$||r||_p = (\int_0^\infty |r(t)|^p dt)^{1/p}$$

for $p \in [1,\infty)$, and say that $r \in \mathcal{L}_p$ when $||r||_p < \infty$.

The two function spaces used in this thesis are the $\mathcal{L}_\infty$ and $\mathcal{L}_2$ spaces.

The $\mathcal{L}_\infty$ norm is defined as

$$||r||_\infty = \sup_{t\geq 0} |r(t)|$$

and $r \in \mathcal{L}_\infty$ whenever $||r||_\infty$ exists. In short, the function space $\mathcal{L}_\infty$ consists of all functions that satisfies $|f(\cdot,t)| < \infty$ for all t.

From Definition 2.3 the $\mathcal{L}_2$ (Euclidian) norm becomes

$$\int_0^\infty \sqrt{f(t)^2}dt, \tag{2.16}$$

and the function space $\mathcal{L}_2$ consists of all functions $f(t)$ with properties such that the integral in Equation 2.16 exists for all t. In short, $\int_0^T f(t)$ must be finite for all $T \in [0, \infty)$.

Throughout the thesis, $|| \cdot ||$ denotes the Euclidian norm of vectors and the induced norm of matrices.

2.6.2 Function properties

Definition 2.4 *A function f(x,t) is said to be Lipschitz if it satisfies the inequality*

$$||f(x,t) - f(y,t)|| \leq L||x - y||$$

$\forall (x,t), (y,t)$ *in some neighbourhood of* (x_0, t_0).

For a function to be considered continuous in a domain, it must be possible to find a Lipschitz constant L which is valid in the entire domain.

Definition 2.5 (Khalil 2000) pp. 144. *A continuous function* $\alpha : [0, a) \to [0, \infty)$ *is said to belong to class* $\mathcal{K}$ *if it is strictly increasing and* $\alpha(0) = 0$. *It is said to belong to class* $\mathcal{K}_\infty$ *if* $a = \infty$ *and* $\alpha(r) \to \infty$ *as* $r \to \infty$.

A special case of class $\mathcal{K}_\infty$ functions is the continuous time variable t.

Definition 2.6 (Khalil 2000) pp. 144. *A continuous function* $\beta : [0, a) \times [0, \infty) \to [0, \infty)$ *is said to belong to class* $\mathcal{KL}$ *if, for each fixed s, the mapping* $\beta(r, s)$ *is decreasing with respect to s and* $\beta(r, s) \to 0$ *as* $s \to \infty$.

2.7 Stability theory

To prove functionality of observers or controllers, it must be shown that the observer or controller error diminishes with time. The main tool used to that end is in this thesis Lyapunov stability theory, as presented in Khalil (2000). The stability property describes whether and how a system converges to an equilibrium state. Using the direct method of Lyapunov, stability can be analysed without solving the differential equations of a system. The main theorems and necessary definitions are included here for convenience.

Lyapunov function candidates must be class $\mathcal{KL}$ if Theorems 2.1 to 2.3 are to be used. They give sufficient conditions for stability, asymptotic stability and exponential stability respectively, and are increasingly strict: Exp.stable systems $\subset$ Asymp.stable systems $\subset$ Stable systems.

Definition 2.7 (Ioannou & Sun 1996), pp. 105. *A state x_e is said to be an equilibrium state of the system described by $\dot{x} = f(x,t)$, $x(t_0) = x_0$ if*

$$f(x_e, t) \equiv 0, \qquad \forall t \geq t_0$$

Theorem 2.1 (Khalil 2000) pp. 151. *Let $x = 0$ be an equilibrium point for $\dot{x} = f(x,t)$ and $D \subset R^n$ be a domain containing $x = 0$. Let $V : [0, \infty) \times D \to R$ be a continuously differentiable function such that*

$$W_1(x) \leq V(x,t) \leq W_2(x)$$

$$\frac{\delta V}{\delta t} + \frac{\delta V}{\delta x} f(x,t) \leq 0 \tag{2.17}$$

$\forall t \geq 0$ and $\forall x \in D$, where $W_1(x)$ and $W_2(x)$ are continuous positive definite functions on D. Then, $x = 0$ is uniformly stable.

Theorem 2.2 (Khalil 2000) pp. 152. *Suppose the assumptions of Theorem 2.1 are satisfied with inequality 2.17 strengthened to*

$$\frac{\delta V}{\delta t} + \frac{\delta V}{\delta x} f(x,t) \leq -W_3(x)$$

$\forall t \geq 0$ and $\forall x \in D$, where $W_3(x)$ is a continuous positive definite function on D. Then, $x = 0$ is uniformly asymptotically stable. Moreover, if r and c are chosen such that $B_r = \{||x|| \leq r\} \subset D$ and $c < min_{||x||=r} W_1(x)$, then every trajectory starting in $\{x \in B_r | w_2(x) \leq c\}$ satisfies

$$||x(t)|| \leq \beta(||x(t_0)||, t - t_0), \qquad \forall t \geq t_0 \geq 0$$

for some class $\mathcal{KL}$ function β. Finally, if $D = R^n$ and $W_1(x)$ is radially unbounded, then $x = 0$ is globally uniformly asymptotically stable.

Theorem 2.3 (Khalil 2000) pp. 154. *Let $x = 0$ be an equilibrium point for $\dot{x} = f(x,t)$ and $D \subset R^n$ be a domain containing $x = 0$. Let $V : [0, \infty) \times D \to R$ be a continuously differentiable function such that*

$$k_1 ||x||^a \leq V(x,t) \leq k_2 ||x||^a$$

$$\frac{\delta V}{\delta t} + \frac{\delta V}{\delta x} f(x,t) \leq -k_3 ||x||^a$$

$\forall t \geq 0$ and $\forall x \in D$, where k_1, k_2, k_3 and a are positive constants. Then, $x = 0$ is exponentially stable. If the assumption hold globally, then $x = 0$ is globally exponentially stable.

Some Lyapunov functions may fail to satisfy Theorems 2.1 to 2.3 because $\dot{V}(\cdot)$ is only negative semidefinite. It may still be possible to show asymptotical or exponential stability by employing the theorem of LaSalle and a corollary:

Theorem 2.4 (Khalil 2000) pp. 128. *Let $\Omega \subset D$ be a compact set that is positively invariant with respect to $\dot{x} = f(x,t)$. Let $V : D \to \mathcal{R}$ be a continuously differentiable function such that $\dot{V}(x) \leq 0$ in Ω. Let E be the set of all points in Ω where $\dot{V}(x) = 0$. Let M be the largest invariant set in E. Then every solution starting in Ω approaches M as $t \to \infty$.*

When the interest is to show that $x(t) \to 0$ as $t \to \infty$, the origin must be established as the largest invariant set in E. This is done by showing that the trivial solution $x(t) \equiv 0$ is the only solution that can stay in E for all time. Theorem 2.4 can be specialized to this case. Corollaries 2.1 and 2.2 shows asymptotical and global asymptotical stability.

Corollary 2.1 (Khalil 2000) pp. 128. *Let $x = 0$ be an equilibrium point for $\dot{x} = f(x,t)$. Let $V : D \to \mathcal{R}$ be a continuously differentiable positive definite function on a domain D containing the origin $x = 0$, such that $\dot{V}(x) \leq 0$ in D. Let $S = \{x \in D | \dot{V}(x) = 0\}$ and suppose that no solution can stay identically in S, other than the trivial solution $x(t) \equiv 0$. Then, the origin is asymptotically stable.*

Corollary 2.2 (Khalil 2000) pp. 129. *Let $x = 0$ be an equilibrium point for $\dot{x} = f(x,t)$. Let $V : \mathcal{R}^n \to \mathcal{R}$ be a continuously differentiable, radially unbounded, positive definite function, such that $\dot{V}(x) \leq 0$ for all $x \in \mathcal{R}^n$. Let $S = \{x \in \mathcal{R}^n | \dot{V}(x) = 0\}$ and suppose that no solution can stay identically in S, other than the trivial solution $x(t) \equiv 0$. Then, the origin is globally asymptotically stable.*

In the case of autonomous systems, the set E may be difficult to define, since $\dot{V}(\cdot)$ is a function of both x and t. Another way to show stability of a function is to consider its integral, as in Barbalat's lemma:

Lemma 2.1 (Khalil 2000) pp. 323. *Let $\phi : \mathcal{R} \to \mathcal{R}$ be a uniformly continuous function on $[0, \infty)$. Suppose that $\lim_{t\to\infty} \int_0^t \phi(\tau) d\tau$ exists and is finite. Then, $\phi(t) \to 0$ as $t \to \infty$.*

A corollary of Barbalat's lemma reformulates the square-integrability condition into consideration of the $\mathcal{L}_p$-belonging of the signals involved. The result is, however, less general:

Corollary 2.3 (Ioannou & Sun 1996) pp. 76. *If f, $\dot{f} \in \mathcal{L}_\infty$ and $f \in \mathcal{L}_p$ for some $p \in [1, \infty)$, then $f(t) \to 0$ as $t \to \infty$.*

As seen with the Lyapunov stability theorems, it is sometimes more useful to compute bounds on the solution of the state equation $\dot{x} = f(x,t)$ than to compute the exact solution. A tool to do this, is the comparison lemma. This may be applied to situations where the inequality $\dot{x} \leq f(x,t)$ is satisfied.

Lemma 2.2 (Khalil 2000) pp. 102. *Consider the scalar differential equation*

$$\dot{u} = f(u,t), \qquad u(t_0) = u_0$$

where $f(u,t)$ is continuous in t and locally Lipschitz in u, for all $t \geq 0$ and all $u \in J \subset R$. Let $[t_0, T)$ (T could be infinity) be the maximal interval of existence of the solution $u(t)$, and suppose $u(t) \in J$ for all $\in [t_0, T)$. Let $v(t)$ be a continuous function whose upper right-hand derivative $D^+v(t)$ satisfies the differential inequality

$$D^+v(t) \leq f(v(t), t), \qquad v(t_0) \leq u_0$$

with $v(t) \in J$ for all $t \in [t_0, T)$. Then, $v(t) \leq u(t)$ for all $t \in [t_0, T)$.

The comparison lemma can also be used to prove exponential stability of an equation. Consider the case where the Lyapunov function candidate V satisfies the inequality $\dot{V} \leq -kV$. Then, by the comparison lemma, there exist constants k_2 and k_3 such that

$$V(x(t), t) \leq V(x(t_0), t_0)e^{-(k_3/k_2)(t-t_0)}.$$

Finally, a definition concerning the passivity of interconnected (closed-loop) systems.

Definition 2.8 (Khalil 2000) pp. 236. *The system*

$$\begin{aligned} \dot{x} &= f(x, u) \\ y &= h(x, u). \end{aligned}$$

is said to be passive if there exists a continuously differentiable positive semidefinite function $V(x)$ (called the storage function) such that

$$u^T y \geq \dot{V} = \frac{\delta V}{\delta x} f(x, u), \qquad \forall (x, u) \in \mathcal{R}^n \times \mathcal{R}^p.$$

Moreover, it is said to be

- *lossless if $u^T y = \dot{V}$*
- *strictly passive if $u^T y \geq \dot{V} + \psi(x)$ for some positive definite function ψ.*

In both cases, the inequality should hold for all (x, u).

Chapter 3

Satellite Model

The differential equations describing satellite attitude are here introduced as a foundation for the control laws and observer algorithms presented in later chapters.

3.1 Kinematic equations

The kinematic equations of a rotating body in space were given in Chapter 2 as:

$$\dot{\eta} = -\frac{1}{2}\boldsymbol{\epsilon}^T\boldsymbol{\omega}^b \tag{3.1}$$

$$\dot{\boldsymbol{\epsilon}} = \frac{1}{2}\left(\eta\boldsymbol{I_{3\times 3}} - \boldsymbol{S}(\boldsymbol{\epsilon})\right)\boldsymbol{\omega}^b \tag{3.2}$$

In compact notation, this will be written as $\boldsymbol{T(q)}\boldsymbol{\omega}^b = [\ \boldsymbol{T}_1(\eta) \quad \boldsymbol{T_2(\epsilon)}\ ]^T\boldsymbol{\omega}^b$.

3.2 Dynamic equations

The equation of motion for rigid-body spacecraft attitude is in its most general form

$$\boldsymbol{J}^b\dot{\boldsymbol{\omega}}^b + N(\boldsymbol{R},\boldsymbol{\omega}^b)\boldsymbol{\omega}^b = \boldsymbol{\tau}^b. \tag{3.3}$$

If the model includes reaction wheel dynamics the $N(\cdot)$ term becomes $N(\boldsymbol{R},\boldsymbol{\omega}^b) = \boldsymbol{S}(\boldsymbol{R}^T\boldsymbol{H}^i)$, where $\boldsymbol{H}^i$ is the total angular momentum of the spacecraft in the inertial frame. Assuming only simple jet actuators, $N(\boldsymbol{R},\boldsymbol{\omega}^b) = \boldsymbol{S}(\boldsymbol{\omega}^b)\boldsymbol{J}^b\boldsymbol{\omega}^b$. The equation of motion is written out in Equation 3.4:

$$\boldsymbol{J}^b\dot{\boldsymbol{\omega}}^b + \boldsymbol{S}(\boldsymbol{\omega}^b)\boldsymbol{J}^b\boldsymbol{\omega}^b = \boldsymbol{\tau}^b \tag{3.4}$$

3.2.1 Open-loop stability

Before complicating the equations, the open-loop equilibrium points should be investigated in the spirit of Josh et al. (1995). Setting all derivatives and inputs of

Equations 3.1 and 3.3 to zero gives:

$$-\frac{1}{2}\boldsymbol{\epsilon}^T\boldsymbol{\omega}^b = 0 \tag{3.5}$$

$$\frac{1}{2}\left(\eta\boldsymbol{I}_{3\times3} - \boldsymbol{S}(\boldsymbol{\epsilon})\right)\boldsymbol{\omega}^b = 0 \tag{3.6}$$

$$\boldsymbol{S}(\boldsymbol{\omega}^b)\boldsymbol{J}^b\boldsymbol{\omega}^b = 0$$

By taking the dot product of $\boldsymbol{\omega}^b$ on both sides of Equation 3.6, $\eta\boldsymbol{I}\boldsymbol{\omega}^b \cdot \boldsymbol{\omega}^b = 0$, which means that either $\eta = 0$, $\boldsymbol{\omega}^b = 0$ or both are zero. Assuming that $\eta = 0$, then by Equations 3.5 and 3.6 $\boldsymbol{\epsilon}^T\boldsymbol{\omega}^b = 0$ and $\boldsymbol{S}(\boldsymbol{\epsilon})\boldsymbol{\omega}^b = 0$, which in turn means that either $\boldsymbol{\omega}^b = 0$, $\boldsymbol{\epsilon} = 0$ or both are zero. However, by the properties of the unit quaternion shown in Equation 2.9, if $\eta = 0$ then $\boldsymbol{\epsilon} \neq 0$. Conclusively, $\boldsymbol{\omega}^b = 0$ when the system is in equilibrium. This will later be used to simplify controller set-points. The equilibrium points of the system are

$$\begin{bmatrix} \eta \\ \boldsymbol{\epsilon} \\ \boldsymbol{\omega}^b \end{bmatrix} = \begin{bmatrix} \pm 1 \\ \mathbf{0} \\ \mathbf{0} \end{bmatrix}. \tag{3.7}$$

3.2.2 Introducing frames

If using the ECI-frame as the inertial frame for a satellite, $\boldsymbol{\omega}^b_{ib}$ can be computed as the sum of the angular velocity in the other frames between the inertial and body frame, as shown in Equation 3.8. Then, the velocities may be decomposed into the new frames.

$$\begin{aligned} \boldsymbol{\omega}^b_{ib} &= \boldsymbol{\omega}^b_{im} + \boldsymbol{\omega}^b_{mo} + \boldsymbol{\omega}^b_{ob} \\ \boldsymbol{\omega}^b_{ib} &= \boldsymbol{R}^b_o\boldsymbol{R}^o_m\boldsymbol{\omega}^m_{im} + \boldsymbol{R}^b_o\boldsymbol{\omega}^o_{mo} + \boldsymbol{\omega}^b_{ob} \end{aligned} \tag{3.8}$$

This yields the velocities $\boldsymbol{\omega}^m_{im} = \begin{bmatrix} 0 & 0 & \boldsymbol{\omega}^m_0 \end{bmatrix}^T$ and $\boldsymbol{\omega}^o_{mo} = \begin{bmatrix} 0 & -\boldsymbol{\omega}^o_0 & 0 \end{bmatrix}^T$, which are approximations of the angular velocity of the moon around the earth and the angular velocity of the satellite around the moon, respectively. Inserting for $\boldsymbol{\omega}^b$ in Equation 3.4 gives:

$$\boldsymbol{J}^b[\frac{d}{dt}(\boldsymbol{R}^b_o\boldsymbol{R}^o_m\boldsymbol{\omega}^m_{im} + \boldsymbol{R}^b_o\boldsymbol{\omega}^o_{mo} + \boldsymbol{\omega}^b_{ob})] + \boldsymbol{S}(\boldsymbol{\omega}^b_{ib})\boldsymbol{J}^b\boldsymbol{\omega}^b_{ib} = \tau^b,$$

which, using Equations 2.3 and 2.13, assuming $\dot{\boldsymbol{\omega}}^m_{im} = \dot{\boldsymbol{\omega}}^o_{mo} = 0$ and rearranging, can be written as

$$\begin{aligned} \dot{\boldsymbol{\omega}}^b_{ob} = (\boldsymbol{J}^b)^{-1}\tau^b &+ \boldsymbol{S}(\boldsymbol{\omega}^o_{mo})\boldsymbol{R}^b_o\boldsymbol{R}^o_m\boldsymbol{\omega}^m_{im} + \boldsymbol{R}^o_m\boldsymbol{S}(\boldsymbol{\omega}^b_{ob})\boldsymbol{R}^b_o\boldsymbol{\omega}^m_{im} + \boldsymbol{S}(\boldsymbol{\omega}^b_{ob})\boldsymbol{R}^b_o\boldsymbol{\omega}^o_{mo} \\ &-(\boldsymbol{J}^b)^{-1}\boldsymbol{S}(\boldsymbol{R}^b_o\boldsymbol{R}^o_m\boldsymbol{\omega}^m_{im} + \boldsymbol{R}^b_o\boldsymbol{\omega}^o_{mo} + \boldsymbol{\omega}^b_{ob})\boldsymbol{J}^b(\boldsymbol{R}^b_o\boldsymbol{R}^o_m\boldsymbol{\omega}^m_{im} + \boldsymbol{R}^b_o\boldsymbol{\omega}^o_{mo} + \boldsymbol{\omega}^b_{ob}) \end{aligned}$$

3.3 State-space model

To simplify analysis, Equation 3.9 can be somewhat simplified. By regarding the Moon as the inertial frame, the motion of the Moon around the Earth is removed. This is desireable, since because of its highly nonlinear characteristics the assumption $\boldsymbol{\omega}_{im}^{m} = 0$ is not always correct. It is assumed that self-adjusting properties of the sensor system will cover the inaccuracies arising from the simplifications.

Using the Moon as the inertial frame and combining with Equation 3.1, it is possible to choose the state vector $\boldsymbol{x} = [\ \eta \quad \epsilon \quad \boldsymbol{\omega}_{ob}^{b}\ ]^T$ and form the state-space model:

$$\begin{bmatrix} \dot{\eta} \\ \dot{\epsilon} \\ \dot{\boldsymbol{\omega}}_{ob}^{b} \end{bmatrix} = \begin{bmatrix} -\frac{1}{2}\boldsymbol{\epsilon}^T\boldsymbol{\omega}_{ob}^{b} \\ \frac{1}{2}\left(\eta\boldsymbol{I} - \boldsymbol{S}(\boldsymbol{\epsilon})\right)\boldsymbol{\omega}_{ob}^{b} \\ (\boldsymbol{J}^b)^{-1}\tau^b + \boldsymbol{S}(\boldsymbol{\omega}_{ob}^{b})\boldsymbol{R}_o^b\boldsymbol{\omega}_{io}^{o} - (\boldsymbol{J}^b)^{-1}\boldsymbol{S}(\boldsymbol{\omega}_{ib}^{b})\boldsymbol{J}^b(\boldsymbol{\omega}_{ib}^{b}) \end{bmatrix}, \quad (3.9)$$

where $\boldsymbol{\omega}_{ib}^{b} = \boldsymbol{R}_o^b\boldsymbol{\omega}_{io}^{o} + \boldsymbol{\omega}_{ob}^{b}$, $\boldsymbol{\omega}_{io}^{o} = [\ 0 \quad \omega_0 \quad 0\ ]$ and $\tau^b = \tau_{tau} + \tau_g$.

This is a standard rigid body model, assuming simple jet actuators in the torque dynamics. Another important assumption is that $\boldsymbol{\omega}^b \in \mathcal{L}_\infty$, i.e. that the angular velocity never approaches infinity. This is a sound decision from a physical point of view, and will be seen to simplify the mathematics. To simplify notation, $\boldsymbol{R}_o^b$ and $\boldsymbol{J}^b$ will in the following be written without sub- and superscripts when the meaning is clear.

3.4 Environment model

Forces affecting the motion of the satellite include atmospheric drag, sun radiation and gravity. The two former are assumed neglectable, along with the gravitational pull of the Earth. Newton's law of gravitation, see Equation 3.10, describes the gravitational force between two masses M and m separated by the distance r. G is the universal gravitational constant, and taking M as the mass of the Moon and m as that of the satellite, $GM = \mu_m$ where μ_m is the magnitude of gravitation on the Moon.

$$\boldsymbol{F} = \mu_m\frac{m}{r^2}\boldsymbol{r} \quad (3.10)$$

Equation 3.10 gives the gravitational force in vector format. Kyrkjebø (2000) shows how the force $\boldsymbol{F}$ can be reformulated as a torque around the z-axis of an orbiting satellite, where $\boldsymbol{I}^b$ is the inertia matrix of the satellite:

$$\begin{aligned} \boldsymbol{c}_3 &= \boldsymbol{R}_o^b\begin{bmatrix} 0 & 0 & 1 \end{bmatrix}^T \\ \boldsymbol{\tau}_g &= \boldsymbol{S}(3{\omega_0}^2\boldsymbol{c}^3)\boldsymbol{I}^b\boldsymbol{c}^3. \end{aligned}$$

3.5 System properties

Most processes can be formulated as Figure 3.1, where *r* is the reference, *u* is the actuating input and *y* the output. The plant consists of one or more processes, and

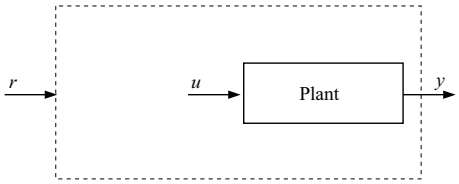

Figure 3.1: Overview of a control system. r, u and y represent reference, actuating input and system output respectively.

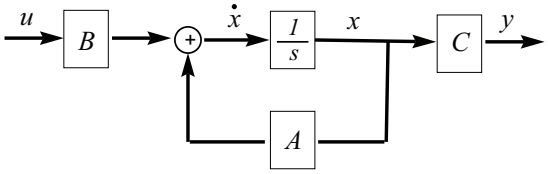

Figure 3.2: Basic linear system. s is the Laplace operator.

the translation from *r* to *u* is usually done by some kind of controller. If this translation is only dependant on *u*, the controller is so-called "open loop". Normally, performance will then be dissatisfactory, because of changes in plant parameters or signal noise that are not accounted for. It is more useful to let the actuating input also rely on the plant output in a feedback control loop. Correctly designed, this will enhance performance by decreasing the effect of parameter variations and suppressing noise and disturbances.

Most real-life processes have nonlinear characteristics. Any linear description will only be an approximation. Process characteristics may also vary with time. Since this complicates equations and notation, only time-invariant systems are presented here. With ordinary differential equations, plants may be modelled linearly as shown in Equation 3.11 and Figure 3.2.

$$\begin{aligned} \dot{\boldsymbol{x}}(t) &= \boldsymbol{A}\boldsymbol{x}(t) + \boldsymbol{B}\boldsymbol{u}(t) \\ \boldsymbol{y}(t) &= \boldsymbol{C}\boldsymbol{x}(t) + \boldsymbol{D}\boldsymbol{u}(t) \end{aligned} \tag{3.11}$$

Plants may be modelled nonlinearly as

$$\Sigma : \begin{array}{l} \dot{\boldsymbol{x}}(t) = f(\boldsymbol{x}(t), \boldsymbol{u}(t)) \\ \boldsymbol{y}(t) = h(\boldsymbol{x}(t)) \end{array} \tag{3.12}$$

where $\boldsymbol{x}(t) \in \mathcal{R}^m, \boldsymbol{u}(t) \in \mathcal{R}^n, \boldsymbol{y}(t) \in \mathcal{R}^p$ and f and h are continuous functions.

State observers is a commonly used tool in control engineering. When designing a control law for the system 3.12, the natural choice is $\boldsymbol{u}(t) = -f(\boldsymbol{x}(t), t)$. This assumes that the entire state vector can be measured and used directly in a feedback connection. In most complex systems, this is not the case. States can be impossible or impractical to measure, or the measurements may suffer from severe

noise pollution. This leaves the control designer with the possibility to predict, or estimate, the unknown states. The observer is a model of the system which on basis of inputs and outputs of the total system estimates the missing states so that the system can be controlled from these. An obvious demand to the system is then that it must be possible to reconstruct its states based on the input and output. A system satisfying this demand is said to observable. The dual of the observability property is the ability to steer the state variables by varying the input. This is called controllability, and may be more intuitively understandable.

3.5.1 Controllability

Linear systems

The controllability property of a linear system indicates whether the states of the state-space equations can be controlled from the input. Chen (1999) gives the definition:

Definition 3.1 *The state equation 3.11 or the pair ($\boldsymbol{A}$, $\boldsymbol{B}$) is said to be controllable if for any initial state $\boldsymbol{x}(0) = \boldsymbol{x}_0$ and any final state $\boldsymbol{x}_1$, there exists an input that transfers $\boldsymbol{x}_0$ to $\boldsymbol{x}_1$ in a finite time. Otherwise 3.11 or ($\boldsymbol{A}$, $\boldsymbol{B}$) is said to be uncontrollable.*

The definition requires that an input should be capable of moving any state to any other state in finite time. For practical purposes, a system might even then be uncontrollable since the definition sets no restraints on the input or the state trajectories from state $\boldsymbol{x}$ to state $\boldsymbol{x'}$, and a physical system will often have such restraints.

Nonlinear systems

Controllability may be defined in essentially the same way as with linear systems (Gershwin & Jacobson 1971). A system such as 3.12 is controllable from $(\boldsymbol{x}_0, t_0)$ to $(0, t_f)$ if, for some control $\boldsymbol{u}(t)$, $t_0 \leq t \leq t_f$, the solution of 3.12 with $\boldsymbol{x}(t_0) = \boldsymbol{x}_0$ is such that $\boldsymbol{x}(t_f) = 0$, where t_f is a preassigned terminal time. t_f ensures that $\boldsymbol{x}(t)$ goes to zero in finite time.

3.5.2 Observability

Where controllability is the concept of steering a state from input, observability is about estimating a state from the output.

Linear systems

Fulfilling the requirements of the observability property guarantees the possibility to design an observer for a linear system. Chen (1999) defines observability as:

Definition 3.2 *The state equation 3.11 is said to be observable if for any unknown initial state $\boldsymbol{x}(0)$, there exists a finite $T > 0$ such that the knowledge of the input $\boldsymbol{u}$ and the output $\boldsymbol{y}$ over $[0, T]$ suffices to determine uniquely the initial state $\boldsymbol{x}(0)$. Otherwise, the equation is said to be unobservable.*

Given the linear time-invariant (LTI) system 3.11, where $\boldsymbol{A}, \boldsymbol{B}$ and $\boldsymbol{C}$ are known, its solution is given by:

$$\boldsymbol{y}(t) = \boldsymbol{C}e^{\boldsymbol{A}t}\boldsymbol{x}(0) + \boldsymbol{C}\int_0^T e^{\boldsymbol{A}(T-t)}\boldsymbol{B}\boldsymbol{u}(t)dt + \boldsymbol{D}\boldsymbol{u}(t), \tag{3.13}$$

where the state $\boldsymbol{x}(0)$ is the only unknown. In order to find a unique solution to Equation 3.13, the system 3.11 must be observable.

Nonlinear systems

For nonlinear systems, the observability property does no longer guarantee the possibility to design an observer. This is because the property is dependant on the actuator input, and one would expect that for nonlinear systems, observer gains would have to vary with the input. Observability for nonlinear systems is explained in Nijmeijer & Fossen (1999), a short summary is given here.

A pair of internal states (x_0, x_0') is said to be *indistinguishable* by u if $\forall t \geq 0$, $g(\mathcal{X}_u(t, x_0)) \equiv g(\mathcal{X}_u(t, x_0'))$. This must be true for all u. Thus, a system such as 3.12 can be said to be observable if it has no indistinguishable state pairs. However, the indistinguishability and observability property does not exclude the possible existence of inputs which makes some states indistinguishable: Since the system may respond differently for different inputs (f is a function of both x and u), the possibility arises that the output y may be the same for different internal states. Given this, the inputs must be considered when designing an observer. It is possible to distinguish between universal and singular inputs. Universal inputs are defined as inputs that does not give any indistinguishable pairs of system states, while all non-universal inputs are called singular.

- If a system has no singular inputs, it *may* be possible to design an observer irrespective of the input. Otherwise it will only be possible to design one that is dependant on the input.
- If a system has singular inputs, an observer will in general have to depend on the input.

Chapter 4

Observer

If system 3.11 is observable, an open-loop estimator can be realised as a model of the plant, as in Figure 4.1. In practice a feedback from the original system is necessary, since the initial $\boldsymbol{x}(t_0)$ may be unknown, and the the two systems will initially give different output values. Also, if the model is not accurate the states $\boldsymbol{x}(t)$ and $\hat{\boldsymbol{x}}(t)$ will drift apart over time. The (t) parameter will often be omitted to simplify notation.

The following is a quick overview on different types of observers. The linear Luenberger observer was the first of its kind, and the theory behind it is an excellent introduction to observer design.

Salcudean (1990) presented what has become the foundation of rigid body observers. Vik (2000) presented an observer based on the rigid body approach, to be used for GPS/INS integration in marine applications. The complementary qualities of the GPS and INS is emphasized, where the GPS has slow update rate but high accuracy, while the INS has fast update rate and lower accuracy. Some parallels can be drawn to a star tracker and sun sensor configuration, where the sun sensor may have sample rates ten times that of the star tracker. This observer has become

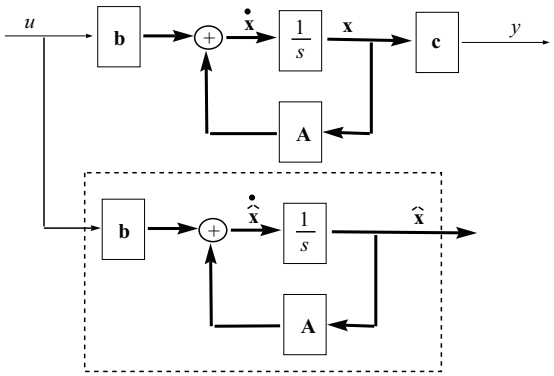

Figure 4.1: Open-loop estimator. $\hat{\boldsymbol{x}}$ is the estimated state

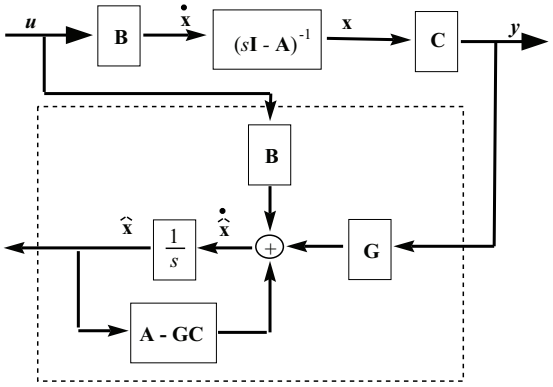

Figure 4.2: Structure of the closed-loop estimator. The state estimate is fed back to a controller.

a text-book example of observers for attitude determination, and is well-suited to be extended with a velocity determination part. It has been subject of further research by Thienel & Sanner (2001), where it was shown that the observer can be made robust to constant bias errors.

The observer of Vik was presented in the pre-project as the recommended observer for the ESMO ADCS. A succesful implementation would demonstrate the versatility of the observer, and be a step towards finding a general structure applicable to other areas of control theory.

4.1 Luenberger observer

The first observer was introduced by Luenberger (1966). There it was shown how an observer could be designed for linear systems based on knowledge of the original system. If the observability property of Definition 3.2 is satisfied, the observer dynamics can be chosen arbitrarily. Convergence to the system states is ensured by choosing the observer poles faster than the system poles. Observer performance is dependant on the accuracy of the model. The Luenberger observer for the system 3.11 can be written as:

$$\dot{\hat{\boldsymbol{x}}} = \boldsymbol{A}\hat{\boldsymbol{x}} + \boldsymbol{B}\boldsymbol{u} + \boldsymbol{G}(\boldsymbol{y} - \boldsymbol{C}\boldsymbol{x})\dot{\hat{\boldsymbol{x}}} = (\boldsymbol{A} - \boldsymbol{G}\boldsymbol{C})\hat{\boldsymbol{x}} + \boldsymbol{B}\boldsymbol{u} + \boldsymbol{G}\boldsymbol{y}, \tag{4.1}$$

where $\boldsymbol{G}$ represents the input structure of the observer, as shown in Figure 4.2. The error dynamics of Equation 4.1 are shown in Equation 4.2, where the convergence is ensured by choosing the poles of $\boldsymbol{A}$-$\boldsymbol{G}\boldsymbol{C}$.

$$\begin{aligned} \boldsymbol{e} =& \boldsymbol{x} - \hat{\boldsymbol{x}} \\ \dot{\boldsymbol{e}} =& (\boldsymbol{A} - \boldsymbol{G}\boldsymbol{C})\boldsymbol{e} \end{aligned} \tag{4.2}$$

4.2 Rigid body observer

Salcudean (1990) presented an observer structure designed for rigid body control. Primarily meant to be used with manipulation of magnetically levitated robot wrists, it has excellent properties for use with a larger group of rigid bodies. It is based on a rigid body dynamic and kinematic model formulated with quaternions, as presented in Equation 2.13. To understand the way of thinking, consider an example where the velocity v of a unit mass is to be estimated from the measured position $\boldsymbol{x}$ and the applied force $\boldsymbol{F}$. An observer can be made as shown in Equation 4.3, where k_f and k_v are positive damping constants. The observer can be thought of as a system that is influenced by the same force $\boldsymbol{F}$ as the actual system, in addition to a correction force in the direction of the position error.

$$\hat{\boldsymbol{v}} = \boldsymbol{f} + k_f(\boldsymbol{x} - \hat{\boldsymbol{x}}); \qquad \hat{\boldsymbol{x}} = \hat{\boldsymbol{v}} + k_v(\boldsymbol{x} - \hat{\boldsymbol{x}}) \tag{4.3}$$

$$\dot{\tilde{\boldsymbol{v}}} = -k_f(\tilde{\boldsymbol{x}}) \qquad \dot{\tilde{\boldsymbol{x}}} = \tilde{\boldsymbol{v}} - k_v(\tilde{\boldsymbol{x}}); \tag{4.4}$$

Error dynamics are made by taking $\tilde{\boldsymbol{x}} = \boldsymbol{x} - \hat{\boldsymbol{x}}$ and $\tilde{\boldsymbol{v}} = \boldsymbol{v} - \hat{\boldsymbol{v}}$, as in Equation 4.4, which implies that the observed velocity will converge to the actual velocity with convergence rates dictated by the damping constants.

The same approach can be taken for the rotational motion of a rigid body. Rotation matrices $\boldsymbol{R}_b^a$ and $\boldsymbol{R}_{\hat{b}}^a$ are used to denote the position of the actual system and the observer model. The position error becomes $\boldsymbol{R}_b^a \boldsymbol{R}_{\hat{b}}^{a^T} = \boldsymbol{R}_{\tilde{b}}^b$. These matrices may be computed as in Equation 2.10, using $\boldsymbol{q}$ and $\hat{\boldsymbol{q}}$. Formulated as in Equation 4.3, with inertia matrix $\boldsymbol{J}$, angular velocity $\boldsymbol{\omega}$ and torque $\boldsymbol{\tau}$, the observer dynamics are given by Equation 4.5. $\tilde{\boldsymbol{\epsilon}}$ and $\tilde{\eta}$ are the components of the quaternion $\tilde{\boldsymbol{q}}$ describing the rotation error.

$$\begin{aligned} \boldsymbol{J}\dot{\hat{\boldsymbol{\omega}}} &= \boldsymbol{\tau} + \frac{1}{2} k_f \boldsymbol{J}^{-1} \tilde{\boldsymbol{\epsilon}} \operatorname{sgn}(\tilde{\eta}) \\ \dot{\boldsymbol{R}}_{\hat{b}}^a &= [\boldsymbol{R}_{\hat{b}}^b (\boldsymbol{\omega} + k_v \boldsymbol{J}^{-1} \tilde{\boldsymbol{\epsilon}} \operatorname{sgn}(\tilde{\eta}))] \boldsymbol{R}_{\hat{b}}^a \end{aligned} \tag{4.5}$$

Deriving the error dynamics is a lengthy exercise, but they are similar to the error dynamics for the observer of Vik in the following section.

4.3 Vik observer

The Vik observer was presented in Vik (2000). It is based on the work of Salcudean (1990), concerning an observer for rigid body robot manipulator control. Its main properties will later be used in stability analysis of the total system, however in a simplified manner when it comes to the error models. The observer in its pure form is therefore analysed here.

$$
\begin{aligned}
\dot{\hat{\boldsymbol{q}}} =& \boldsymbol{T}_{\hat{q}}(\hat{\boldsymbol{q}})\tilde{\boldsymbol{R}}\left[(I+\hat{\boldsymbol{\Delta}})\boldsymbol{\omega}_{imu}+\hat{\boldsymbol{b}}+\boldsymbol{K}_1\tilde{\boldsymbol{\epsilon}}\,\mathrm{sgn}(\tilde{\eta})\right] \\
\dot{\hat{\boldsymbol{b}}} =& -\boldsymbol{T}_1^{-1}\hat{\boldsymbol{b}}+\frac{1}{2}\boldsymbol{K}_2\tilde{\boldsymbol{\epsilon}}\,\mathrm{sgn}(\tilde{\eta}) \\
\dot{\hat{s}} =& -\boldsymbol{T}_2^{-1}\hat{\boldsymbol{s}}+\frac{1}{2}\boldsymbol{K}_3\,\mathrm{diag}(\tilde{\boldsymbol{\epsilon}})\boldsymbol{\omega}_{imu}\,\mathrm{sgn}(\tilde{\eta}) \\
\dot{\hat{\phi}} =& -\boldsymbol{T}_3^{-1}\hat{\boldsymbol{\phi}}+\frac{1}{2}\boldsymbol{K}_4\Gamma(\tilde{\boldsymbol{\epsilon}})\boldsymbol{\omega}_{imu}\,\mathrm{sgn}(\tilde{\eta})
\end{aligned}
\tag{4.6}
$$

where $\boldsymbol{s} = [\ s_x \quad s_y \quad s_z\ ]$ and

$$
\boldsymbol{\phi} = \begin{bmatrix} \phi_{xy} \\ \phi_{xz} \\ \phi_{yx} \\ \phi_{yz} \\ \phi_{zx} \\ \phi_{zy} \end{bmatrix} \quad \boldsymbol{\Gamma}(\tilde{\boldsymbol{\epsilon}}) = \begin{bmatrix} 0 & \tilde{\epsilon}_1 & 0 \\ 0 & 0 & \tilde{\epsilon}_1 \\ \tilde{\epsilon}_2 & 0 & 0 \\ 0 & 0 & \tilde{\epsilon}_2 \\ \tilde{\epsilon}_3 & 0 & 0 \\ 0 & \tilde{\epsilon}_3 & 0 \end{bmatrix} \quad \tilde{\boldsymbol{\Delta}} = \begin{bmatrix} s_x & \phi_{xy} & \phi_{xz} \\ \phi_{yx} & s_y & \phi_{yz} \\ \phi_{zx} & \phi_{zy} & s_z \end{bmatrix}
$$

4.3.1 Stability analysis

Lyapunov's direct method is used to establish global exponential stability. Taking the observer error dynamics as the difference between $\boldsymbol{q}$ and $\hat{\boldsymbol{q}}$, the error dynamics become

$$
\begin{aligned}
\dot{\tilde{\boldsymbol{q}}} =& \boldsymbol{T}_{\tilde{q}}(\tilde{\boldsymbol{q}})\left[(\tilde{\boldsymbol{\Delta}})\boldsymbol{\omega}_{imu}+\tilde{\boldsymbol{b}}+\boldsymbol{K}_1\tilde{\boldsymbol{\epsilon}}\,\mathrm{sgn}(\tilde{\eta})\right] \\
\dot{\tilde{\boldsymbol{b}}} =& -\boldsymbol{T}_1^{-1}\tilde{\boldsymbol{b}}-\frac{1}{2}\boldsymbol{K}_2\tilde{\boldsymbol{\epsilon}}\,\mathrm{sgn}(\tilde{\eta}) \\
\dot{\tilde{\boldsymbol{s}}} =& -\boldsymbol{T}_2^{-1}\tilde{\boldsymbol{s}}-\frac{1}{2}\boldsymbol{K}_3\,\mathrm{diag}(\tilde{\boldsymbol{\epsilon}})\boldsymbol{\omega}_{imu}\,\mathrm{sgn}(\tilde{\eta}) \\
\dot{\tilde{\boldsymbol{\phi}}} =& -\boldsymbol{T}_3^{-1}\tilde{\boldsymbol{\phi}}-\frac{1}{2}\boldsymbol{K}_4\Gamma(\tilde{\boldsymbol{\epsilon}})\boldsymbol{\omega}_{imu}\,\mathrm{sgn}(\tilde{\eta}).
\end{aligned}
\tag{4.7}
$$

The following Lyapunov function is proposed for the error dynamics:

$$
\boldsymbol{V} = \frac{1}{2}\tilde{\boldsymbol{b}}^T\boldsymbol{K}_2^{-1}\tilde{\boldsymbol{b}}+\frac{1}{2}\tilde{\boldsymbol{s}}^T\boldsymbol{K}_3^{-1}\tilde{\boldsymbol{s}}+\frac{1}{2}\tilde{\boldsymbol{\phi}}^T\boldsymbol{K}_4^{-1}\tilde{\boldsymbol{\phi}}+\begin{pmatrix} (\tilde{\eta}-1)^2+\tilde{\boldsymbol{\epsilon}}^T\tilde{\boldsymbol{\epsilon}}\,\text{if}\,\tilde{\eta}\geq 0 \\ (\tilde{\eta}+1)^2+\tilde{\boldsymbol{\epsilon}}^T\tilde{\boldsymbol{\epsilon}}\,\text{if}\,\tilde{\eta}<0 \end{pmatrix}
$$

The derivative of $\boldsymbol{V}$ is given by

$$
\dot{\boldsymbol{V}} = \tilde{\boldsymbol{b}}^T\boldsymbol{K}_2^{-1}\dot{\tilde{\boldsymbol{b}}}+\tilde{\boldsymbol{s}}^T\boldsymbol{K}_3^{-1}\dot{\tilde{\boldsymbol{s}}}+\tilde{\boldsymbol{\phi}}^T\boldsymbol{K}_4^{-1}\dot{\tilde{\boldsymbol{\phi}}}+\begin{pmatrix} 2(\tilde{\eta}-1)\dot{\tilde{\eta}}+2\tilde{\boldsymbol{\epsilon}}^T\dot{\tilde{\boldsymbol{\epsilon}}}\,\text{if}\,\tilde{\eta}\geq 0 \\ 2(\tilde{\eta}+1)\dot{\tilde{\eta}}+2\tilde{\boldsymbol{\epsilon}}^T\dot{\tilde{\boldsymbol{\epsilon}}}\,\text{if}\,\tilde{\eta}<0 \end{pmatrix}
$$

Inserting for $\dot{\tilde{\eta}}$, $\dot{\tilde{\boldsymbol{\epsilon}}}$, $\dot{\tilde{\boldsymbol{b}}}$, $\dot{\tilde{\boldsymbol{s}}}$ and $\dot{\tilde{\boldsymbol{\phi}}}$ now gives the whole expression. Cancellation of terms, use of Equation 2.3 and that

$$
\tilde{\boldsymbol{\epsilon}}^T\tilde{\Delta}\boldsymbol{\omega}_{IMU} = (\tilde{\boldsymbol{s}}^T\,\mathrm{diag}\,\tilde{\boldsymbol{\epsilon}}+\tilde{\boldsymbol{\phi}}^T\Gamma(\tilde{\boldsymbol{\epsilon}})),
$$

Error	Origin
$\boldsymbol{\omega}_{gyro}$	The true angular velocity
$\boldsymbol{\Delta\omega}_{gyro}$	3-by-3 matrix with coupling errors from misalignment angles and regular scale factor errors along the diagonal
$\boldsymbol{b}$	Bias term representing mechanical drifts after long-term operation or constant disturbances like solar wind
$\boldsymbol{w}_n$	Bounded unmodeled errors and measurement noise

Table 4.1: Gyro errors

ultimately yields

$$\dot{\boldsymbol{V}} = \tilde{\boldsymbol{b}}^T \boldsymbol{K}_2^{-1}\boldsymbol{T}_1^{-1}\tilde{\boldsymbol{b}} - \tilde{\boldsymbol{s}}^T \boldsymbol{K}_3^{-1}\boldsymbol{T}_2^{-1}\tilde{\boldsymbol{s}} + \tilde{\boldsymbol{\phi}}^T \boldsymbol{K}_4^{-1}\boldsymbol{T}_3^{-1}\tilde{\boldsymbol{\phi}} - \tilde{\boldsymbol{\epsilon}}^T K_1 \tilde{\boldsymbol{\epsilon}} \leq 0.$$

Due to boundedness of the unit quaternion, $\dot{V}$ will be zero for $\tilde{\boldsymbol{\epsilon}} = [\ 1 \quad 1 \quad 1\ ]$ and strictly negative else. Theorem 2.3 could now indicate that the observer is globally exponentially stable, but it is worth to remark here that the global property is mathematically incorrect due to the multiple equilibria $\eta = \pm 1$. These do however correspond to the same physical attitude, and Salcudean (1990) uses the term *globally convergent*. It can thus be said that the observer error dynamics are globally exponentially stable from a practical point of view.

4.3.2 Simplified observer

The observer used for analysis in this project is based on the work of Salcudean (1990). It has later been extended with sensor error models by Vik (2000). The sensor errors are in the following modelled in a simpler fashion, however equivalent as far as stability analysis is concerned. Tuning of the observer gains is the only affected area, as the different types of errors in the angular velocities are lumped together in a single subsystem $\boldsymbol{\Delta}$. The original observer of Vik used two separate subsystems $\boldsymbol{s}$ and $\boldsymbol{\phi}$.

Angular velocities are usually measured with gyros, which are prone to different types of errors and noise. This observer assumes that the angular velocity measurement can be decomposed as $\boldsymbol{\omega}_{msr} = [\boldsymbol{I} - \boldsymbol{\Delta}]\,\boldsymbol{\omega}_{gyro} - \boldsymbol{b} - \boldsymbol{w}_n$. (See Table 4.1 and Vik (2000)). $\boldsymbol{\omega}_{gyro}$ will in the following be written simply as $\boldsymbol{\omega}$. The errors in $\boldsymbol{\Delta}$ are small, so an approximation can be made:

$$\begin{aligned}\boldsymbol{\omega} &= (\boldsymbol{I} - \boldsymbol{\Delta})^{-1}(\boldsymbol{\omega}_{msr} + \boldsymbol{b} + \boldsymbol{w}_n) \\ &\approx (\boldsymbol{I} + \boldsymbol{\Delta})(\boldsymbol{\omega}_{msr} + \boldsymbol{b} + \boldsymbol{w}_n) \\ &\approx \boldsymbol{\omega} = (\boldsymbol{I} + \boldsymbol{\Delta})\boldsymbol{\omega}_{msr} + \boldsymbol{b} + \boldsymbol{w}_n.\end{aligned}$$

The estimated velocity thus becomes $\hat{\boldsymbol{\omega}} = (\boldsymbol{I} + \hat{\boldsymbol{\Delta}})\boldsymbol{\omega}_{msr} + \hat{\boldsymbol{b}} + \boldsymbol{K}_1\tilde{\boldsymbol{\epsilon}}\,\mathrm{sgn}\,\tilde{\eta}$.

Based on the satellite dynamics, the new observer is proposed as:

$$\begin{aligned}
\dot{\hat{\boldsymbol{q}}} =& \boldsymbol{T}(\hat{\boldsymbol{q}})\tilde{\boldsymbol{R}}\left[(\boldsymbol{I}+\hat{\boldsymbol{\Delta}})\boldsymbol{\omega}_{msr}+\hat{\boldsymbol{b}}+\boldsymbol{K}_1\tilde{\boldsymbol{\epsilon}}\,\mathrm{sgn}(\tilde{\eta})\right]\\
\dot{\hat{\boldsymbol{b}}} =& -\boldsymbol{T}_1^{-1}\hat{\boldsymbol{b}}+\frac{1}{2}\boldsymbol{K}_2\tilde{\boldsymbol{\epsilon}}\,\mathrm{sgn}(\tilde{\eta})\\
\dot{\hat{\Delta}} =& -\boldsymbol{T}_2^{-1}\hat{\boldsymbol{\Delta}}+\frac{1}{2}\boldsymbol{K}_3\,\mathrm{diag}(\tilde{\boldsymbol{\epsilon}})\boldsymbol{\omega}_{msr}\,\mathrm{sgn}(\tilde{\eta})
\end{aligned}$$

Observer error dynamics

The attitude error in the observer is defined as $\tilde{\boldsymbol{q}} = \boldsymbol{q}\otimes\hat{\boldsymbol{q}}^{-1}$. Bias and angular velocity errors are defined as $\tilde{\boldsymbol{b}} = \boldsymbol{b}-\hat{\boldsymbol{b}}$ and $\tilde{\boldsymbol{\omega}} = \boldsymbol{\omega}-\hat{\boldsymbol{\omega}}$. The observer error dynamics are then:

$$\begin{aligned}
\dot{\tilde{\boldsymbol{q}}} =& \boldsymbol{T}(\tilde{\boldsymbol{q}})\left[(\tilde{\Delta}\omega+\tilde{\boldsymbol{b}}-\boldsymbol{K}_1\tilde{\boldsymbol{\epsilon}}\,\mathrm{sgn}(\tilde{\eta})\right]\\
\dot{\tilde{\boldsymbol{b}}} =& -\boldsymbol{T}_1^{-1}\tilde{\boldsymbol{b}}-\frac{1}{2}\boldsymbol{K}_2\tilde{\boldsymbol{\epsilon}}\,\mathrm{sgn}(\tilde{\eta})\\
\dot{\tilde{\Delta}} =& -\boldsymbol{T}_2^{-1}\tilde{\boldsymbol{\Delta}}-\frac{1}{2}\boldsymbol{K}_3\boldsymbol{\omega}\tilde{\boldsymbol{\epsilon}}^T\,\mathrm{sgn}(\tilde{\eta})
\end{aligned}\tag{4.8}$$

Stability analysis of the error dynamics is done by choosing the Lyapunov function

$$\begin{aligned}
V_o &= \frac{1}{2}\tilde{\boldsymbol{b}}^T\boldsymbol{K}_2^{-1}\tilde{\boldsymbol{b}}+\frac{1}{2}\tilde{\boldsymbol{\Delta}}^T\boldsymbol{K}_3^{-1}\tilde{\boldsymbol{\Delta}}+\begin{pmatrix}(\tilde{\eta}-1)^2+\tilde{\boldsymbol{\epsilon}}^T\tilde{\boldsymbol{\epsilon}}\,\text{if}\,\tilde{\eta}\geq 0\\(\tilde{\eta}+1)^2+\tilde{\boldsymbol{\epsilon}}^T\tilde{\boldsymbol{\epsilon}}\,\text{if}\,\tilde{\eta}<0\end{pmatrix}\\
\dot{V}_o &= \tilde{\boldsymbol{b}}^T\boldsymbol{K}_2^{-1}\dot{\tilde{\boldsymbol{b}}}+\tilde{\boldsymbol{\Delta}}^T\boldsymbol{K}_3^{-1}\dot{\tilde{\boldsymbol{\Delta}}}+\begin{pmatrix}2(\tilde{\eta}-1)\dot{\tilde{\eta}}+2\tilde{\boldsymbol{\epsilon}}^T\dot{\tilde{\boldsymbol{\epsilon}}}\,\text{if}\,\tilde{\eta}\geq 0\\2(\tilde{\eta}+1)\dot{\tilde{\eta}}+2\tilde{\boldsymbol{\epsilon}}^T\dot{\tilde{\boldsymbol{\epsilon}}}\,\text{if}\,\tilde{\eta}<0\end{pmatrix}
\end{aligned}$$

Expressions for $\dot{\tilde{\eta}}$, $\dot{\tilde{\boldsymbol{\epsilon}}}$, $\dot{\tilde{\boldsymbol{b}}}$ and $\dot{\tilde{\boldsymbol{\Delta}}}$ from Equations 4.8 are now inserted, and cancellation of terms and use of 2.3 ultimately yields

$$\dot{V}_o = -\tilde{\boldsymbol{b}}^T\boldsymbol{K}_2^{-1}\boldsymbol{T}_1^{-1}\tilde{\boldsymbol{b}}-\tilde{\boldsymbol{\Delta}}^T\boldsymbol{K}_3^{-1}\boldsymbol{T}_2^{-1}\tilde{\boldsymbol{\Delta}}-\tilde{\boldsymbol{\epsilon}}^T K_1\tilde{\boldsymbol{\epsilon}}.$$

$\dot{\boldsymbol{V}}_o$ is not in itself strictly negative, but if the unit quaternion property $\eta^2+\boldsymbol{\epsilon}^T\boldsymbol{\epsilon}=1$ is considered, $\dot{\boldsymbol{V}}_o$ will be zero for $\tilde{\boldsymbol{\epsilon}} = [\ 1\quad 1\quad 1\ ]$ and strictly negative else. As with the original observer in Equation 4.6, it can only be said that the observer error dynamics are GES from a practical point of view due to the multiple equlibria $\eta = \pm 1$.

Chapter 5

Controllers

Common for all attitude controllers in this chapter is that they are nonlinear, and that they use quaternion feedback as opposed to Euler angles. The term $\boldsymbol{\omega}_{io}^{o}$ in Equation 3.9, which describes the velocity of the orbit frame with respect to the inertial frame, introduces a slight dilemma for the control strategy. In situations where it is desireable to compensate for this motion, a nominal term should be included in the controller to translate the equilibrium point of the closed-loop system. The result will be that the orbit frame will not rotate around itself as its origin translates around the origin of the moon-centered frame. This compensation is done in all control laws herein.

All controllers describe the velocity error as $\tilde{\boldsymbol{\omega}} = \boldsymbol{\omega}^b - \boldsymbol{\omega}_d$ and the attitude error with the parameters of the error rotation matrix $\tilde{\boldsymbol{R}} = \boldsymbol{R}_d \boldsymbol{R}^b$, namely $\tilde{\eta}$ and $\tilde{\boldsymbol{\epsilon}}$. $\tilde{\boldsymbol{R}} = \boldsymbol{I}$ corresponds to $\tilde{\eta} = \pm 1$ and $\tilde{\boldsymbol{\epsilon}} = \boldsymbol{0}$. From Equation 2.8, $\tilde{\eta}$ and $\tilde{\boldsymbol{\epsilon}}$ are bounded inside the unit ball, and from Equation 2.13 it is clear that $\dot{\tilde{\eta}}$ and $\dot{\tilde{\boldsymbol{\epsilon}}}$ are bounded whenever $\tilde{\boldsymbol{\omega}}$ is bounded.

It seems most controllers developed for spacecraft try to linearize the system by neutralizing the nonlinear dynamics, see e.g. Byrnes & Isidori (1991), Wen & Kreutz-Delgado (1991) or Lam & Morgan (1992). This can be done either with basis in the model equation of motion or, more advanced, by including an adaptive term that takes into account model uncertainties. Some model-independent robust controllers also exist. One adaptive controller and one robust controller are presented in this chapter. Aside from the differences in design, it is worth to note the differences in how the problem of multiple equlibrium points are treated in the stability analyses. The adaptive controller makes use of a Lyapunov function candidate $V(\cdot, \boldsymbol{\epsilon})$ and uses the unit quaternion property in Equation 2.9 to include η in the analysis. The robust controller shifts the equilibriums $\eta = \pm 1$ to $\eta = 0$ and $\eta = -2$ and shows that one equilibrium is attractive and the other is repelling.

Finally, a PD-controller is presented. While perhaps inferior in control performance, a PD control algorithm may be easier to understand and maintain, thus being more cost effective.

5.1 Adaptive controller

Egeland & Godhavn (1994) propose an adaptive controller. First, the angular velocity error term $\tilde{\boldsymbol{\omega}} = \boldsymbol{\omega} - \boldsymbol{\omega}_d$ and the tracking error $\boldsymbol{e}(t) \in \mathcal{R}^3$ are defined. $\boldsymbol{\omega}_d$ and $\dot{\boldsymbol{\omega}}_d$ are assumed bounded, along with $\boldsymbol{\omega}$. $\boldsymbol{e}(t)$ is a parameterization of $\tilde{\boldsymbol{R}}(t)$, hence $\dot{\boldsymbol{e}}$ is bounded whenever $\tilde{\boldsymbol{\omega}}$ is bounded. The equation describing the system is

$$\boldsymbol{M}\dot{\boldsymbol{s}} + N(\boldsymbol{R}, \boldsymbol{\omega})\boldsymbol{s} + \boldsymbol{K}_D\boldsymbol{s} = \boldsymbol{\nu} \tag{5.1}$$

Here, $N(\cdot)$ is the same as in Equation 3.3, $\boldsymbol{K}_d$ is a positive definite gain matrix and $\boldsymbol{s}$ is given by

$$\boldsymbol{s} = \tilde{\boldsymbol{\omega}} + \kappa\boldsymbol{e}, \qquad \kappa > 0. \tag{5.2}$$

It is necessary to show that Equation 5.2 converges. In that case, the error manifold $\boldsymbol{s}$ has the property $\boldsymbol{s} \to 0$ as $t \to \infty$. This can be shown with Barbalat's lemma 2.1, if it can be established that $\boldsymbol{s} \in \mathcal{L}_2$ and $\boldsymbol{s}, \dot{\boldsymbol{s}} \in \mathcal{L}_\infty$.

If the mapping $-\boldsymbol{s} \to \boldsymbol{\nu}$ is passive, i.e.

$$\int_0^T -\boldsymbol{s}^T(t)\boldsymbol{\nu}(t)dt \geq -k_1, \tag{5.3}$$

then $\boldsymbol{s} \in \mathcal{L}_2$. Ortega & Spong (1988) propose the Lyapunov function

$$V = \frac{1}{2}\boldsymbol{s}^T\boldsymbol{M}\boldsymbol{s} + k_1 - \int_0^T -\boldsymbol{s}^T(t)\boldsymbol{\nu}(t)dt. \tag{5.4}$$

Originally intended for use with robot arm dynamics, Equation 5.4 can be applied to a satellite system as well. Note that V is positive definite because of Equation 5.3. Differentiating along the trajectories of Equation 5.1 gives

$$\dot{V} = \boldsymbol{s}^T\boldsymbol{M}\dot{\boldsymbol{s}} - \boldsymbol{s}^T\nu = -\boldsymbol{s}^T\boldsymbol{K}_D\boldsymbol{s} - \boldsymbol{s}^T N(\boldsymbol{R}, \boldsymbol{\omega})\boldsymbol{s}. \tag{5.5}$$

Hence $\dot{V} \leq 0$ for sufficiently large $\boldsymbol{K}_D$. Conclusively, $\boldsymbol{s} \in \mathcal{L}_2$. By Corollary 2.3, $\boldsymbol{s} \to 0$ as $t \to \infty$.

Two assumptions must now be made, namely that the mapping $\tilde{\boldsymbol{\omega}} \to \boldsymbol{e}$ is passive and that $\dot{\boldsymbol{e}} \in \mathcal{L}_2$ when $\tilde{\boldsymbol{\omega}} \in \mathcal{L}_2$. Both are sound assumptions based on the model dynamics of Equation 3.1. Egeland & Godhavn (1994) then show that

$$||\boldsymbol{s}||^2 = ||\tilde{\boldsymbol{\omega}} + \kappa\boldsymbol{e}||^2 = ||\tilde{\boldsymbol{\omega}}||^2 + \kappa^2||\boldsymbol{e}||^2 + 2\kappa < \boldsymbol{e}, \tilde{\boldsymbol{\omega}} > . \tag{5.6}$$

Since $\tilde{\boldsymbol{\omega}} \to \boldsymbol{e}$ is passive, a constant k_2 exists so that $||\tilde{\boldsymbol{\omega}}||^2 + \kappa^2||\boldsymbol{e}||^2 \leq ||\boldsymbol{s}||^2 - 2\kappa k_2$, and thus $\tilde{\boldsymbol{\omega}}, \boldsymbol{e} \in \mathcal{L}_2$. It follows from the properties of the unit quaternions and Equation 3.1 that $\dot{\boldsymbol{e}} \in \mathcal{L}_2$ and $\boldsymbol{e} \in \mathcal{L}_\infty$. By Corollary 2.3 $\boldsymbol{e}(t) \to 0$ as $t \to \infty$. From Equation 5.1, $\tilde{\boldsymbol{\omega}}, \boldsymbol{e} \in \mathcal{L}_\infty$ gives $\boldsymbol{s} \in \mathcal{L}_\infty$. Using $\boldsymbol{s}, \boldsymbol{\nu} \in \mathcal{L}_\infty$ in Equation 5.1 yields $\dot{\boldsymbol{s}} \in \mathcal{L}_\infty$. It has already been shown that $\boldsymbol{s} \in \mathcal{L}_2$, hence Corollary 2.3 can be employed to show convergence of Equation 5.2.

It is worth to remark that with the implementation of a linearizing term in Equation 5.1, Equation 5.5 will be strictly negative for all $\boldsymbol{K}_D > 0$. Egeland & Godhavn (1994) define the term $\boldsymbol{\omega}_r = \boldsymbol{\omega}_d - \kappa \boldsymbol{e}$, so that $\boldsymbol{s}$ can be written $\boldsymbol{s} = \boldsymbol{\omega} - \boldsymbol{\omega}_r$. The adaptive control term is then defined: Take $\boldsymbol{\theta}$ as the vector of unknown model parameters. $\tilde{\boldsymbol{\theta}} = \hat{\boldsymbol{\theta}} - \boldsymbol{\theta}$ expresses the parameter estimation error. A parameterization is proposed as

$$\boldsymbol{M}\dot{\boldsymbol{\omega}}_r + N(\boldsymbol{R}, \boldsymbol{\omega})\boldsymbol{\omega}_r = \boldsymbol{Y}(\boldsymbol{R}, \boldsymbol{\omega}, \boldsymbol{\omega}_r, \dot{\boldsymbol{\omega}})\boldsymbol{\theta}. \tag{5.7}$$

That $\boldsymbol{Y}$ is bounded follows from the definition of $\boldsymbol{\omega}_r$ and the earlier assumptions that $\boldsymbol{\omega}_d$ and $\dot{\boldsymbol{\omega}}$ are bounded. An adaptive controller is then formulated as

$$\begin{aligned} \boldsymbol{\tau} &= \boldsymbol{Y}\hat{\boldsymbol{\theta}} - \boldsymbol{K}_D \boldsymbol{s} \\ \dot{\hat{\boldsymbol{\theta}}} &= -\boldsymbol{\Gamma}^{-1}\boldsymbol{Y}^T \boldsymbol{s}, \end{aligned} \tag{5.8}$$

where Γ and $\boldsymbol{K}_D$ are constant, symmetric and positive definite matrices.

The $\boldsymbol{e}$ term in $\boldsymbol{s} = \tilde{\boldsymbol{\omega}} + \kappa \boldsymbol{e}$ can now be tweaked, as long as it is a function of the Euler parameters in $\tilde{\boldsymbol{R}}$. Egeland & Godhavn (1994) propose and analyse the two versions $\boldsymbol{s} = \tilde{\boldsymbol{\omega}} + \kappa\tilde{\boldsymbol{\epsilon}}$ and $\boldsymbol{s} = \tilde{\boldsymbol{\omega}} + \kappa\tilde{\eta}\tilde{\boldsymbol{\epsilon}}$. The former of the two controllers inspired the controller used in the total stability analysis in Chapter 7, therefore its stability analysis is presented in the following.

5.1.1 Stability analysis

The stability proof has the form of a theorem, which makes use of two lemmas. It is already established that $\tilde{\boldsymbol{\epsilon}}$ is bounded, and that $\dot{\tilde{\boldsymbol{\epsilon}}}$ is bounded when $\tilde{\boldsymbol{\omega}}$ is bounded. Since $\boldsymbol{K}_D$ is positive definite, there is a constant $k_D = \lambda_{min}(\boldsymbol{K}_D)$ that denotes the smallest eigenvalue of $\boldsymbol{K}_D$. The theorem and lemmas are not given here exactly as in Egeland & Godhavn (1994), some minor details are simplified.

Lemma 5.1 *The mapping $\tilde{\boldsymbol{\omega}} \rightarrow \tilde{\boldsymbol{\epsilon}}$ is passive, and*

$$< \tilde{\boldsymbol{\epsilon}}, \tilde{\boldsymbol{\omega}} >= 2[\tilde{\eta}(0) - \tilde{\eta}(T)] \qquad \forall T \geq 0$$

Lemma 5.2 *If $\tilde{\boldsymbol{\omega}} \in \mathcal{L}_2$, then $\dot{\tilde{\boldsymbol{\epsilon}}} \in \mathcal{L}_2$.*

Theorem 5.1 *Consider the system given by Equation 3.3 with the control law 5.8 and $\boldsymbol{s} = \tilde{\boldsymbol{\omega}} + \kappa\tilde{\boldsymbol{\epsilon}}$. Then $\lim_{t\to\infty} \tilde{\boldsymbol{\omega}}(t) = 0$ and $\lim_{t\to\infty} \tilde{\boldsymbol{\epsilon}}(t) = 0$, while $\tilde{\eta}(t) \rightarrow 1$ or $\tilde{\eta}(t) \rightarrow -1$ as $t \rightarrow \infty$. If*

$$\tilde{\eta}(0) > -1 + \frac{1}{8\kappa k_D}\left[\boldsymbol{s}(0)^T \boldsymbol{M}\boldsymbol{s}(0) + \tilde{\boldsymbol{\theta}}^T \Gamma \tilde{\boldsymbol{\theta}}(0)\right] + \delta_\epsilon \tag{5.9}$$

for some small constant $\delta_\epsilon > 0$, then $\tilde{\eta}(t) > -1 + \delta_\epsilon$ for all $t \geq 0$ and $\lim_{t\to\infty} \tilde{\eta}(t) = 1$. The mapping $\boldsymbol{s} \rightarrow \tilde{\boldsymbol{\epsilon}}$ with initial state $\tilde{\boldsymbol{\epsilon}} = 0$, $\tilde{\eta} = 1$ is $\mathcal{L}_2$ stable.

The theorem gives a stability proof and conditions for the system to converge to the equilibrium $\tilde{\eta} = 1$. Now the parameterization of Equation 5.7 can be subtracted from the system equation of motion, namely Equation 3.3. If then the control law in Equation 5.8 is inserted, the result is Equation 5.1 where $\boldsymbol{\nu} = Y\tilde{\boldsymbol{\theta}}$. The mapping $-\boldsymbol{s} \rightarrow \boldsymbol{\phi}$ has been shown to be passive. It follows from Theorem 5.1 and Lemmas 5.1 and 5.2 that $\lim_{t\to\infty} \tilde{\boldsymbol{\epsilon}}(t) = 0$. Hence, $\tilde{\eta}$ approaches 1 or -1. To show stability properties of the theorem, consider the Lyapunov function

$$V = \frac{1}{2}(\boldsymbol{s}^T \boldsymbol{M} \boldsymbol{s} + \tilde{\boldsymbol{\theta}}^T \boldsymbol{\Gamma} \tilde{\boldsymbol{\theta}}). \tag{5.10}$$

Following the procedure of Slotine & Li (1988), Chapter 2.2, the time derivative is

$$\dot{V} = -\boldsymbol{s}^T \boldsymbol{K}_D \boldsymbol{s} \leq 0 \tag{5.11}$$

$\boldsymbol{s}$ and $\boldsymbol{\theta}$ are bounded, since V is nonincreasing. From Lemma 5.1, $\boldsymbol{\nu}$ is bounded and Theorem 5.1 then implies $\lim_{t\to\infty} \tilde{\boldsymbol{\omega}} = 0$. Combining Equations 5.6 and Lemma 5.2 yields

$$||\boldsymbol{s}||^2 \geq 2\kappa < \tilde{\boldsymbol{\epsilon}}, \tilde{\boldsymbol{\omega}} >_T = 4\kappa \left[\tilde{\eta}(0) - \tilde{\eta}(T)\right],$$

which gives a bound on $\tilde{\eta}(T)$:

$$\tilde{\eta}(T) \geq \tilde{\eta}(0) - \frac{1}{4\kappa}||\boldsymbol{s}||^2 \qquad \forall T \geq 0.$$

Now, from the Lyapunov function and its derivative in Equations 5.10 and 5.11, it can be seen that

$$||\boldsymbol{s}||_T^2 \leq \frac{1}{k_D} \int_0^T \boldsymbol{s}^T \boldsymbol{K}_D \boldsymbol{s} dt \leq \frac{1}{k_D} V(0) \forall T \geq 0.$$

This means that the error manifold s has a bound

$$||\boldsymbol{s}||^2 \leq \frac{1}{2k_D} \left[\boldsymbol{s}(0)^T \boldsymbol{M} \boldsymbol{s}(0) dt + \tilde{\boldsymbol{\theta}}(0)^T \boldsymbol{\Gamma} \tilde{\boldsymbol{\theta}}(0)\right].$$

Therefore, if Equation 5.9 holds, then $\tilde{\eta}(t) > -1 + \delta_\epsilon$ for all $t \geq 0$. $\tilde{\eta}$ can then not converge to -1. Hence, $\lim_{t\to\infty} \tilde{\eta}(t) = 1$, as long as $\tilde{\eta}(0) \neq -1$.

5.1.2 Model-dependent linearizing controller

Based on the controller of Egeland & Godhavn (1994) a model-dependent linearizing controller is designed. To achieve the desired performance, the attitude $\boldsymbol{q}(t)$ should asymptotically track a desired attitude $\boldsymbol{q}_d(t)$. The tracking error is defined by the inverse quaternion product as

$$\boldsymbol{q}_e(t) = \begin{bmatrix} \eta_e(t) \\ \boldsymbol{\epsilon}_e(t) \end{bmatrix} = \boldsymbol{q}(t) \otimes \boldsymbol{q}_d^{-1}(t). \tag{5.12}$$

The velocity error is defined as $\tilde{\boldsymbol{\omega}}(t) = \boldsymbol{\omega}(t) - \boldsymbol{\omega}_d(t)$, and the tracking error then obeys the kinematics of $\dot{\tilde{\boldsymbol{q}}} = 1/2T(\tilde{\boldsymbol{q}})\tilde{\boldsymbol{\omega}}$. Based on system 3.9, a state feedback control law is proposed:

$$\boldsymbol{\tau}' = -\boldsymbol{J}^{-1}\boldsymbol{S}(\boldsymbol{\omega})\boldsymbol{\omega}_{io}^{b} + \boldsymbol{S}(\boldsymbol{\omega}_{\boldsymbol{io}}^{\boldsymbol{b}} + \boldsymbol{\omega})\boldsymbol{J}(\boldsymbol{\omega}_{\boldsymbol{io}}^{\boldsymbol{b}} + \boldsymbol{\omega}) - \boldsymbol{\tau}_g - \boldsymbol{K_D}\tilde{\boldsymbol{\omega}} - \boldsymbol{K_D}\kappa\tilde{\boldsymbol{\epsilon}} - \boldsymbol{J}\boldsymbol{a}. \tag{5.13}$$

The first three terms cancel the nominal terms of the system, while the three latter ensure convergence. This can be proven with the direct method of Lyapunov. Inserting the control law $\boldsymbol{\tau}'$ into Equation 3.9 yields

$$\boldsymbol{J}\dot{\boldsymbol{\omega}} = -\boldsymbol{K}_D\tilde{\omega} - \boldsymbol{K}_D\kappa\tilde{\boldsymbol{\epsilon}} - \boldsymbol{J}\boldsymbol{a}. \tag{5.14}$$

Whenever $\tilde{\boldsymbol{q}} = 0$ the desired angular velocity is zero, so the velocity error becomes $\boldsymbol{\omega}(t) - \boldsymbol{\omega}_d(t) = \boldsymbol{\omega}(t)$. Then the analysis can be simplified using $\boldsymbol{s} = \boldsymbol{\omega} + \kappa\tilde{\boldsymbol{\epsilon}}$ (Thienel & Sanner 2001) and $\boldsymbol{a} = \kappa\boldsymbol{T}_2(\tilde{\boldsymbol{\epsilon}})\boldsymbol{\omega}$ in Equation 5.14, which allows to write the dynamics as

$$\boldsymbol{J}\dot{\boldsymbol{s}} - \boldsymbol{J}\kappa\dot{\epsilon} = -\boldsymbol{K}_D\boldsymbol{s} - \boldsymbol{J}\kappa\boldsymbol{T}_2(\tilde{\boldsymbol{\epsilon}})\boldsymbol{\omega} \tag{5.15}$$

$$\boldsymbol{J}\dot{\boldsymbol{s}} = -\boldsymbol{K}_D\boldsymbol{s}. \tag{5.16}$$

Choosing $\boldsymbol{V} = 1/2\boldsymbol{s}^T\boldsymbol{J}\boldsymbol{s}$ as Lyapunov function candidate, it can be shown that its derivative along the trajectories of 5.15 is $\dot{\boldsymbol{V}} = -\boldsymbol{s}^T\boldsymbol{K_D}\boldsymbol{s} \leq -\boldsymbol{s}^T k_D\boldsymbol{s}$, where $k_D = \lambda_{min}(\boldsymbol{K_D})$.

The unit property of quaternions and Equation 5.12 ensures that $\tilde{\boldsymbol{\epsilon}} \in \mathcal{L}_\infty$. $\boldsymbol{\omega} \in \mathcal{L}_2$ is already assumed, and thus $\boldsymbol{s} \in \mathcal{L}_\infty$. Equation 5.15 implies then that $\dot{\boldsymbol{s}} \in \mathcal{L}_\infty$. For positive definite $\boldsymbol{K_D}$, $\dot{\boldsymbol{V}}(s)$ is strictly negative for all $\boldsymbol{s}$ except the equilibrium. This implies by Equation 2.16 that $\boldsymbol{s} \in \mathcal{L}_2$, since for all t

$$\begin{aligned}
\dot{\boldsymbol{V}}_{\boldsymbol{c}} \leq & -\boldsymbol{s}^T k_d\boldsymbol{s} \\
\int_{t_0}^{T} \boldsymbol{s}^T\boldsymbol{s}\,dt \leq & -\frac{1}{k_D}\int_{t_0}^{T} \dot{\boldsymbol{V}}_c\,dt \\
\leq & \frac{1}{k_D}(\boldsymbol{V}(t_0) - \boldsymbol{V}(T)),
\end{aligned}$$

which shows that $\boldsymbol{s}$ is square-integrable. In sum, $\boldsymbol{s}(t), \dot{\boldsymbol{s}}(t) \in \mathcal{L}_\infty$ and $\boldsymbol{s}(t) \in \mathcal{L}_2$, which by Barbalat's lemma 2.1 implies that $\lim_{t\to\infty} ||\boldsymbol{s}(t)|| = 0$.

To establish convergence of the attitude error $\tilde{\boldsymbol{\epsilon}}(t)$, observe that $\boldsymbol{\omega} \in \mathcal{L}_\infty$ and $\tilde{\boldsymbol{\epsilon}} \in \mathcal{L}_\infty$ implies that $\dot{\tilde{\boldsymbol{\epsilon}}}(t) \in \mathcal{L}_\infty$ because of $\dot{\tilde{\boldsymbol{\epsilon}}} = \boldsymbol{T}_2(\tilde{\boldsymbol{\epsilon}})\boldsymbol{\omega}$. $\tilde{\boldsymbol{\epsilon}}$ is also in $\mathcal{L}_2$, since $\kappa\tilde{\boldsymbol{\epsilon}} = \boldsymbol{s} - \boldsymbol{\omega}$, where $\boldsymbol{s} \in \mathcal{L}_2$ and the mapping $\boldsymbol{\omega} \to \tilde{\boldsymbol{\epsilon}}$ can be shown to be passive (Egeland & Gravdahl 2002):

Using that

$$\dot{\tilde{\eta}} = -\frac{1}{2}\tilde{\boldsymbol{\epsilon}}^T\tilde{\boldsymbol{\omega}},$$

passivity can be shown by

$$\begin{aligned}\int_0^T \tilde{\boldsymbol{\epsilon}}^T \tilde{\boldsymbol{\omega}} \; dt = & \quad -2\int_0^T \dot{\tilde{\eta}} dt \\ = & \quad -2(\tilde{\eta}(T) - \eta(0)) \\ \geq & \quad 2(\tilde{\eta}(0) - 1).\end{aligned}$$

Comparing with Definition 2.8, the system can be said to be strictly passive.

$\dot{\boldsymbol{\epsilon}}_e, \boldsymbol{\epsilon}_e \in \mathcal{L}_\infty$ and $\boldsymbol{\epsilon}_e \in \mathcal{L}_2$ are now established, and Barbalat's lemma 2.1 can again be invoked to show that $\lim_{t\to\infty} ||\boldsymbol{\epsilon}_e(t)|| = 0$. Thus, global asymptotic stability is proven for Equation 5.14 using Equation 5.13 as control law.

5.2 Robust Stabilizing Controller

The robustness of a controller is an important issue. The robustness of the adaptive controller presented in the previous section depends on the convergence of the estimated parameters to the true parameters. Josh et al. (1995) presents a controller which is model-independent and therefore robust in that aspect.

Consider the control law

$$\boldsymbol{\tau}' = -\frac{1}{2}[(\tilde{\eta}\boldsymbol{I} + \boldsymbol{S}(\tilde{\boldsymbol{\epsilon}}))\boldsymbol{K}_P + \gamma(1-\tilde{\eta})\boldsymbol{I}]\tilde{\boldsymbol{\epsilon}} - \boldsymbol{K}_D\tilde{\boldsymbol{\omega}}, \tag{5.17}$$

where γ is a positive definite scalar and $\boldsymbol{K}_P, \boldsymbol{K}_D$ are positive definite symmetric matrices. $\tilde{\boldsymbol{q}} = \boldsymbol{q} \otimes \hat{\boldsymbol{q}}$ and $\tilde{\boldsymbol{\omega}} = \boldsymbol{\omega} - \boldsymbol{\omega}_d$. The stability proof begins by establishing the equilibrium points of the closed-loop system resulting from the insertion of Equation 5.17 into the system 3.9. From the equilibrium point analysis of the open-loop system in Chapter 3.2.1 it is known that $\boldsymbol{\omega} = 0$ leads to $\tau' = 0$. Using this in the control law 5.17 yields

$$[\tilde{\eta}\boldsymbol{I} + \boldsymbol{S}(\boldsymbol{\epsilon})\boldsymbol{K}_P + \gamma(1-\tilde{\eta})\boldsymbol{I}]\tilde{\boldsymbol{\epsilon}} = 0, \tag{5.18}$$

which can further be simplified by premultiplying with $\tilde{\boldsymbol{\epsilon}}^T$:

$$\tilde{\boldsymbol{\epsilon}}^T\boldsymbol{A}\tilde{\boldsymbol{\epsilon}} = 0, \qquad \boldsymbol{A} = [\tilde{\eta}\boldsymbol{K}_P + \gamma(1-\tilde{\eta})\boldsymbol{I}]. \tag{5.19}$$

Hence, the eigenvalues of $\boldsymbol{A}$ are the eigenvalues of the controller. Singularities occur when one or more of the eigenvalues $\lambda_i(\boldsymbol{A}) = \tilde{\eta}\lambda_i(\boldsymbol{K}_P) + \gamma(1-\tilde{\eta})\boldsymbol{I}$ are zero. The constants $\boldsymbol{K}_P$ and γ are design parameters to be chosen arbitrarily, whereas η is a state variable. Rearranging with respect to $\tilde{\eta}$ allows for an examination of possible singularities:

$$\tilde{\eta} = \frac{-\gamma}{\lambda_i(\boldsymbol{K}_P) - \gamma} \Rightarrow \lambda_i(\boldsymbol{A}) = 0 \tag{5.20}$$

From Equation 5.20 it can be seen that

$$\lambda_i(\boldsymbol{K}_P) > 2\gamma \Rightarrow \tilde{\eta} < -1$$
$$\lambda_i(\boldsymbol{K}_P) = 2\gamma \Rightarrow \tilde{\eta} = -1$$
$$\lambda_i(\boldsymbol{K}_P) < 2\gamma \Rightarrow \tilde{\eta} > -1,$$

so that whenever $\lambda_i(\boldsymbol{K}_P) > 2\gamma$ there are feasible values of $\tilde{\eta}$ that gives singularities in A. The singularity at $\tilde{\eta} = -1$ coincides with an equilibrium point of the open-loop system. In sum, this imposes a restriction on the design parameters $\lambda_i(\boldsymbol{K}_P) \leq 2\gamma \ \forall i$. As long as this restriction is upheld, the equilibrium points of the closed-loop system are the same as in Equation 3.7.

5.2.1 Stability analysis

To use the direct method of Lyapunov, the equilibrium of the system should lie in the origin of the state space. Initially, the closed-loop system has equilibriums in $\tilde{\eta} = \pm 1$. Josh et al. (1995) translates the equilibriums by introducing the variable $\beta = \tilde{\eta} - 1$. Accordingly, the control becomes

$$\boldsymbol{\tau}' = -\frac{1}{2}[((\beta + 1)\boldsymbol{I} + \boldsymbol{S}(\tilde{\boldsymbol{\epsilon}}))\boldsymbol{K}_P - \gamma\beta\boldsymbol{I}]\tilde{\boldsymbol{\epsilon}} - \boldsymbol{K}_D\boldsymbol{\omega}. \tag{5.21}$$

Consider now the Lyapunov function candidate

$$\boldsymbol{V} = \boldsymbol{\omega}^T\boldsymbol{M}\boldsymbol{\omega} + \tilde{\boldsymbol{\epsilon}}^T\boldsymbol{K}_P\tilde{\boldsymbol{\epsilon}} + \gamma\beta^2. \tag{5.22}$$

Taking the time derivative of $\boldsymbol{V}$ yields

$$\dot{\boldsymbol{V}} = 2\boldsymbol{\omega}^T[-\boldsymbol{S}(\boldsymbol{\omega})\boldsymbol{M}\boldsymbol{\omega} + \boldsymbol{\tau}'] + \tilde{\boldsymbol{\epsilon}}^T\boldsymbol{K}_P(\boldsymbol{S}(\boldsymbol{\omega})\tilde{\boldsymbol{\epsilon}} + (\beta + 1)\boldsymbol{\omega}) - \gamma\beta\boldsymbol{\omega}^T\tilde{\boldsymbol{\epsilon}}, \tag{5.23}$$

which can, using Equation 2.3 and substituting for the control law 5.21, be shortened to $\dot{\boldsymbol{V}} = -2\boldsymbol{\omega}^T\boldsymbol{K}_D\boldsymbol{\omega}$. Hence, $\dot{\boldsymbol{V}}$ is only negative semidefinite. Repeating the procedure in Equations 5.18 to 5.20 with the control law in Equation 5.21 shows that $\dot{\boldsymbol{V}} = 0$ only at the equilibrium points

$$\begin{bmatrix} \beta \\ \tilde{\boldsymbol{\epsilon}} \\ \boldsymbol{\omega} \end{bmatrix} = \begin{bmatrix} 0 \vee -2 \\ \mathbf{0} \\ \mathbf{0} \end{bmatrix}.$$

These values correspond to the same physical states. Also, from the Lyapunov function 5.22, any perturbation from the equilibrium point $\beta = -2$ results in a decrease in $\boldsymbol{V}$. $\dot{\boldsymbol{V}} < 0$ everywhere in the feasible state space, and therefore also in the neighbourhood of $\beta = -2$. Hence, $\beta = -2$ is a repelling equilibrium point as opposed to $\beta = 0$ which is attracting. In sum, if the initial conditions of the system is anywhere but at the equilibrium corresponding to $\beta = -2$, it will approach the origin. If the initial conditions is exactly at the point $\beta = -2$, it will stay there for all time. The two equilibria correspond to the same value in the phsyical space, and Josh et al. (1995) states that global asymptotic stability can be concluded by La'Salle's Theorem 2.4.

5.3 PD-controller

The advantages of a simple PD-controller can be many. There are few parameters to tune, the algorithm is easy to maintain and it demands very little computing power. Also, it is independent of the model, which adds to its robustness and usability. The drawbacks may be poor control performance and slow convergence.

Taking the desired velocity $\boldsymbol{\omega}_d = 0$, the setpoint control law is

$$\boldsymbol{\tau}' = -\boldsymbol{K}_P\tilde{\boldsymbol{\epsilon}} - \boldsymbol{K}_D\boldsymbol{\omega}. \tag{5.24}$$

The resulting system dynamics are

$$\boldsymbol{J}\dot{\boldsymbol{\omega}} = -\boldsymbol{K}_P\tilde{\boldsymbol{\epsilon}} - \boldsymbol{K}_D\boldsymbol{\omega}.$$

5.3.1 Stability analysis

Assuming again that $\boldsymbol{\omega}, \dot{\boldsymbol{\omega}} \in \mathcal{L}_\infty$, the law ensures that $\tilde{\boldsymbol{\epsilon}}(t), \boldsymbol{\omega}(t) \to 0$ as $t \to \infty$. This can be proven with a Lyapunov function candidate similar but not identical to the one found in Wen & Kreutz-Delgado (1991), Theorem 1:

$$V = (\boldsymbol{K}_P + k\boldsymbol{K}_D)((\tilde{\eta} - 1)^2 + \tilde{\boldsymbol{\epsilon}}^T\tilde{\boldsymbol{\epsilon}}) + \frac{1}{2}\tilde{\boldsymbol{\omega}}\boldsymbol{J}\tilde{\boldsymbol{\omega}} + k\tilde{\boldsymbol{\epsilon}}\boldsymbol{J}\tilde{\boldsymbol{\omega}}.$$

V can be bounded below by the function

$$V \geq \boldsymbol{x}^T\boldsymbol{P}_c\boldsymbol{x},$$

where

$$\begin{aligned}\boldsymbol{x} &= \begin{bmatrix} ||\tilde{\boldsymbol{\epsilon}}|| \\ ||\tilde{\boldsymbol{\omega}}|| \end{bmatrix} \\ \boldsymbol{P}_c &= \frac{1}{2}\begin{bmatrix} 2(\boldsymbol{K}_P + k\boldsymbol{K}_D) & k||\boldsymbol{J}|| \\ k||\boldsymbol{J}|| & ||\boldsymbol{J}|| \end{bmatrix}.\end{aligned}$$

$\boldsymbol{P}_c$ is positive definite for small enough values of k. Taking the time derivative along the solutions of Equation 3.3 gives

$$\begin{aligned}\dot{V} = &(\boldsymbol{K}_P + k\boldsymbol{K}_D)\left[-(\tilde{\eta}1)\tilde{\boldsymbol{\epsilon}}^T\tilde{\boldsymbol{\omega}} + \tilde{\boldsymbol{\epsilon}}^T\tilde{\eta}\tilde{\boldsymbol{\omega}}\right] \\ &+ \tilde{\boldsymbol{\omega}}^T(\boldsymbol{\tau} - N(\boldsymbol{R}, \boldsymbol{\omega})\tilde{\boldsymbol{\omega}}) + k\tilde{\boldsymbol{\epsilon}}(\boldsymbol{\tau} - N\tilde{\boldsymbol{\omega}}) + k\dot{\tilde{\boldsymbol{\epsilon}}}^T\boldsymbol{J}\tilde{\boldsymbol{\omega}}\end{aligned}$$

Inserting for the control law 5.24 gives

$$\begin{aligned}\dot{V} &= -\tilde{\boldsymbol{\omega}}^T\boldsymbol{K}_D\tilde{\boldsymbol{\omega}} - \tilde{\boldsymbol{\omega}}^T N(\boldsymbol{R}, \boldsymbol{\omega})\tilde{\boldsymbol{\omega}} - k\tilde{\boldsymbol{\epsilon}}N(\boldsymbol{R}, \boldsymbol{\omega})\tilde{\boldsymbol{\omega}} + k\dot{\tilde{\boldsymbol{\epsilon}}}^T\boldsymbol{J}\tilde{\boldsymbol{\omega}} \\ &= -\boldsymbol{x}^T\boldsymbol{Q}_c\boldsymbol{x} + \boldsymbol{p}\boldsymbol{x} \\ &\leq -\lambda||\boldsymbol{x}||^2 + \rho(t)||\boldsymbol{x}||,\end{aligned} \tag{5.25}$$

where

$$\begin{aligned}
\boldsymbol{Q}_c &= \begin{bmatrix} k\boldsymbol{K}_P & \frac{1}{2}kN \\ \frac{1}{2}kN & \boldsymbol{K}_D + N \end{bmatrix}, \\
\lambda &\triangleq \lambda_{min}(\boldsymbol{Q}_c), \\
\boldsymbol{p} &= [\ 0 \quad k\dot{\tilde{\boldsymbol{\epsilon}}}\boldsymbol{J}\ ], \\
\rho(t) &\triangleq \sqrt{1-k^2}k\dot{\tilde{\boldsymbol{\epsilon}}}\boldsymbol{J} \qquad (||\rho|| \geq ||\boldsymbol{p}||).
\end{aligned}$$

For sufficiently small k the eigenvalue $\lambda > 0$ and $\boldsymbol{Q}_c$ is thus positive definite.

The rest of the stability proof uses the same techniques as Wen & Kreutz-Delgado (1991). Integrating both sides of Equation 5.25 gives

$$V_T - V_0 \leq \lambda \int_0^T ||\boldsymbol{x}(t)||^2 dt + \int_0^T \rho(t)||\boldsymbol{x}(t)||dt$$

which can in turn be written as

$$\lambda \int_0^T ||\boldsymbol{x}(t)||^2 dt - \int_0^T ||\boldsymbol{x}(t)||^2 dt \leq V_0. \tag{5.26}$$

It is now useful to show that $\rho(t) \in \mathcal{L}_2$. This can be done by introducing the surface $s = \tilde{\boldsymbol{\epsilon}} + \lambda\tilde{\boldsymbol{\omega}}$, assuming that the mapping $\tilde{\boldsymbol{\omega}} \rightarrow \tilde{\boldsymbol{\epsilon}}$ is passive and following the same reasoning as in Chapter 5.1, in particular concerning Equations 5.4 to 5.6.

Since $\rho(t) \in \mathcal{L}_2$, the Schwarz inequality can be applied to the second term on the left hand side of Equation 5.26: $\int_0^T \rho(t)||\boldsymbol{x}(t)||dt \leq ||\rho||||\boldsymbol{x}||$. Rearranging now gives

$$\begin{aligned}
\lambda||\boldsymbol{x}||^2 &\leq V_0 + ||\rho||||\boldsymbol{x}|| \\
\lambda||\boldsymbol{x}||^2 + \frac{||\rho||}{2}^2 &\leq V_0 + ||\rho||||\boldsymbol{x}|| + \frac{||\rho||}{2}^2 \\
||\boldsymbol{x}|| &\leq \left[\frac{1}{\lambda}(V_0 + \frac{||\rho||^2}{4\lambda})\right]^{1/2} + \frac{||\rho||}{2\lambda}.
\end{aligned} \tag{5.27}$$

Equation 5.27 expresses a bound on $||\boldsymbol{x}||$, hence $\boldsymbol{x} \in \mathcal{L}_2$. Inserting the bound into Equation 5.26 shows that V is uniformly bounded for all t. From the kinematic and dynamic equations in Chapter 3, $\dot{\boldsymbol{x}} \in \mathcal{L}_2$ which means that x is uniformly continuous. Barbalat's lemma then shows that $\boldsymbol{x}(t) \rightarrow 0$ as $t \rightarrow \infty$.

For predetermined $\boldsymbol{K}_P$ and $\boldsymbol{K}_D$, there exists a range of possible k such that $\boldsymbol{P}_c$ and $\boldsymbol{Q}_c$ are positive definite. The k parameter decides the convergence rate of the system, and since it is not part of the control law it can be chosen freely (apart from the stated requirements).

Chapter 6

Separation Principle

The implementation of a nonlinear feedback controller gives the opportunity to design the transient behaviour of the total system and to place the system poles such that some degree of stability is achieved. For state feedback systems, i.e. systems where all necessary states are available for measurement, this is quite straightforward as the only alteration of the system dynamics originates in the controller itself. Control of output feedback systems is made possible with the addition of an observer. The observer/controller configuration is in itself an interconnected system (ICS). The data fed from the observer to the controller are only estimates, and this requires the observer error to have some properties of convergence. Rather than analysing the ICS stability directly, stability analysis can be done by separating the ICS into subsystems, establish stability properties for each subsystem and then draw conclusions for the overall system. The structure of the ICS determines how the subsystems may be formed. In general, a *separation principle* is said to exist if a problem can be divided into simpler subproblems, which may in turn be solved and have their solutions combined to give the solution of the original problem.

6.1 Linear systems

For linear systems there exist a separation principle which simplifies the stability analysis. The separation principle states that if a controller is designed using an observer and a state-feedback matrix, the observer gains and the feedback gains can be designed separately. The eigenvalues of the ICS will be the union of the eigenvalues of the observer and those due to the feedback controller. The proof of this can be found in most books on linear systems, e.g. Chen (1999), pp. 254. The properties of the linear separation principles is summarized here because of its structural likeness to the cascaded system that will be encountered later.

Consider the system

$$\begin{aligned}\dot{\boldsymbol{x}} =& \boldsymbol{A}\boldsymbol{x} + \boldsymbol{B}u \\ y =& \boldsymbol{C}\boldsymbol{x}.\end{aligned}$$

As long as $(\boldsymbol{A}, \boldsymbol{B})$ is controllable, the state feedback $u = r - \boldsymbol{K}\boldsymbol{x}$ can place the eigenvalues of $\boldsymbol{A} - \boldsymbol{B}\boldsymbol{K}$ in any desired position. If $(\boldsymbol{A}, \boldsymbol{C})$ is observable, an observer with arbitrary eigenvalues may be constructed. Take the Luenberger observer from Chapter 4: $\dot{\hat{\boldsymbol{x}}} = (\boldsymbol{A} - \boldsymbol{G}\boldsymbol{C})\hat{\boldsymbol{x}} + \boldsymbol{B}\boldsymbol{u} + \boldsymbol{G}\boldsymbol{y}$. Now, let the controller use the estimated state feedback $u = r - \boldsymbol{K}\hat{\boldsymbol{x}}$. The total system becomes

$$\begin{bmatrix} \dot{\boldsymbol{x}} \\ \dot{\hat{\boldsymbol{x}}} \end{bmatrix} = \begin{bmatrix} \boldsymbol{A} & -\boldsymbol{B}\boldsymbol{K} \\ \boldsymbol{G}\boldsymbol{C} & \boldsymbol{A} - \boldsymbol{G}\boldsymbol{C} - \boldsymbol{B}\boldsymbol{K} \end{bmatrix} \begin{bmatrix} \boldsymbol{x} \\ \hat{\boldsymbol{x}} \end{bmatrix} + \begin{bmatrix} \boldsymbol{B} \\ \boldsymbol{B} \end{bmatrix}.$$

By writing the observation error as $\boldsymbol{e} = \boldsymbol{x} - \hat{\boldsymbol{x}}$, an equivalent presentation of the total system is

$$\begin{bmatrix} \dot{\boldsymbol{x}} \\ \dot{\boldsymbol{e}} \end{bmatrix} = \begin{bmatrix} \boldsymbol{A} - \boldsymbol{B}\boldsymbol{K} & \boldsymbol{B}\boldsymbol{K} \\ \boldsymbol{0} & \boldsymbol{A} - \boldsymbol{G}\boldsymbol{C} \end{bmatrix} \begin{bmatrix} \boldsymbol{x} \\ \boldsymbol{e} \end{bmatrix} + \begin{bmatrix} \boldsymbol{B} \\ \boldsymbol{0} \end{bmatrix}. \tag{6.1}$$

Since the square matrix in Equation 6.1 is block triangular, its eigenvalues are the union of those on the diagonal, namely the eigenvalues of $\boldsymbol{A} - \boldsymbol{B}\boldsymbol{K}$ and $\boldsymbol{A} - \boldsymbol{G}\boldsymbol{C}$. These are the original eigenvalues of the controller and the observer respectively, and it is clear that basing the control law on state estimates does not alter the eigenvalues of the two subsystems, nor does it introduce any new eigenvalues.

6.2 Nonlinear systems

A similar general principle has yet to be found for nonlinear systems, and proving stability is more complicated. However, separation principles have been proved for some classes of nonlinear systems. When designing a control system it is a regular goal that the interconnected system should fit into one of the classes that have already established stability theorems and methods of analysis. This thesis takes the approach of cascaded interconnected systems, on which examples of previous work can be found in Michel et al. (1978), Vidyasagar (1980*a*), Jankovic et al. (1996), Panteley & Loria (1997) etc. These will be referenced as needed throughout the presentation. Stability analyses are done in the sense of Lyapunov as shown in Theorems 2.1- 2.3.

6.2.1 ICS with additive subsystems

Consider a system described by an ordinary differential equation of the form

$$\dot{z} = b(z, t) \tag{6.2}$$

where $z \in \mathcal{R}^m$, t is the regular time-function and $b : \mathcal{R}^m \rightarrow \mathcal{R}^m$ is a smooth function and locally Lipschitz. Michel et al. (1978) explains Lyapunov analysis of an ICS which is composed by simple addition of its subsystems. Decomposing system 6.2 into subsystems allows rewriting as $\dot{z}_i = b_i(z_i, t)$. By renumbering,

and if necessary aggregating the state variables, a *hierarchical structure* may be obtained where each subsystem is only affected by itself and 'lower' subsystems:[1]

$$\dot{x}_i = f_i(x_i, t)) + \Sigma_{j=1}^{i-1} \boldsymbol{G}_{ij}(x_j, t) \tag{6.3}$$

Here $f_i(\cdot)$ represents the local mapping and $\boldsymbol{G}_{ij}(\cdot)$ is a matrix containing mappings of the contributions from the 'lower' subsystems. $f(\cdot)$ and $\boldsymbol{G}(\cdot)$ inherit the properties of $b(\cdot)$ in 6.2.

The mappings in $\boldsymbol{G}_{ij}(\cdot)$ are decisive in the stability analysis. Take $g : x_j \times t \rightarrow y_j$, where g is an element of $\boldsymbol{G}$. g is then said to be *stability preserving* if $y_j(t) = g(x_j, t)$ has the same stability properties as $x_j(t)$ and this holds for all t. Thomas (1964) showed that g is stability preserving if g is a *homeomorphism*:

Definition 6.1 *g is a homeomorphism if it has the following properties:*

- *g is a one-to-one mapping between x_j and y_j.*
- *g is continuous.*
- *g^{-1} exists and is continuous.*

Equivalently, Hahn (1967) showed that g preserve uniform stability and uniform asymptotic stability if it fulfils the Lipschitz-like criterion

$$|y_2(t) - y_1(t)| < \alpha(|x_2(t) - x_1(t)|) \forall t \geq 0, \tag{6.4}$$

where $\alpha(\cdot)$ is a class $\mathcal{K}$ function. The mapping g is exponential stability preserving if it fulfils 6.4 and there exist constants $k_1, k_2, k_3 > 0$ such that $\alpha(|\Delta x|) \leq k_1(|\Delta x|)^{k_2}$ when $0 < \Delta x < k_3$. If $\alpha(\cdot)$ is of the class $\mathcal{K}_\infty$, the results are global.

Using the passivity preserving property of g_{ij} and direct Lyapunov analysis as presented in Chapter 2, Michel et al. (1978) proves Theorem 6.1:

Theorem 6.1 *The equilibrium $x_i = 0$ of system 6.3 is (globally) stable, respectively (globally) exponentially/asymptotically stable, if all subsystems x_j are (globally) stable, respectively (globally) exponentially/asymptotically stable.*

6.2.2 ICS with nonadditive subsystems

Often, the ICS can not be formed by simply adding its subcomponents. Consider again Equation 6.2, written in the hierarchical form

$$\dot{x}_i(t) = \boldsymbol{F}_i(x_1(t), ..., x_i(t), t), \qquad i = 1, ..., m \tag{6.5}$$

[1]The procedure of decomposing a graph into strongly connected subcomponents falls outside the scope of this thesis. As becomes clear later, it is not necessary for the special case of ICS's which an observer/controller system amounts to. Theories on graph decomposition can be found in e.g. Harary (1962), Kevorkian & Snoek (1973), and Kevorkian (1975).

where m is the number of subsystems. It is now interesting to relate the stability properties of the ICS with the properties of each isolated subsystem

$$\dot{x}_i(t) = f_i(0, ...0, x_i(t), t), \tag{6.6}$$

as in Vidyasagar (1980*a*). In addition to $\boldsymbol{F}_i$ being smooth, Assumption 6.1 and 6.2 must hold.

Assumption 6.1

$$\boldsymbol{F}_i(0, ..., 0, t) = 0 \qquad \forall i, t \geq 0$$

Assumption 6.2

$$\sup_{||\boldsymbol{w}_i|| \leq c} ||\nabla \boldsymbol{F}_i(\boldsymbol{w}_i, t)|| < \infty \qquad \forall i, t \geq 0,$$

where $\boldsymbol{w}_i = [x_1, ..., x_i]$.

With these assumptions, Vidyasagar proves Theorem 6.2

Theorem 6.2 *$x = 0$ is a uniform exponentially/asymptotically stable equilibrium point of 6.5 if and only if $x_i = 0$ is a uniform exponentially/asymptotically stable equilibrium point of 6.6 for all i. If Assumption 6.2 is strenghtened with $c = \infty$, the results hold globally.*

Theorem 6.2 gives necessary and sufficient conditions. Another theorem, which is a generalization of Theorem 6.1, gives only sufficient conditions:

Theorem 6.3 *Suppose that $x_i = 0$ is a globally asymptotically stable equilibrium point of Equation 6.6 for all i, and that there exist Lyapunov functions V_i that fulfils the criterions of Theorem 2.2 for all i and all t. Also, suppose that $\lim_{||x_i|| \to \infty} ||\nabla_{x_i} V_i(x_i, t)/W_{i3}(||x_i||) = 0$, that Assumption 6.1 holds and that there exist class $\mathcal{K}$ functions α_i such that*

$$||f_i(w_i, t) - f_i(0, ..., x_i)|| \leq \alpha_i(||\boldsymbol{w}_i||) \forall t \geq 0, x. \tag{6.7}$$

Then, $x_i = 0$ is a globally asymptotically stable equilibrium point of system 6.5.

It is worth noting that Equation 6.7 ensures that the contributions from lower subsystems do not violate the stability preserving property.

6.2.3 Cascaded systems

The term *cascaded systems* indicates here that the system has the structure of a controller/observer control system as shown in Figure 6.1. Until now only autonomous systems have been discussed. An observer/controller cascade is nonautonomous, since the observer dynamics depends on the output. Two different approaches to stability analysis are presented. The first approach treats the interconnection term $g(\cdot)$ implicitly, while $g(\cdot)$ is separated from the subsystems in the second approach. The latter allows for specific requirements on the interconnection term, at the same time easing the requirements on the subsystems.

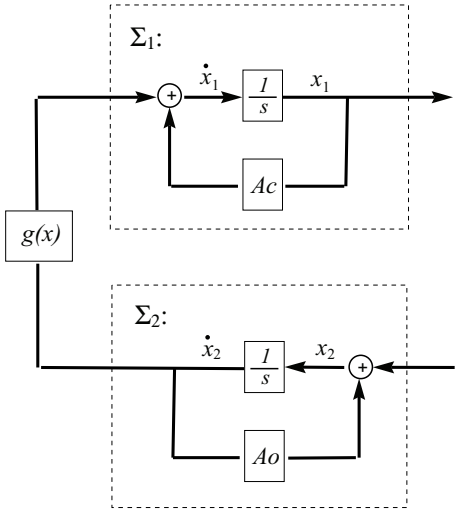

Figure 6.1: The controller observer configuration viewed as a cascade. Σ_1 is the controller system, Σ_2 the observer system.

Implicit interconnection term

Vidyasagar (1980*b*) discusses a special case of ICS with nonadditive subsystems, more precisely the case where a feedback control law is used for stabilizing the nonlinear system. The method of designing the control system is as follows:

1. Find a function $f(\cdot)$ based on true states $\boldsymbol{x}(t)$, that has the desired stabilizing effect on the system.
2. Implement an observer that generates the state estimates $\hat{\boldsymbol{x}}(t)$ such that $\hat{\boldsymbol{x}}(t) - \boldsymbol{x}(t) \to 0$ for $t \to \infty$.
3. Base the function $f(\cdot)$ on $\hat{\boldsymbol{x}}(t)$ instead of $\boldsymbol{x}(t)$.

To certify this method it must be shown that the function $f(\hat{\boldsymbol{x}}(t), t)$ from step 3 has the same stabilizing properties as $f(\boldsymbol{x}(t), t)$ in step 1.

Consider the system

$$\begin{aligned} \dot{\boldsymbol{x}}(t) &= f(\boldsymbol{x}(t), \boldsymbol{u}(t), t) \\ \boldsymbol{y} &= c(\boldsymbol{x}(t), t), \end{aligned} \tag{6.8}$$

where $\boldsymbol{x}(t)$, $\boldsymbol{y}(t)$ and $\boldsymbol{u}(t)$ represents the state, output and input of the system, respectively. $f(\cdot)$ and $c(\cdot)$ are continuous functions and $\boldsymbol{x}(t) \in \mathcal{R}^n$, $\boldsymbol{y}(t) \in \mathcal{R}^m$, $\boldsymbol{u}(t) \in \mathcal{R}^l$. Further, the following assumption is made:

Assumption 6.3 *$c(0,0,t) = 0$, $f(0,0,t) = 0$ and there exist constants k and δ such that*

$$||\nabla_x f(\boldsymbol{x}, \boldsymbol{u}, t)|| \leq k, \quad ||\nabla_u f(\boldsymbol{x}, \boldsymbol{u}, t)|| \leq k, \quad \forall t \geq 0, \ \boldsymbol{x} \in B_\delta, \boldsymbol{u} \in B_\delta.$$

Now, system 6.8 is said to be asymptotically/exponentially *stabilizable* if there exist a function $\tau(\cdot) : \mathcal{R}^n \times \mathcal{R}_+ \rightarrow \mathcal{R}^l$ that has the following properties:

- $\tau(\cdot)$ is continuously differentiable
- $||\nabla_x \tau(\boldsymbol{x}, t)|| \leq \beta(||\boldsymbol{x}||) \quad \forall t, \boldsymbol{x} \in B_c$, where $\beta(\cdot)$ is of class $\mathcal{KL}$
- $\boldsymbol{x} = 0$ is a uniformly asymptotically/exponentially stable equilibrium point of

$$\dot{\boldsymbol{x}} = f(\boldsymbol{x}(t), \tau(\boldsymbol{x}(t), t), t). \tag{6.9}$$

If a known function $\tau(\cdot)$ stabilizes the system 6.8, $\tau(\cdot)$ is referred to as the *control law*.

As for the implementation of an observer, the system 6.8 is sait to be *weakly exponentially detectable* if there exist functions $g(\cdot) : \mathcal{R}^n \times \mathcal{R}^m \times \mathcal{R}^l \times \mathcal{R}_+ \rightarrow \mathcal{R}^n$ and $V(\cdot) : \mathcal{R}^n \times \mathcal{R}^n \times \mathcal{R}_+ \rightarrow \mathcal{R}_+$ such that

- $h(\cdot)$ is continuously differentiable
- $h(0, 0, 0, t) = 0 \forall t$
- there exist constants k_1, k_2 and k_3 such that $V(\cdot)$ is a Lyapunov function for the system $\dot{\boldsymbol{e}} = d(\boldsymbol{e}, \boldsymbol{u}, t)$ where $\boldsymbol{e} = \boldsymbol{x} - \hat{\boldsymbol{x}}$, and Theorem 2.3 is valid with $V(\cdot)$ and $\dot{V}(\cdot)$.

The function $\dot{\boldsymbol{e}} = d(\cdot)$ in the last bullet represents the error dynamics of the observer

$$\dot{\hat{\boldsymbol{x}}} = h(\hat{\boldsymbol{x}}(t), \boldsymbol{y}(t), \boldsymbol{u}(t), t), \quad \hat{\boldsymbol{x}}(t) \in B_\delta, \boldsymbol{u}(t) \in B_\delta \tag{6.10}$$

and if Theorem 2.3 is valid with $V(\cdot)$, the error dynamics are locally exponentially stable.[2] Thus, Equation 6.10 is an observer for system 6.8.

Based on these premises Vidyasagar (1980*b*) proves the following theorem:

Theorem 6.4 (Vidyasagar 1980*b*) *Suppose the system*

$$\begin{aligned} \dot{\boldsymbol{x}}(t) &= f(\boldsymbol{x}(t), \tau(\hat{\boldsymbol{x}}(t), t), t) \\ \dot{\hat{\boldsymbol{x}}}(t) &= h(\hat{\boldsymbol{x}}(t), c(\boldsymbol{x}(t), t), \tau(\hat{\boldsymbol{x}}(t), t), t) \end{aligned} \tag{6.11}$$

is exponentially stabilizable and weakly exponentially detectable. Then $\boldsymbol{x} = 0$, $\hat{\boldsymbol{x}} = 0$ is a uniformly stable equilibrium point of the system 6.11.

The previous stability analysis of system 6.11 holds only locally, due to the restrictions $\boldsymbol{x}(t), \boldsymbol{u}(t), \hat{\boldsymbol{x}}(t) \in B_\delta$. Finally, Vidyasagar (1980*b*) proves a theorem that gives global exponential stability.

Theorem 6.5 (Vidyasagar 1980*b*) *Suppose the following conditions hold.*

[2] Theorem 2.3 normally proves global stability, but here it is assumed that $\boldsymbol{x}(t) \in B_\delta, \boldsymbol{u}(t) \in B_\delta, \hat{\boldsymbol{x}}(t) \in B_\delta$ and the result will only hold locally.

i) The system 6.9 is globally exponentially stable.

ii) The solution trajectories of 6.11 satisfy

$$||\boldsymbol{x}(t) - \hat{\boldsymbol{x}}(t)|| \leq k_4||\boldsymbol{x}(t_0) - \hat{x}(t_0)||e^{-k_5(t-t_0)}$$

for some positive constants k_4 and k_5.

iii) The function $f(\cdot)$ satisfies

$$\sup_{t\geq 0}\sup_{\boldsymbol{x}\in\mathcal{R}^n} ||\nabla_x f(\boldsymbol{x}, \tau(\boldsymbol{x}(t), t), t)|| < \infty$$

iv) The system 6.11 satisfies

$$\sup_{t\geq 0}\sup_{\boldsymbol{x},\hat{\boldsymbol{x}}\in\mathcal{R}^n} \max\{\mu_{11}, \mu_{12}, \mu_{21}, \mu_{22}\} = k_5 < \infty$$

where

$$\begin{aligned}
\mu_{11} =& \nabla_x f(\boldsymbol{x}, \tau(\hat{\boldsymbol{x}}, t), t)\\
\mu_{12} =& \nabla_{\hat{x}} f(\boldsymbol{x}, \tau(\hat{\boldsymbol{x}}, t), t)\\
\mu_{21} =& \nabla_x h(\hat{\boldsymbol{x}}, c(\boldsymbol{x}, t), \tau(\hat{\boldsymbol{x}}, t), t)\\
\mu_{22} =& \nabla_{\hat{x}} h(\hat{\boldsymbol{x}}, c(\boldsymbol{x}, t), \tau(\hat{\boldsymbol{x}}, t), t)
\end{aligned}$$

Under these conditions, the system 6.11 is globally exponentially stable.

In words, *iii*) and iv) in Theorem 6.5 states that the gradients with respect to $\boldsymbol{x}$ and $\hat{\boldsymbol{x}}$ along the solutions of system 6.11 need to be in $\mathcal{L}_\infty$. These requirements are analogous to the stability preserving requirements on the $\boldsymbol{G}(\cdot)$ mappings in Equation 6.4.

Explicit interconnection term

The cascaded system in Figure 6.1 can be described by

$$\begin{aligned}
\Sigma_1 : \dot{\boldsymbol{x}}_1 &= f(\boldsymbol{x}_1, t) + g(\boldsymbol{x}, t)\boldsymbol{x}_2\\
\Sigma_2 : \dot{\boldsymbol{x}}_2 &= h(\boldsymbol{x}_2, t),
\end{aligned} \tag{6.12}$$

where $\boldsymbol{x}_1 \in \mathcal{R}^n, \boldsymbol{x}_2 \in \mathcal{R}^m, \boldsymbol{x} = \text{col}[\boldsymbol{x}_1, \boldsymbol{x}_2]$. The functions $f(\cdot), h(\cdot)$ and $g(\cdot)$ are continuously differentiable in their respective arguments and locally Lipschitz. Panteley & Loria (1997) gives sufficient theorems to show global stability and global asymptotic stability for the system 6.12:

Theorem 6.6 *If Assumptions 6.4 to 6.6 below are satisfied, then the cascaded system 6.12 is globally uniformly stable.*

Assumption 6.4 *The system $\dot{\boldsymbol{x}} = f(\boldsymbol{x}_1, t)$ is globally uniformly stable with a Lyapunov function $V(\boldsymbol{x}_1, t)$, $V : \mathcal{R}_{\geq 0} \times \mathcal{R}^n \rightarrow \mathcal{R}_{\geq 0}$ positive definite (that is $V(0,t) = 0$ and $V(\boldsymbol{x}_1, t) > 0$ for all $\boldsymbol{x}_1 \neq 0$) and proper (that is, radially unbounded) which satisfies*

$$\left|\left|\frac{\delta V}{\delta \boldsymbol{x}_1}\right|\right| ||\boldsymbol{x}_1|| \leq k_1 V(\boldsymbol{x}_1, t) \qquad \forall ||\boldsymbol{x}_1|| \geq \upsilon \tag{6.13}$$

where $k_1, \upsilon > 0$. We also assume that $\delta V / \delta \boldsymbol{x}_1(\boldsymbol{x}_1, t)$ is bounded uniformly in t for all $||\boldsymbol{x}_1|| \leq \upsilon$, that is, there exists a constant $k_2 > 0$ such that for all $t \geq t_0 \geq 0$

$$||\frac{\delta V}{\delta \boldsymbol{x}_1}|| \leq k_2 \qquad \forall ||\boldsymbol{x}_1|| \geq \upsilon$$

Assumption 6.5 *The function $g(\boldsymbol{x}, t)$ satisfies*

$$||g(\boldsymbol{x}, t)|| \leq \theta_1(||\boldsymbol{x}_2||) + \theta_2(||\boldsymbol{x}_2||)||\boldsymbol{x}_1||$$

where $\theta_1, \theta_2 : \mathcal{R}_{\geq 0} \rightarrow \mathcal{R}_{\geq}$ are continuous.

Assumption 6.6 *Equation $\dot{\boldsymbol{x}}_2 = h(\boldsymbol{x}_2, t)$ is globally uniformly asymptotically stable and for all $t_0 \geq 0$,*

$$\int_{t_0}^{\infty} ||\boldsymbol{x}_2(\boldsymbol{x}_2(t_0), t_0, t)|| dt \leq \alpha(||\boldsymbol{x}_2(t_0)||)$$

where function $\alpha(\cdot)$ is a class $\mathcal{K}$ function.

Theorem 6.7 *Consider the cascaded system of 6.12. Assume that the system $\dot{\boldsymbol{x}}_1 = f_1(x_1, t)$ is globally uniformly asymptotically stable with a Lyapunov function satisfying the inequality 6.13 and Assumptions 6.4 and 6.5 of Theorem 6.6. Then the cascaded system is globally uniformly stable.*

Chapter 7

ADCS Stability Analysis

There are two possible lines of action in the stability analysis. These are designing the controller in such a way that a separation principle exists for a given system, or designing the controller independently and then prove the total system to have properties such that a separation principle exists. The latter method is taken here, where the ADCS is analysed using the controllers from Chapter 5.

7.1 Method

The construction of the control system is done according to the procedure of Chapter 6.2.3, where a controller and an observer are designed and analyzed in turn before the total ICS is treated. Due to the cascaded structure of the ICS, the method of stability analysis will be use of Theorem 6.7. To do this, the system must be written on the form

$$\begin{aligned} \Sigma_1 : \dot{\boldsymbol{x}}_1 &= \boldsymbol{A}_c(\boldsymbol{x}_1)\boldsymbol{x}_1 + g(\boldsymbol{x})\boldsymbol{x}_2 \\ \Sigma_2 : \dot{\boldsymbol{x}}_2 &= \boldsymbol{A}_o(\boldsymbol{x}_1)\boldsymbol{x}_2 \end{aligned} \tag{7.1}$$

which is similar to the system in Equation 6.12. With this method of separating the subsystems, the controller ($\boldsymbol{A}_c$) and the observer ($\boldsymbol{A}_o$) can be designed independently whenever Assumptions 1-3 below are satisfied. The function $g(\cdot)$ represents the interconnection dynamics, see Figure 6.1.

Assumption 1: The state feedback controller is proven globally asymptotically stable or better.

Assumption 2: The observer is proven globally asymptotically stable or better.

Assumption 3: The interconnection dynamics are uniformly bounded, fulfils the Lipschitz criterion and is continuous for all time.

Observer error:	$\tilde{\boldsymbol{q}} = \boldsymbol{q} \otimes \hat{\boldsymbol{q}}^{-1}$
State feedback controller error:	$\boldsymbol{q}_e = \boldsymbol{q} \otimes \boldsymbol{q}_d^{-1}$
Output feedback controller error:	$\hat{\boldsymbol{q}}_e = \hat{\boldsymbol{q}} \otimes \boldsymbol{q}_d^{-1}$
Interconnection controller error:	$\tilde{\boldsymbol{q}_e} = \boldsymbol{q}_e \otimes \hat{\boldsymbol{q}}_e^{-1} = \boldsymbol{q} \otimes \hat{\boldsymbol{q}}^{-1}$

Table 7.1: An overview of the errors in the controller and observer

7.2 Separation principle

So far, the satellite is proven asymptotically stable with the state feedback controllers in Chapter 5. Also, a globally exponentially stable observer has been designed. The question of overall stability arises when the controller uses the estimated states instead of the actual states, so that a cascaded system is formed.

Some changes in notation are necessary: The controller errors will now be denoted $\boldsymbol{q}_e$ and $\boldsymbol{\omega}_e$, while $\tilde{\boldsymbol{q}}$ and $\tilde{\boldsymbol{\omega}}$ denotes errors in the observer estimates. The controller error based on the attitude estimate becomes $\hat{\boldsymbol{q}}_e = \hat{\boldsymbol{q}} \otimes \boldsymbol{q}_d$, and so the total attitude error including the estimation error is described by $\tilde{\boldsymbol{q}}_e = \boldsymbol{q}_e \otimes \hat{\boldsymbol{q}}_e = \boldsymbol{q} \otimes \hat{\boldsymbol{q}}$, see Table 7.1.

7.2.1 PD-controller

It has been shown in Chapter 5.3 that the control law

$$\boldsymbol{\tau}' = -\boldsymbol{K}_P \boldsymbol{\epsilon}_e - \boldsymbol{K}_D \boldsymbol{\omega}$$

corresponds to the system dynamics

$$\boldsymbol{J}\dot{\boldsymbol{\omega}} = -\boldsymbol{K}_P \tilde{\boldsymbol{\epsilon}} - \boldsymbol{K}_D \boldsymbol{\omega}.$$

Changing $\boldsymbol{\tau}'$ into an output feedback controller yields

$$\boldsymbol{\tau} = -\boldsymbol{K}_P \hat{\boldsymbol{\epsilon}} - \boldsymbol{K}_D \hat{\boldsymbol{\omega}}$$

The tracking and observer error can now be defined in the fashion of 7.1: $\boldsymbol{x}_1 = \begin{bmatrix} \boldsymbol{q}_e & \boldsymbol{\omega} \end{bmatrix}$ and $\boldsymbol{x}_2 = \begin{bmatrix} \tilde{\boldsymbol{q}} & \tilde{\boldsymbol{b}} & \tilde{\boldsymbol{\Delta}} \end{bmatrix}$. The tracking error dynamics become

$$\begin{bmatrix} \dot{\boldsymbol{q}}_e \\ \dot{\boldsymbol{\omega}} \end{bmatrix} = \boldsymbol{A}_c \begin{bmatrix} \boldsymbol{q}_e \\ \boldsymbol{\omega} \end{bmatrix}, \quad \boldsymbol{A}_c = \begin{bmatrix} 0 & \boldsymbol{T}(\boldsymbol{q}_e) \\ -\boldsymbol{J}^{-1}\boldsymbol{K}_P\boldsymbol{E} & -\boldsymbol{J}^{-1}\boldsymbol{K}_D \end{bmatrix},$$

and the observer error dynamics are

$$\begin{bmatrix} \dot{\tilde{\boldsymbol{q}}} \\ \dot{\tilde{\boldsymbol{b}}} \\ \dot{\tilde{\boldsymbol{\Delta}}} \end{bmatrix} = \boldsymbol{A}_o \begin{bmatrix} \tilde{\boldsymbol{q}} \\ \tilde{\boldsymbol{b}} \\ \tilde{\boldsymbol{\Delta}} \end{bmatrix}, \quad \boldsymbol{A}_o = \begin{bmatrix} -\boldsymbol{K}_1\boldsymbol{T}(\tilde{\boldsymbol{q}})f(\tilde{\boldsymbol{q}}) & \boldsymbol{T}(\tilde{\boldsymbol{q}}) & \boldsymbol{T}(\tilde{\boldsymbol{q}})\boldsymbol{\omega}_{gyro} \\ -\frac{1}{2}\boldsymbol{K}_2 f(\tilde{\boldsymbol{q}}) & -\boldsymbol{T}^{-1} & 0 \\ -\frac{1}{2}\boldsymbol{K}_3\boldsymbol{\omega}_{gyro} f(\tilde{\boldsymbol{q}}) & 0 & -\boldsymbol{T}_2^{-1} \end{bmatrix},$$

where $f(\tilde{\boldsymbol{q}}) = \tilde{\boldsymbol{\epsilon}}\,\mathrm{sgn}(\tilde{\eta})$ and $\boldsymbol{E}$ is a 3×4 matrix such that $\tilde{\boldsymbol{\epsilon}} = \boldsymbol{E}\tilde{\boldsymbol{q}}$.

Interconnection dynamics

From Figure 6.1 it can be seen that the control input can be written as $\boldsymbol{\tau} = \boldsymbol{\tau}' + g(\boldsymbol{x})\boldsymbol{x}_2$. The function $g(\cdot)$ represents the errors arising from basing the control law on the estimated states instead of the true ones.

Now, the control and observer dynamics are defined, so in order to analyse the stability properties of the interconnected system, the interconnection dynamics $g(\cdot)$ must fulfil certain requirements, as presented in Chapter 6. Computing the interconnection dynamics yields:

$$g(\boldsymbol{x})\boldsymbol{x}_2 = \boldsymbol{\tau} - \boldsymbol{\tau}'$$

The immediate goal is to factorize the right-hand side so that $\boldsymbol{x}_2$ may be cancelled and $g(\boldsymbol{x})$ analyzed separately. Inserting for the control laws gives

$$\begin{aligned} g(\boldsymbol{x})\boldsymbol{x}_2 =& \boldsymbol{K}_P\tilde{\boldsymbol{\epsilon}} + \boldsymbol{K}_D\tilde{\omega} \\ =& \begin{bmatrix} \boldsymbol{K}_P & \boldsymbol{K}_D \end{bmatrix} \boldsymbol{x}_2 \end{aligned} \tag{7.2}$$

Completeness

The cascaded system can now be written on the form

$$\begin{aligned} \Sigma_1 : \dot{\boldsymbol{x}}_1 =& \boldsymbol{A}_c(\boldsymbol{x}_1)\boldsymbol{x}_1 + g(\boldsymbol{x})\boldsymbol{x}_2 \\ \Sigma_2 : \dot{\boldsymbol{x}}_2 =& \boldsymbol{A}_o(\boldsymbol{x}_1)\boldsymbol{x}_2. \end{aligned} \tag{7.3}$$

Notice that the dynamics of Σ_2 are not decoupled from that of Σ_1 due to the presence of ω_{gyro} in Σ_2. So in order to consider the total system as a cascade, it must be shown that the system is complete. I.e. that the solutions $\boldsymbol{x}_1(t), \boldsymbol{x}_2(t)$ exist for all time.

Consider the Lyapunov function candidate

$$V(\boldsymbol{x}) = \frac{1}{2}{\boldsymbol{x}_1}^T P_c \boldsymbol{x}_1 + \frac{1}{2}{\boldsymbol{x}_2}^T P_o \boldsymbol{x}_2. \tag{7.4}$$

Its derivative along the trajectories of Equation 7.3 is

$$\dot{V}(\boldsymbol{x}) = -{\boldsymbol{x}_1}^T P_c \boldsymbol{A}_c \boldsymbol{x}_1 + {\boldsymbol{x}_1}^T P_c g(\boldsymbol{x})\boldsymbol{x}_2 - {\boldsymbol{x}_2}^T P_o \boldsymbol{A}_o \boldsymbol{x}_2. \tag{7.5}$$

Global exponential stability has been proved for the controller and observer dynamics, hence $P_c, P_o \in \mathcal{R}_{>0}$ is a safe assumption. Accordingly, Equation 7.5 may be written as

$$\dot{V}(\boldsymbol{x}) = -{\boldsymbol{x}_1}^T Q_c \boldsymbol{x}_1 + {\boldsymbol{x}_1}^T P_c g(\boldsymbol{x})\boldsymbol{x}_2 - {\boldsymbol{x}_2}^T Q_o \boldsymbol{x}_2, \tag{7.6}$$

where $\boldsymbol{Q}_c, \boldsymbol{Q}_o \in \mathcal{R}_{>0}$. As for the interconnection term, Equation 7.2 shows that it is bounded for any $\boldsymbol{x}$. This comes from the facts that $\boldsymbol{q}$ is bounded by definition, and that the assumption $\boldsymbol{\omega} \in \mathcal{L}_\infty$ gives $\tilde{\boldsymbol{\omega}} \in \mathcal{L}_\infty$ due to the exponential stability of

the observer. Hence, there exist a constant $k_1 > 0$ such that $||\boldsymbol{g}(\boldsymbol{x})|| \leq k_1$ for all $\boldsymbol{x}$. Equation 7.6 can now be shortened to

$$\dot{V}(\boldsymbol{x}) \leq \lambda k_1 ||\boldsymbol{x}_1|| ||\boldsymbol{x}_2||,$$

where $\lambda = \lambda_{max}(\boldsymbol{P}_c) < \infty$ is the largest eigenvalue of P_c. The Schwarz inequality (2.15) now gives

$$\dot{V}(\boldsymbol{x}) \leq \lambda k_1 ||\boldsymbol{x}_1|| ||\boldsymbol{x}_2|| \leq 2\lambda k_1 (||\boldsymbol{x}_1||^2 + ||\boldsymbol{x}_2||^2). \tag{7.7}$$

From this, by combining Equations 7.7 and 7.4, it is clear that there exists a constant k_2 such that $\dot{V}(\boldsymbol{x}) \leq k_2 V(\boldsymbol{x})$. By the comparison lemma (2.2) it follows that there exists a constant k_3 such that $V(\boldsymbol{x}, t) \leq k_2 V(\boldsymbol{x}, t_0) e^{-k_3(t-t_0)}$. This proves that $V(\boldsymbol{x})$ exists and is bounded for all bounded t. Since $V(\boldsymbol{x})$ is a Lyapunov function for the system 7.3 it can be concluded that the solutions $\boldsymbol{x}(t)$ exist and can be continued for all t. The closed-loop system is complete. The observer dynamics $\dot{\boldsymbol{x}}_2 = \boldsymbol{A}_o(\boldsymbol{x}_1(t))$ can be written as $\dot{\boldsymbol{x}}_2 = \boldsymbol{A}_o(t)$.

Stability analysis of the cascade

Established properties of the ICS are:

i) The observer is globally exponentially stable uniformly in the tracking error $\boldsymbol{x}_1$.

ii) The controller is globally asymptotically stable.

iii) The solutions of the closed-loop system exist for all $t \geq 0$.

iv) The ICS has a cascaded structure.

Also, the system fulfils the following requirements raised by Theorem 6.7:

Assumption 6.4: The following Lyapunov function have been established:

$$V = (\boldsymbol{K}_P + k\boldsymbol{K}_D)((\tilde{\eta} - 1)^2 + \tilde{\boldsymbol{\epsilon}}^T \tilde{\boldsymbol{\epsilon}}) + \frac{1}{2}\tilde{\boldsymbol{\omega}} \boldsymbol{J} \tilde{\boldsymbol{\omega}} + k\tilde{\boldsymbol{\epsilon}} \boldsymbol{J} \tilde{\boldsymbol{\omega}}.$$

Notice that

$$||\frac{\delta V}{\delta \boldsymbol{x}_1}|| ||\boldsymbol{x}_1|| \leq max\{2\lambda_{max}(\boldsymbol{K}_P), 2k\lambda_{max}(\boldsymbol{K}_D), \lambda_{max}(\boldsymbol{J}), k\lambda_{max}(\boldsymbol{J}), 1\} ||\boldsymbol{x}_1||^2.$$

From this it can be seen that

$$||\frac{\delta V}{\delta \boldsymbol{x}_1}|| ||\boldsymbol{x}_1|| \leq k_4 V_c(\boldsymbol{x}_1, t) \qquad \forall ||\boldsymbol{x}_1|| \geq \upsilon$$

where $k_4, \upsilon > 0$ is satisfied choosing

$$k_4 \geq \frac{max\{2\lambda_{max}(\boldsymbol{K}_P), 2k\lambda_{max}(\boldsymbol{K}_D), \lambda_{max}(\boldsymbol{J}), k\lambda_{max}(\boldsymbol{J}), 1\}}{min\{2\lambda_{max}(\boldsymbol{K}_P), 2k\lambda_{max}(\boldsymbol{K}_D), \lambda_{max}(\boldsymbol{J}), k\lambda_{max}(\boldsymbol{J}), 1\}}$$

Assumption 6.5: The growth rate of the interconnection dynamics due to the tracking error satisfies

$$||g(\boldsymbol{x})|| \leq || \begin{bmatrix} \boldsymbol{K}_P & \boldsymbol{K}_D \end{bmatrix}$$
$$||g(\boldsymbol{x})|| \leq \lambda_{max}(\boldsymbol{K}_P) + \lambda_{max}(\boldsymbol{K}_D).$$

Assumption 6.6: Since the observer error dynamics are exponentially stable, there will for all initial conditions $x_1(t_0)$ exist some positive constants k_5 and k_6 such that $||\boldsymbol{x}_2(t)|| \leq k_5||\boldsymbol{x}_2(t_0)||e^{-k_6(t-t_0)}$. This suggests to choose e.g. $\alpha(||\boldsymbol{x}_2(t_0)||) = (k_5)||\boldsymbol{x}_2(t_0)||$.

By Theorem 6.7, the ICS in 7.3 is globally uniformly asymptotically stable.

7.2.2 Model-dependent linearizing controller

It has been shown that the control law

$$\boldsymbol{\tau}' = -\boldsymbol{J}^{-1}\boldsymbol{S}(\boldsymbol{\omega})\boldsymbol{\omega}_{io}^b + \boldsymbol{S}(\boldsymbol{\omega}_{\boldsymbol{io}}^{\boldsymbol{b}} + \boldsymbol{\omega})\boldsymbol{J}(\boldsymbol{\omega}_{\boldsymbol{io}}^{\boldsymbol{b}} + \boldsymbol{\omega}) - \boldsymbol{\tau}_g - \boldsymbol{K_D}\boldsymbol{\omega_e} - \boldsymbol{K_D}\kappa\boldsymbol{\epsilon}_e - \boldsymbol{Ja}$$

corresponds to the system dynamics

$$\boldsymbol{J}\dot{\boldsymbol{\omega}} = -\boldsymbol{K}_D\omega_e - \boldsymbol{K}_D\kappa\boldsymbol{\epsilon}_e - \boldsymbol{Ja}.$$

Changing $\boldsymbol{\tau}'$ into an output feedback controller yields

$$\boldsymbol{\tau} = -\boldsymbol{JS}(\hat{\boldsymbol{\omega}})\boldsymbol{\omega}_{io}^b + \boldsymbol{S}(\boldsymbol{\omega}_{io}^b + \hat{\boldsymbol{\omega}}) - \boldsymbol{\tau}_g - \boldsymbol{K_D}\hat{\boldsymbol{\omega}} - \boldsymbol{K_D}\kappa\hat{\boldsymbol{\epsilon}}_e(t) - \boldsymbol{J}\kappa\boldsymbol{T}_2(\hat{\epsilon})\hat{\boldsymbol{\omega}}.$$

The tracking and observer error can now be defined in the fashion of 7.1: $\boldsymbol{x}_1 = \begin{bmatrix} \boldsymbol{q}_e & \boldsymbol{\omega} \end{bmatrix}$ and $\boldsymbol{x}_2 = \begin{bmatrix} \tilde{\boldsymbol{q}} & \tilde{\boldsymbol{b}} & \tilde{\boldsymbol{\Delta}} \end{bmatrix}$. The tracking error dynamics become

$$\begin{bmatrix} \dot{\boldsymbol{q}}_e \\ \dot{\boldsymbol{\omega}} \end{bmatrix} = \boldsymbol{A}_c \begin{bmatrix} \boldsymbol{q}_e \\ \boldsymbol{\omega} \end{bmatrix}, \quad \boldsymbol{A}_c = \begin{bmatrix} 0 & \boldsymbol{T}(\boldsymbol{q}_e) \\ -\boldsymbol{J}^{-1}\kappa\boldsymbol{K}_D\boldsymbol{E} & -\boldsymbol{J}^{-1}\boldsymbol{K}_D - \kappa\boldsymbol{T}_2(\boldsymbol{\epsilon}_e) \end{bmatrix},$$

and the observer error dynamics are

$$\begin{bmatrix} \dot{\tilde{\boldsymbol{q}}} \\ \dot{\tilde{\boldsymbol{b}}} \\ \dot{\tilde{\boldsymbol{\Delta}}} \end{bmatrix} = \boldsymbol{A}_o \begin{bmatrix} \tilde{\boldsymbol{q}} \\ \tilde{\boldsymbol{b}} \\ \tilde{\boldsymbol{\Delta}} \end{bmatrix}, \quad \boldsymbol{A}_o = \begin{bmatrix} -\boldsymbol{K}_1\boldsymbol{T}(\tilde{\boldsymbol{q}})f(\tilde{\boldsymbol{q}}) & \boldsymbol{T}(\tilde{\boldsymbol{q}}) & \boldsymbol{T}(\tilde{\boldsymbol{q}})\boldsymbol{\omega}_{gyro} \\ -\frac{1}{2}\boldsymbol{K}_2 f(\tilde{\boldsymbol{q}}) & -\boldsymbol{T}^{-1} & 0 \\ -\frac{1}{2}\boldsymbol{K}_3\boldsymbol{\omega}_{gyro}f(\tilde{\boldsymbol{q}}) & 0 & -\boldsymbol{T}_2^{-1} \end{bmatrix},$$

where $f(\tilde{\boldsymbol{q}}) = \tilde{\boldsymbol{\epsilon}}\,\mathrm{sgn}(\tilde{\eta})$ and $\boldsymbol{E}$ is a 3×4 matrix such that $\tilde{\boldsymbol{\epsilon}} = \boldsymbol{E}\tilde{\boldsymbol{q}}$.

Interconnection dynamics

From Figure 6.1 it can be seen that the control input can be written as $\boldsymbol{\tau} = \boldsymbol{\tau}' + g(\boldsymbol{x})\boldsymbol{x}_2$. The function $g(\cdot)$ represents the errors arising from basing the control law on the estimated states instead of the true ones.

Now, the control and observer dynamics are defined, so in order to analyse the stability properties of the interconnected system, the interconnection dynamics $g(\cdot)$ must fulfil certain requirements, as presented in Chapter 6. Computing the interconnection dynamics yields:

$$g(\boldsymbol{x})\boldsymbol{x}_2 = \boldsymbol{\tau} - \boldsymbol{\tau}^{'}$$

The immediate goal is to factorize the right-hand side so that $\boldsymbol{x}_2$ may be cancelled and $g(\boldsymbol{x})$ analyzed separately. Inserting for the control laws gives

$$\begin{aligned} g(\boldsymbol{x})\boldsymbol{x}_2 =& \boldsymbol{J}^{-1}\boldsymbol{S}(\tilde{\boldsymbol{\omega}})\boldsymbol{\omega}_{io}^b \\ &- \left[\boldsymbol{S}(\boldsymbol{\omega}_{io}^b + \hat{\boldsymbol{\omega}})\boldsymbol{J}(\boldsymbol{\omega}_{io}^b + \hat{\boldsymbol{\omega}}) - \boldsymbol{S}(\boldsymbol{\omega}_{io}^b + \boldsymbol{\omega})\boldsymbol{J}(\boldsymbol{\omega}_{io}^b + \boldsymbol{\omega})\right] \\ &+ \boldsymbol{K}_D(\tilde{\boldsymbol{\omega}} + \kappa\tilde{\boldsymbol{\epsilon}}_e) \\ &+ \frac{1}{2}\kappa(\tilde{\eta}\boldsymbol{I} + \boldsymbol{S}(\tilde{\epsilon}_e))\tilde{\boldsymbol{\omega}} + \tilde{\boldsymbol{\tau}}_g \end{aligned} \tag{7.8}$$

Using the property of skew-symmetric matrices in Equation 2.2 allows to rewrite some terms in Equation 7.8:

$$\boldsymbol{J}^{-1}\boldsymbol{S}(\tilde{\boldsymbol{\omega}})\boldsymbol{\omega}_{io}^b = \boldsymbol{J}^{-1}\boldsymbol{S}(\boldsymbol{\omega}_{io}^b)^T\tilde{\boldsymbol{\omega}}$$

$$\begin{aligned} &\boldsymbol{S}(\boldsymbol{\omega}_{io}^b + \hat{\boldsymbol{\omega}})\boldsymbol{J}(\boldsymbol{\omega}_{io}^b + \hat{\boldsymbol{\omega}}) - \boldsymbol{S}(\boldsymbol{\omega}_{io}^b + \boldsymbol{\omega})\boldsymbol{J}(\boldsymbol{\omega}_{io}^b + \boldsymbol{\omega}) \\ =& -\boldsymbol{S}(\boldsymbol{\omega}_{io}^b)\boldsymbol{J}\tilde{\boldsymbol{\omega}} + \boldsymbol{S}(\boldsymbol{J}\boldsymbol{\omega}_{io}^b)\tilde{\boldsymbol{\omega}} + [\boldsymbol{S}(\hat{\boldsymbol{\omega}})\boldsymbol{J}\hat{\omega} - \boldsymbol{S}(\boldsymbol{\omega})\boldsymbol{J}\omega] \end{aligned} \tag{7.9}$$

$$\tilde{\boldsymbol{\tau}}_g = 3{\omega_0}^2\left[\boldsymbol{S}(\hat{\boldsymbol{c_3}})\boldsymbol{J}\hat{c_3} - \boldsymbol{S}(\boldsymbol{c_3})\boldsymbol{J}\boldsymbol{c_3}\right]$$

Now there are two terms in square brackets in Equation 7.9 which need to be rewritten in a way that allows factorization. It is practical to introduce the matrix $\Upsilon_{\boldsymbol{\upsilon},\hat{\boldsymbol{\upsilon}}} \subset \mathcal{R}^{3\times 3}$ where $\tilde{\upsilon}_i = \upsilon_i - \hat{\upsilon}_i$, with elements

$$\begin{aligned} \Upsilon_{11} &= -j_7\upsilon_2 + j_4\upsilon_3 \\ \Upsilon_{12} &= -j_7(\upsilon_1 - \tilde{\upsilon}_1) - j_8(2\upsilon_2 - \tilde{\upsilon}_2) + j_5(\upsilon_3 - \tilde{\upsilon}_3) - j_9\upsilon_3 \\ \Upsilon_{13} &= j_4(\upsilon_1 - \tilde{\upsilon}_1) - j_9(\upsilon_2 - \tilde{\upsilon}_2) + j_6(2\upsilon_3 - \tilde{\upsilon}_3) + j_5\upsilon_2 \\ \Upsilon_{21} &= j_7(2\upsilon_1 - \tilde{\upsilon}_1) + j_8(\upsilon_2 - \tilde{\upsilon}_2) - j_1(\upsilon_3 - \tilde{\upsilon}_3) + j_9\upsilon_3 \\ \Upsilon_{22} &= j_8\upsilon_1 - j_2\upsilon_3 \\ \Upsilon_{23} &= j_9(\upsilon_1 - \tilde{\upsilon}_1) - j_2(\upsilon_2 - \tilde{\upsilon}_2) + j_3(2\upsilon_3 - \tilde{\upsilon}_3) - j_1\upsilon_1 \\ \Upsilon_{31} &= -j_4(2\upsilon_1 - \tilde{\upsilon}_1) + j_1(\upsilon_2 - \tilde{\upsilon}_2) - j_6(\upsilon_3 - \tilde{\upsilon}_3) - j_5\upsilon_2 \\ \Upsilon_{32} &= -j_5(\upsilon_1 - \tilde{\upsilon}_1) + j_2(2\upsilon_2 - \tilde{\upsilon}_2) + j_3(\upsilon_3 - \tilde{\upsilon}_3) + j_1\upsilon_1 \\ \Upsilon_{33} &= -j_6\upsilon_1 + j_3\upsilon_2 \end{aligned} \tag{7.10}$$

such that

$$[\boldsymbol{S}(\hat{\boldsymbol{\upsilon}})\boldsymbol{J}\hat{\upsilon} - \boldsymbol{S}(\boldsymbol{\upsilon})\boldsymbol{J}\boldsymbol{\upsilon}] = \Upsilon_{\boldsymbol{\upsilon},\hat{\boldsymbol{\upsilon}}}\tilde{\boldsymbol{\upsilon}},$$

It can then be shown that the bracketed expressions may be written as

$$[\boldsymbol{S}(\hat{\boldsymbol{\omega}})\boldsymbol{J}\hat{\omega} - \boldsymbol{S}(\boldsymbol{\omega})\boldsymbol{J}\omega] = \Upsilon_{\boldsymbol{\omega},\hat{\boldsymbol{\omega}}}\tilde{\boldsymbol{\omega}}$$
$$\tilde{\boldsymbol{\tau}}_g = 3{\omega_0}^2\Upsilon_{\boldsymbol{c_3},\hat{\boldsymbol{c}}_3}\tilde{\boldsymbol{c}}_3.$$

The term $\tilde{\boldsymbol{c}}_3$ corresponds to the third column of direction cosines in the rotation matrix in Equation 2.10:

$$\boldsymbol{c}_3 = \begin{bmatrix} 2(\epsilon_1\epsilon_3 + \eta\epsilon_2) \\ 2(\epsilon_2\epsilon_3 - \eta\epsilon_1) \\ \eta^2 - \epsilon_1^2 - \epsilon_2^2 + \epsilon_3^2 \end{bmatrix}$$

Rewriting allows to factorize as

$$\begin{aligned} \boldsymbol{c}_3 =& \begin{bmatrix} 2\tilde{\epsilon}_2 & 2\tilde{\epsilon}_3 & 0 & 0 \\ -2\tilde{\epsilon}_1 & 0 & 2\tilde{\epsilon}_3 & 0 \\ \tilde{\eta} & -\tilde{\epsilon}_1 & -\tilde{\epsilon}_2 & \tilde{\epsilon}_3 \end{bmatrix} \begin{bmatrix} \tilde{\eta} \\ \tilde{\epsilon}_1 \\ \tilde{\epsilon}_2 \\ \tilde{\epsilon}_3 \end{bmatrix} \\ =& \boldsymbol{c}(\tilde{\boldsymbol{q}})\tilde{\boldsymbol{q}}. \end{aligned} \tag{7.11}$$

Finally, Equation 7.8 can be simplified:

$$g(\boldsymbol{x})\boldsymbol{x}_2 = \begin{bmatrix} \boldsymbol{K}_D\lambda + 3{\omega_0}^2\Upsilon_{\boldsymbol{c_3},\hat{\boldsymbol{c}}_3}c(\tilde{\boldsymbol{q}}) \\ G_3 \end{bmatrix}^T \begin{bmatrix} \tilde{\boldsymbol{q}} \\ \tilde{\omega} \end{bmatrix}$$

$$g(\boldsymbol{x})\boldsymbol{x}_2 = \begin{bmatrix} \boldsymbol{K}_D\lambda + 3{\omega_0}^2\Upsilon_{\boldsymbol{c_3},\hat{\boldsymbol{c}}_3}c(\tilde{\boldsymbol{q}}) \\ G_3 \end{bmatrix}^T \boldsymbol{C_x} \begin{bmatrix} \tilde{\boldsymbol{q}} \\ \tilde{\boldsymbol{b}} \\ \tilde{\Delta} \end{bmatrix}. \tag{7.12}$$

In Equation 7.12, the measurement matrix $C_{\tilde{\eta}}$ defined as

$$C_{\tilde{\eta}} = \begin{bmatrix} 1 & 0 & 0 \\ -K_1 f(\tilde{\eta})\boldsymbol{E} & 1 & \boldsymbol{\omega}_{gyro} \end{bmatrix}$$

combines the measured bias and scale factor errors into angular velocity errors:

$$\begin{bmatrix} \tilde{\boldsymbol{q}} \\ \tilde{\omega} \end{bmatrix} = \boldsymbol{C_x} \begin{bmatrix} \tilde{\boldsymbol{q}} \\ \tilde{\boldsymbol{b}} \\ \tilde{\Delta} \end{bmatrix}$$

The errors arising from the angular velocity are for readability lumped together in $G_3 = -\boldsymbol{M}^{-1}\boldsymbol{S}(\omega_{io}^b) - \boldsymbol{S}(\boldsymbol{\omega}_{io}^b)\boldsymbol{M} + \boldsymbol{S}(\boldsymbol{M}\boldsymbol{\omega}_{io}^b) + \Upsilon_{\boldsymbol{\omega},\hat{\boldsymbol{\omega}}} + \boldsymbol{K}_D + \lambda(\tilde{\eta}\mathcal{I} - \boldsymbol{S}(\tilde{\epsilon}))$.

Completeness

The cascaded system can now be written on the form

$$\begin{aligned} \Sigma_1 : \dot{\boldsymbol{x}}_1 =& \boldsymbol{A}_c(\boldsymbol{x}_1)\boldsymbol{x}_1 + g(\boldsymbol{x})\boldsymbol{x}_2 \\ \Sigma_2 : \dot{\boldsymbol{x}}_2 =& \boldsymbol{A}_o(\boldsymbol{x}_1)\boldsymbol{x}_2. \end{aligned} \tag{7.13}$$

The observer is the same as in the case with the PD-controller, so the dynamics of Σ_2 are also here not decoupled from that of Σ_1 due to the presence of ω_{gyro} in Σ_2. In order to consider the total system as a cascade, it must be shown that the system is complete. I.e. that the solutions $\boldsymbol{x}_1(t), \boldsymbol{x}_2(t)$ exist for all time. The proof of this can be done in the same way as in the case of the PD-controller.

Stability analysis of the cascade

Established properties of the ICS are:

i) The observer is globally exponentially stable uniformly in the tracking error $\boldsymbol{x}_1$.

ii) The controller is globally asymptotically stable.

iii) The solutions of the closed-loop system exist for all $t \geq 0$.

iv) The ICS has a cascaded structure.

Also, the system fulfils the following requirements raised by Theorem 6.7:

Assumption 6.4: The following Lyapunov function have been established:

$$\boldsymbol{V} = 1/2\boldsymbol{s}^T\boldsymbol{J}\boldsymbol{s}.$$

Notice that

$$||\frac{\delta V_c}{\delta \boldsymbol{x}_1}||||\boldsymbol{x}_1|| \leq max\{\lambda_{max}(\boldsymbol{J}), \kappa\lambda_{max}(\boldsymbol{J}), 1\}||\boldsymbol{x}_1||^2.$$

From this it can be seen that

$$\begin{aligned} ||\frac{\delta V_c}{\delta \boldsymbol{x}_1}||||\boldsymbol{x}_1|| \leq & k_4 V_c(\boldsymbol{x}_1, t) \qquad \forall ||\boldsymbol{x}_1|| \geq \upsilon \\ ||\boldsymbol{s}^T\boldsymbol{J}||||\boldsymbol{s}|| \leq & \frac{k_4}{2} \end{aligned} \tag{7.14}$$

where $k_4, \upsilon > 0$, is satisfied choosing

$$k_4 \geq \frac{max\{\lambda_{max}(\boldsymbol{J}), \kappa\lambda_{max}(\boldsymbol{J}), 1\}}{min\{\lambda_{min}(\boldsymbol{J}), \kappa\lambda_{min}(\boldsymbol{J}), 1\}}.$$

Assumption 6.5: The growth rate of the interconnection dynamics due to the tracking error satisfies

$$||g(\boldsymbol{x})|| \leq || \begin{bmatrix} \boldsymbol{K}_D\lambda + 3{\omega_0}^2\Upsilon_{\boldsymbol{c_3},\tilde{\boldsymbol{c}}_3}c(\tilde{\boldsymbol{q}}) \\ G_3 \end{bmatrix}^T ||||C_{\tilde{\eta}}||.$$

Assumption 6.6: Since the observer error dynamics are exponentially stable, there will for all initial conditions $x_1(t_0)$ exist some positive constants k_5 and k_6 such that $||\boldsymbol{x}_2(t)|| \leq k_5||\boldsymbol{x}_2(t_0)||e^{-k_6(t-t_0)}$. This suggests to choose e.g. $\alpha(||\boldsymbol{x}_2(t_0)||) = (k_5)||\boldsymbol{x}_2(t_0)||$.

By Theorem 6.7, the ICS in Equation 7.13 is globally uniformly asymptotically stable.

7.2.3 Robust controller

The method of analysis used with the two first controllers was unsuccessful with the robust controller. Consider the state feedback control law

$$\boldsymbol{\tau}^{'} = -\frac{1}{2}[(\eta_e \boldsymbol{I} + \boldsymbol{S}(\boldsymbol{\epsilon}_e))\boldsymbol{K}_P + \gamma(1-\eta_e)\boldsymbol{I}]\boldsymbol{\epsilon}_e - \boldsymbol{K}_D\boldsymbol{\omega}_e$$

and the output feedback control law

$$\boldsymbol{\tau}^{=} - \frac{1}{2}[(\hat{\eta}\boldsymbol{I} + \boldsymbol{S}(\hat{\boldsymbol{\epsilon}}))\boldsymbol{K}_P + \gamma(1-\hat{\eta})\boldsymbol{I}]\hat{\boldsymbol{\epsilon}} - \boldsymbol{K}_D\hat{\boldsymbol{\omega}}.$$

Computing the interconnection dynamics as $g(\boldsymbol{x})\boldsymbol{x}_2 = \boldsymbol{\tau} - \boldsymbol{\tau}^{'}$ yields an expression which is nonlinear in $\boldsymbol{x}$ and very difficult to factorize.

Still not successful, but closer, is Theorem 6.5:

Condition i**)** It has been shown that the system is asymptotically stable with state feedback.

Condition ii**)** It has been shown that the observer is exponentially stable.

Condition iii**)** The system with state feedback is asymptotically stable uniformly in time.

Condition iv**)** The partial derivatives $\nabla_x h(\cdot), \nabla_{\hat{x}} h(\cdot)$ are bounded, since the observer is exponentially stable uniformly in time. The partial derivatives $\nabla_x f(\cdot, \tau(\hat{\boldsymbol{x}}, \cdot)), \nabla_{\hat{x}} f(\cdot, \tau(\hat{\boldsymbol{x}}, \cdot))$ are difficult to compute, shown in Equation 7.15.

$$\dot{\boldsymbol{\omega}} = -\boldsymbol{J}^{-1}\boldsymbol{S}(\boldsymbol{\omega})\boldsymbol{J}\boldsymbol{\omega} - \frac{1}{2}[(\hat{\eta}\boldsymbol{I} + \boldsymbol{S}(\hat{\boldsymbol{\epsilon}}))\boldsymbol{K}_P + \gamma(1-\hat{\eta})\boldsymbol{I}]\hat{\boldsymbol{\epsilon}} - \boldsymbol{K}_D\hat{\boldsymbol{\omega}} \quad (7.15)$$

Hence, with the assumption that the partial derivatives $\nabla_x f(\cdot), \nabla_{\hat{x}} f(\cdot) < \infty$ for all time, the system is globally uniformly asymptotically stable.

Chapter 8

Results

To be of use, the control system must provide a certain accuracy in the attitude control. The goal for the ESEO satellite was a maximum attitude uncertainty of $\pm 0.0001^{\circ}$. However, a satellite has numerous operating modes, with different demands to the level of accuracy. When the satellite is in motion, it will have to rotate continuously to stay with e.g. a camera pointing toward a fixed point in space or on the moon surface. In orbit, the satellite will have to compensate for the forward velocity and the force of gravity. Therefore, some tests should be performed to investigate the tracking abilities of the controllers. Other times it might be desirable to simply change the satellite attitude from a to b. A simple step-test will in this case reveal which level of performance the controller can deliver.

In order to do the simulations, a system model was made using Matlab with Simulink, see Figure 8.1 and Table 8.1. The same set of sensors were used in all tests, namely a star tracker developed at the Danish Technical University (Jørgensen et al. 2001) and a ring laser gyro (Fossen (2002) pp. 195). The Simulink models, simulation data and controller gains can be found on the project CD.

The performance of the ADCS is analysed using three of the controllers in

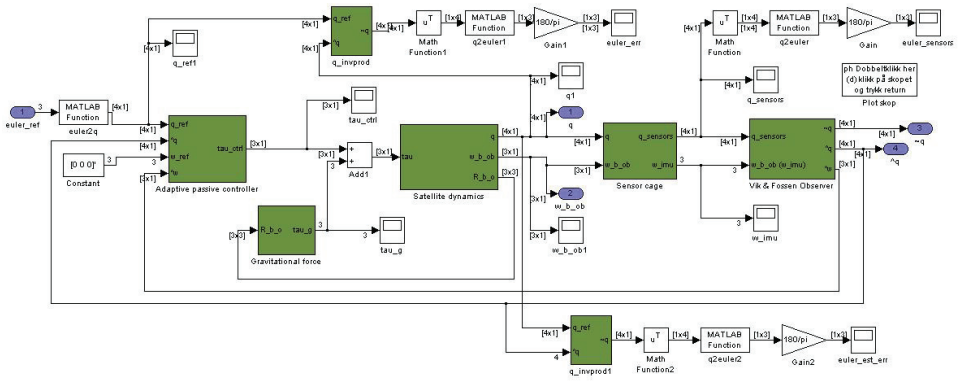

Figure 8.1: Overview of the ESMO ADCS model.

Software:	Matlab 7.2 (R2006a) with Simulink 6.4 (R2006a)
Solver:	ode45(Dormand-Prince)
Relative tolerance:	1e-3
Step sizes:	auto

Table 8.1: Simulink simulation parameters.

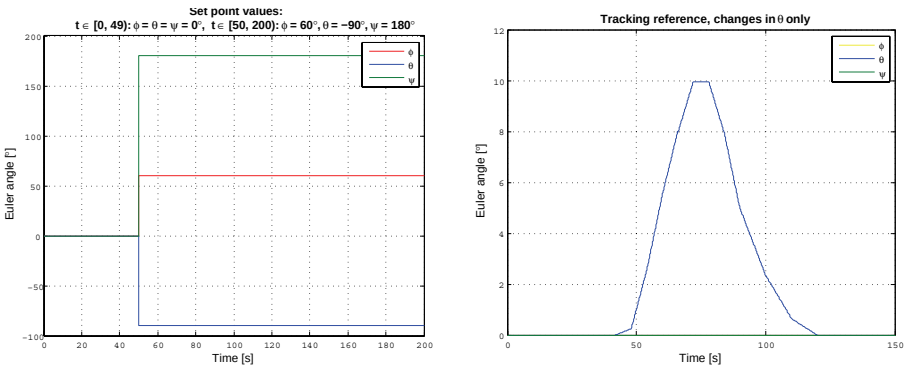

Figure 8.2: The setpoint values. Steps at $t \approx 50$.

Chapter 5. The same two tests were carried out for all three controllers:

1. A change in the attitude setpoints simultanously for all three angles. This type of test was chosen for two reasons: First, it represents a worst-case situation, since there are large deviations between setpoint and actual position and therefore a large amount of torque on the system. Second, it might also be a realistic scenario to adjust all setpoints at once, since from a user point of view one would like to simply input the desired orientation, without having to worry about which order of axis rotation will be taken.

2. A tracking test where a sinusoid signal is an approximation of the trajectory that needs to be followed if a satellite in orbit wants to keep an instrument directed towards a fixed point on the surface of the moon during in a period of time.

The setpoints are shown in Figure 8.2. The controllers are first studied one by one, then they are compared with regards to convergence, amount of noise and accuracy. As in the case of the ESMO satellite, $\pm 0.0001^\circ$ will be the definitive bound on oscillations accepted during steady-state operation. In addition to this, the initial states of the model was chosen arbitrarily to be far from the initial setpoints. Also, the initial states of the observer were chosen to reflect a worst-case situation e.g. if the observer algorithm is switched off and then on again after a period of time during which the attitude of the satellite has changed. For larger versions of the plots, see Appendix A.

8.1 Setpoint control

For comparison, the tests will be done for the controllers using both output feedback and state feedback. This might indicate the amount of impact the use of estimates has on the different controllers. The observer estimation errors are also plotted, to show to which extent the control torque influences the observer.

8.1.1 Model-based linearizing controller

The plots in Figure 8.3 show the attitude error $\boldsymbol{q}_e = \boldsymbol{q} \otimes \boldsymbol{q}_d^{-1}$ converted to Euler angles. Approximately 60 seconds pass after the step before the satellite regains steady-state. The controller is relatively fast in the beginning of the transient period and comes into a $< 10^\circ$ range of the setpoints after only 10 seconds. Convergence after that is slow. If actuator dynamics and physical limitations in the thrusters were taken into account, it is probable that performance would aggravate severly since it would take a long time for the error even to enter the $< 10^\circ$ range. By adjusting the controller gains it is possible to speed up convergence, but at the cost of signal noise with amplitude well above the 0.0001° bound.

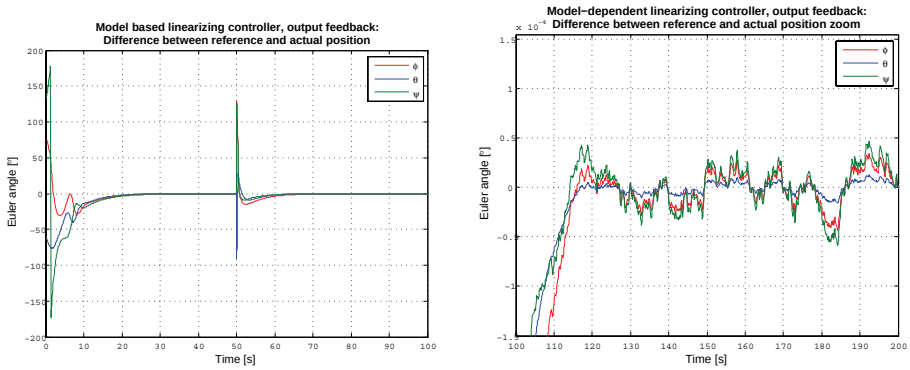

Figure 8.3: Plots of the deviation between setpoints and actual position when the control system consists of observer and linearizing controller.

The plots in Figure 8.4 shows how the estimation error $\tilde{\boldsymbol{q}} = \boldsymbol{q} \otimes \hat{\boldsymbol{q}}^{-1}$ takes approximately 60 seconds to converge. The performance of the observer is clearly best during steady-state operation. This is not surprising, since it was designed mainly to filter noise, not predict changes in the attitude.

The performance of the controller when using the actual states is interesting to note. Figure 8.5 shows a considerable improvement in the convergence rate, compared to Figure 8.3. Clearly, the performance of the controller is prone to suffer during feedback from estimated states. This weakness might come from the control law being model-dependent.

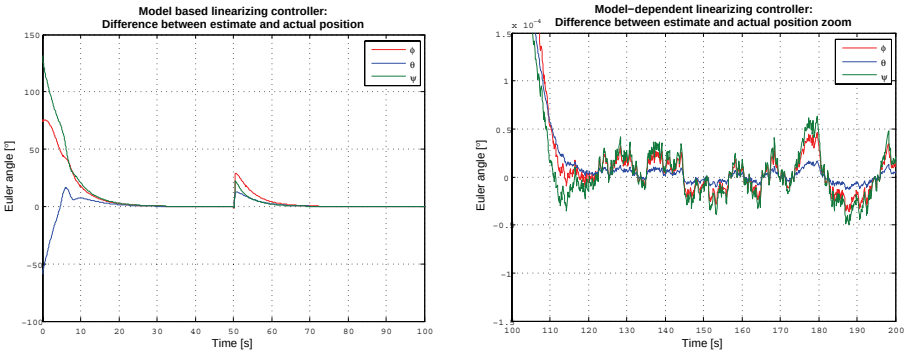

Figure 8.4: Plots of the estimation error with the linearizing controller.

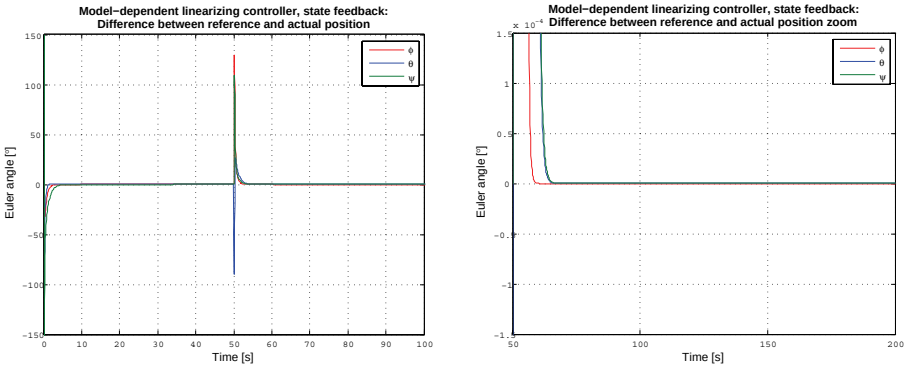

Figure 8.5: Plots of the deviation between setpoints and actual position during state feedback.

8.1.2 Robust controller

The plots in Figure 8.6 show the attitude error $\boldsymbol{q}_e = \boldsymbol{q} \otimes \boldsymbol{q}_d^{-1}$ converted to Euler angles. Almost 60 seconds pass after the step before the satellite regains steady-state. The controller is converges slowly right after the setpoints change, but converges to steady-state in the same amount of time as the linearizing controller. The inclusion of actuator dynamics and physical limitations in the thrusters would probably make the controller more desirable, because convergence is relatively fast towards the end of the transient. Adjustment of the controller gains did not improve performance.

Due to the relatively slow changes in the attitude after the change in setpoint, the observer error is very small during the entire period of time as can be seen from Figure 8.7. Since this controller uses less rapid application of torque, the observer is less disturbed.

Figure 8.8 indicates that the robust controller shows no performance improvement when the true system states are fed back. This in contrast to the model-dependent linearizing controller, which improved severely. The robust controller

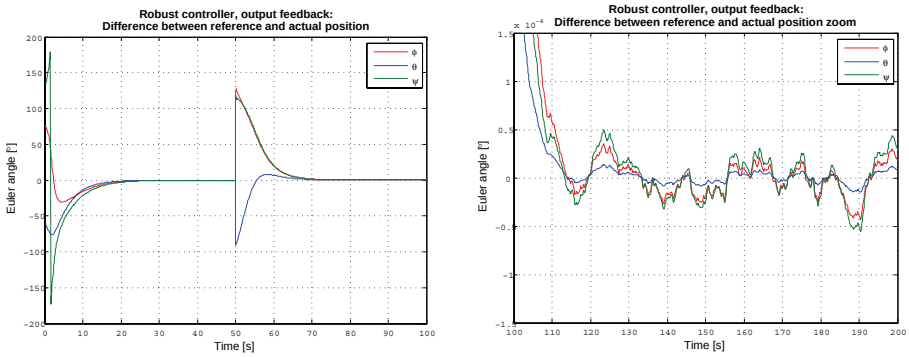

Figure 8.6: Plots of the deviation between setpoints and actual position when the control system consists of observer and robust controller.

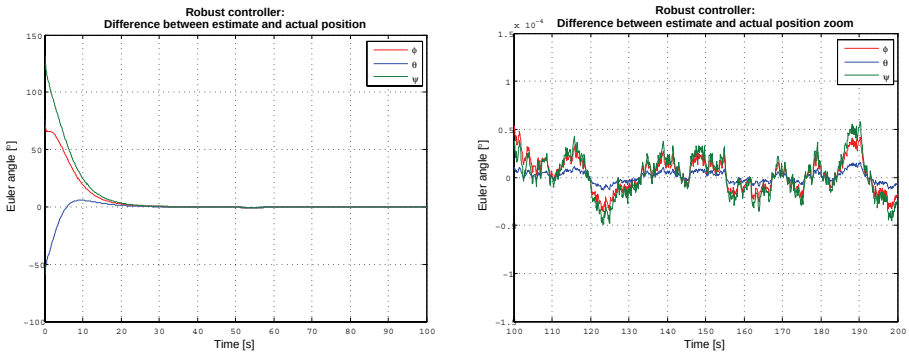

Figure 8.7: Plots of the estimation error with the robust controller.

is clearly robust with respect to noise and model uncertainties.

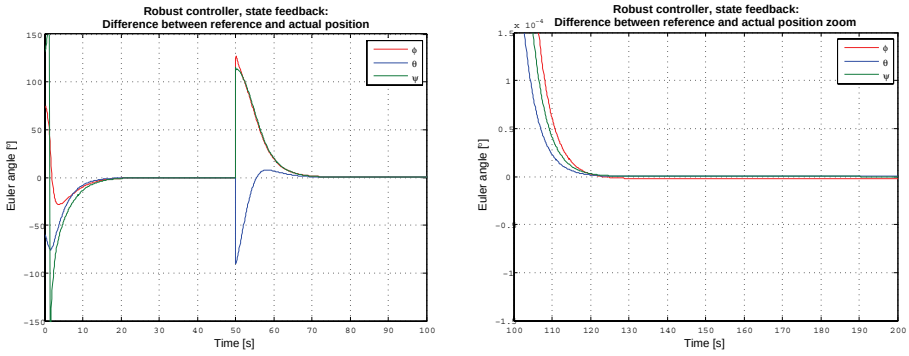

Figure 8.8: Plots of the deviation between setpoints and actual position during state feedback.

8.1.3 PD-controller

The plots in Figure 8.9 show the attitude error $\boldsymbol{q}_e = \boldsymbol{q} \otimes \boldsymbol{q}_d^{-1}$ converted to Euler angles. Approximately 20 seconds pass after the step before the satellite regains steady-state, and it is thus the fastest of the three controllers. The oscillations during steady-state are more significant than in the other controllers, but are kept inside the bound. The convergence ratio seems to be approximately constant, so it is not probable that the controller would be less or more desirable if actuator dynamics and physical limitations in the thrusters were taken into account. By adjusting the controller gains it is possible to speed up convergence, but at the cost of signal noise with amplitude above the $0.0001°$ bound.

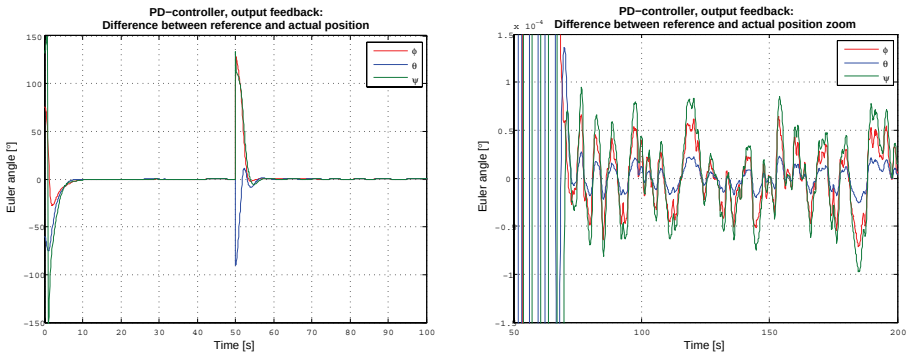

Figure 8.9: Plots of the deviation between setpoints and actual position when the control system consists of observer and PD-controller.

The observer error in Figure 8.10 is very small during the entire period of time. Comparing the zoomed plots of estimation error in the three control systems shows that the estimation error is the same for steady-state operation in all three cases.

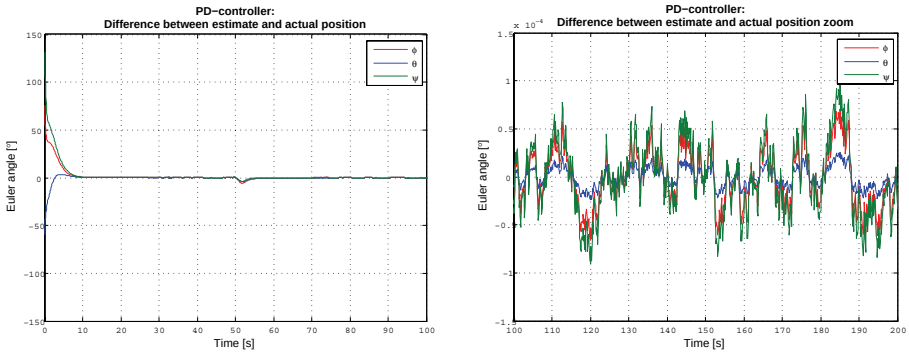

Figure 8.10: Plots of the estimation error with the PD-controller.

The PD-controller shows no or very little performance improvement when the true system states are fed back, see Figure 8.11. It is therefore robust with respect to noise and model uncertainties.

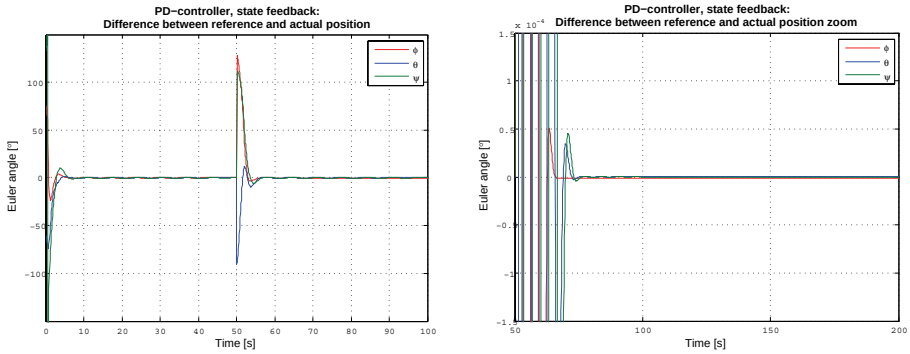

Figure 8.11: Plots of the deviation between setpoints and actual position during state feedback.

8.2 Tracking control

Tracking a constantly changing reference is different from adjusting to setpoint changes. None of the control laws tested here include terms that take into account the rate of change of $\boldsymbol{q}_d$, and excellent performance can therefore not be expected.

8.2.1 Model-based linearizing controller

From Figure 8.12 it can be seen that the linearizing controller actually performs worse in the case of state feedback than with output feedback. The difference is, however, relatively small.

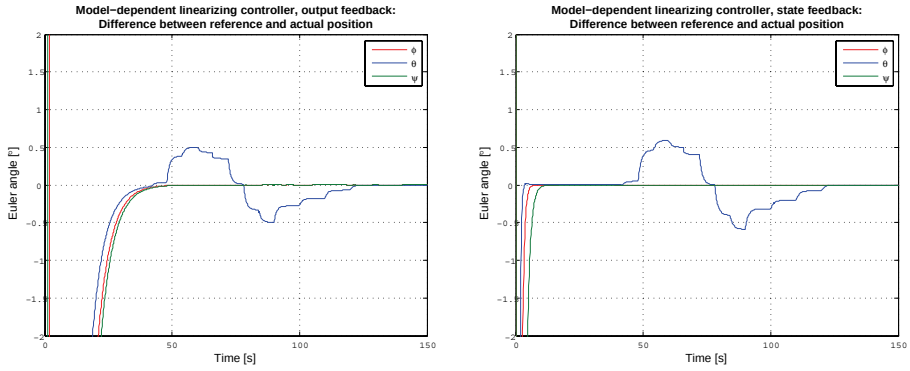

Figure 8.12: Tracking error of the linearizing controller.

8.2.2 Robust controller

The robust controller performs identically in the two cases shown in Figure 8.13. The error is up to 4 times that of the linearizing controller. This reflects what was shown in the setpoint tests; the robust controller is slow.

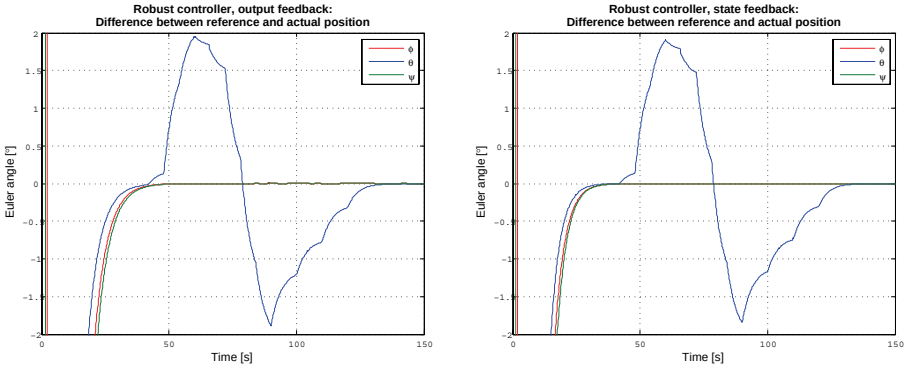

Figure 8.13: Tracking error of the robust controller.

8.2.3 PD-controller

The PD-controller showed to be fastest during the setpoint test. As seen from Figure 8.14, it performs very similar to the linearizing controller when tracking a reference.

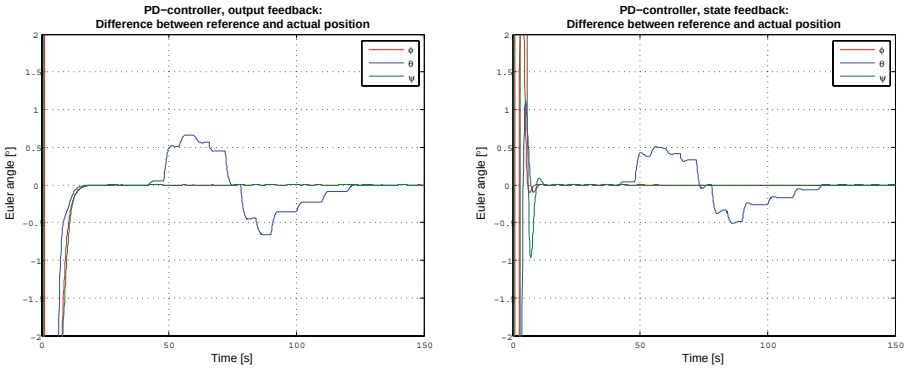

Figure 8.14: Tracking error of the PD-controller.

8.3 Recommendation

Of the three controllers presented here, the PD-controller is the best choice. It is approximately three times faster than the other two controllers. It has is more noisy oscillations during steady-state operation, but with tuning this can be smoothed without having to reduce the convergence speed down to the level of the other controllers. Additionally, it has been shown to be robust against modelling errors, and the PD control law algorithm is easy to understand and maintain.

The other two controllers might have more potential. They are more difficult to tune than the PD-controller, and it might be that more effort put into the tuning procedure would result in improved performance. Egeland & Godhavn (1994)

presents an expansion of the linearizing controller which includes an adaptive term in the control law. Such an adaptive term will make the control law more dynamic and less dependent on the model. If the adaptive update law is sufficiently fast, the controller might gain some robustness against noise and will probably perform better during tracking.

Chapter 9

Conclusions

As a large part of the thesis has been theoretical proofs of stability, the only practical results to comment are the simulation results of Chapter 8. The proofs of total stability in Chapter 7 were tedious and time consuming to work out, but their contribution is in practice simply to validate which controllers can be chosen for testing. On the other hand, without a proof of total stability, no controller/observer system is safe to use. In addition, since the stability proofs show for each control system the existence of a separation principle, the tuning procedures of the controllers and observers can be performed independently.

The ADCS was not shown globally uniformly asymptotically stable with the robust controller. The difficulties seem to arise from the structure of the control law, i.e. that it is difficult to write on the form $\dot{\boldsymbol{x}}_1 = \boldsymbol{A}_c(\boldsymbol{x}_1)\boldsymbol{x}_1$. This may indicate the the analysis method of cascaded systems is not well-suited for certain controllers, especially those not based on the plant model. On the other hand, it seems that the analysis method of cascaded systems can be said to work particularly well with model-dependent controllers.

9.1 Discussion of the results

All control configurations passed the setpoint tests with below 70 seconds of converge time. In the tracking test, none of the controllers performed entirely to satisfaction. One can not expect the same accuracy during tracking as during steady-state operation, but errors of $> 0.5^\circ$ may be too large to successfully operate a camera. If the purpose is to use equipment that has lower demands to accuracy, e.g. antennas, the accuracy obtained here for two of the controllers may suffice.

The PD-controller showed to be the fastest and one of the most robust alternatives. This came as a surprise, since it is also the simplest control algorithm. Especially, when comparing the system dynamics using the control law of the PD-controller, see Equation 5.24, to the system dynamics using the control law of the linearizing controller, see Equation 5.13, it is clear that the linearizing controller reduces to a PD-controller when the linearizing terms are cancelled. What is left is

a PD-controller and some (presumably small) nonlinear terms due to model noise and inaccuracies. In this light, the linearizing controller should outperform the PD-controller as long as the linearizing terms are close to being equal to the nonlinear terms of the model. With that said, the linearizing controller is somewhat more difficult to tune which may account for some of the unexpected performance.

9.2 Further work

Based on the work carried out during this thesis, some suggestions can be made as to how it can be improved.

Expand the satellite model: Before further analysis is done, the model should include reaction wheels and possibly other actuator dynamics, physical limitations and time delays.

Enhance the controllers presented herein: Especially, equip the linearizing controller with an adaptive term. This was suggested in Chapter 8 as the improvement with the most potential.

Complete the total stability proofs: The ADCS with the robust controller was not shown globally uniformly asymptotically stable. If the controller is to be used, a proof must be worked out.

Test the ADCS on a physical model: The Department of Engineering Cybernetics at NTNU have a gyro rig under development, which can be controlled from Matlab. Finishing the rig and testing the performance of the ADCS in practice with real-life data is a logical step towards a complete ADCS proposition.

Establish a documentation standard for proofs of stability: When implementing a control algorithm into a physical system, there should be a requirements to have documented proofs of stability. This should be interesting for e.g. insurance companies and all companies concerned with health, environment and safety standards. As of now, safety requirements include for the large part only physical barriers and emergency switches.

Bibliography

ADCS group Narvik (2006), Call for proposals.

Angeli, D. & Sontag, E. (1999), 'Characterizations of forward completeness', *Proceedings of the 38th Conference on Decision and Control* pp. 2551–2556.

Atassi, A. N. & Khalil, H. K. (1999), 'A separation principle for the stabilization of a class of nonlinear systems', *IEEE Transactions on Automatic Control* **44**, 1672–1687.

Byrnes, C. I. & Isidori, A. (1991), 'On the attitude stabilization of rigid spacecraft', *Automatica* **27**, 87–95.

Chen, C.-T. (1999), *Linear System Theory and Design*, Oxford University Press.

Egeland, O. & Godhavn, J.-M. (1994), 'Passivity-based adaptive attitude control of a rigid spacecraft', *IEEE Transactions on Automatic Control* **39**, 842–846.

Egeland, O. & Gravdahl, J. (2002), *Modelling and Simulation for Automatic Control*, Marine Cybernetics.

Fjellstad, O. (1994), Control of unmanned water underwater vehicles in six degrees of freedom, PhD thesis, Norwegian University of Science and Technology.

Fossen, T. (2002), *Marine Control Systems*, Marine Cybernetics.

Gershwin, S. & Jacobson, D. (1971), 'A controllability theory for nonlinear systems', *IEEE transactions on automatic control* .

Hahn, W. (1967), 'Über stabilitätserhaltende abbildungen und ljapunovsche funktionen', *J. für die reine und angewandte Mathematik* **228**, 189–192.

Harary, F. (1962), 'A graph theoretic approach to matrix inversion by partitioning', *Numer. Math.* **4**, 128–135.

Ioannou, P. & Sun, J. (1996), *Robust Adaptive Control*, Prentice-Hall PTR.

Jankovic, M., Sepulchre, R. & Kokotovic, P. V. (1996), 'Constructive lyapunov stability of nonlinear cascade systems', *IEEE transactions on automatic control* **41**, 1723–1735.

Josh, S. M., Kelkar, A. G. & Wen, J. T. Y. (1995), 'Robust attitude stabilization of spacecraft using nonlinear attitude quaternion feedback', *IEEE Transactions on Automatic Control* **40**, 1800–1803.

Jørgensen, J., Denver, T., Betto, M. & Jørgensen, P. (2001), 'Microasc - a miniature star tracker', *Technical University of Denmark, Dept. of Measurement and Instrumentation* .

Kevorkian, A. K. (1975), 'A decomposition algorithm for the solution of large systems of linear algebraic equations', *Proc. 1975 IEEE Int. Symp. Circuits Syst.* pp. 116–120.

Kevorkian, A. K. & Snoek, J. (1973), 'Decomposition in large scale systems: Theory and applications of structural analysis in partitioning, disjoining and constructing hierarchical systems', *Decomposition of Large Scale Problems* .

Khalil, H. (2000), *Nonlinear Systems*, Prentice-Hall Inc.

Kyrkjebø, E. (2000), Satellite attitude determination. Master thesis, Norwegian University of Science and Technology.

Lam, Q. M. & Morgan, R. N. (1992), 'Spacecraft control law design using lyapunov-based adaptive controllers', pp. 348–350.

Loria, A. (2004), 'Cascaded nonlinear time-varying systems: Analysis and design', *Lecture notes from FAP 2004* .

Loria, A., Fossen, T. I. & Panteley, E. (2000), 'A separation principle for dynamic positioning of ships: Theoretical and experimental results', *IEEE Transactions on Control Systems Technology* **8**, 332–343.

Luenberger, D. G. (1966), 'Observers for multivariable systems', *IEEE Transactions on Automatic Control* **AC-11 No. 2**, 190–197.

Michel, A. N., Miller, R. K. & Tang, W. (1978), 'Lyapunov stability of interconnected systems: Decomposition into strongly connected subsystems', *IEEE Transactions on circuits and systems* **CAS-25**, 799–809.

Nijmeijer, H. & Fossen, T. (1999), *New Directions in Nonlinear Observer Design*, Springer-Verlag London.

Ortega, R. & Spong, M. W. (1988), 'Adaptive motion control of rigid robots: A tutorial', *Proceedings of the 27th Conference on Decision and Control* pp. 1575–1584.

Panteley, E. & Loria, A. (1997), 'On global uniform asymptotiv stability of nonlinear time-varying systems in cascade', *Systems and Control Letters* .

Saberi, A., Kokotovic, P. V. & Sussmann, H. J. (1989), 'Global stabilization of partially linear composite systems', *Proceedings of the 28th Conference on Decision and Control* pp. 1385–1391.

Salcudean, S. (1990), 'A globally convergent angular velocity observer for rigid body motion', *IEEE Transactions on Automatic Control* **36**, 1493 – 1497.

Sciavicco, L. & Siciliano, B. (1996), *Modelling and Control of Robot Manipulators*, Springer.

Slotine, J.-J. & Li, W. (1988), 'Adaptive manipulator control', *IEEE Transactions on Automatic Control* **33**, 995–1003.

Sontag, E. (1989), 'Remarks on stabilization and input-to-state stability', *Proceedings of the 28th Conference on Decision and Control* pp. 1376–1378.

SSETI Homepage (2007), http://www.sseti.net/. The SSETI web pages.

Sunde, B. (2005), Sensor modelling and attitude determination for micro-satellite.

Thienel, J. & Sanner, R. (2001), 'A coupled nonlinear spacecraft attitude controller/observer with an unknown constant gyro bias', *Proceedings of the 40th IEEE Conference on Decision and Control* **044**, 3441 – 3446.

Thomas, J. (1964), 'Über die invarianz der stabilität bei einem phasenraumhomöomorphismus', *J. für die reine und angewandte Mathematik* **213**, 147–150.

Vidyasagar, M. (1980*a*), 'Decomposition techniques for large-scale systems with nonadditive interactions: Stability and stabilizability', *IEEE transactions on automatic control* **AC-25**, 773–779.

Vidyasagar, M. (1980*b*), 'On the stabilization of nonlinear systems using state detection', *IEEE transactions on automatic control* **AC-25**, 504–509.

Vik, B. (2000), Nonlinear Design and Analysis of Integrated GPS and Inertial Navigation Systems, PhD thesis, Norwegian University of Science and Technology.

Waarum, I. K. (2006), Attitude determination for spacecraft in moon orbit: Nonlinear observer. Project, Norwegian University of Science and Technology.

Wen, J. T. Y. & Kreutz-Delgado, K. (1991), 'The attitude control problem', *IEEE Transactions on Automatic Control* **36**, 1148–1162.

Young, N. (1988), *An Introduction to Hilbert Space*, Cambridge University Press.

Appendix A

CD-ROM files

The attached CD contains the following:

ESMO_ADCS: Simulink model of satellite, environment and ADCS.

sat_obs_init: Initializes variables used in the Simulink model.

CONTROLLERS: Three different controllers, to be used with the ADCS.

IMU: Models of gyros, to be used with the ADCS.

STAR_TRACKERS: Models of star tracker, to be used with the ADCS.

SUN_SENSORS: Models of sun sensors, to be used with the ADCS.

Rquat: Quaternion rotation matrix.

q2euler: Converts quaternions to Euler angles.

Sk_matrix: Computes the skew matrix of a vector.

marine_gnc: Folder with tools for Matlab.

phlib: Folder with tools for Matlab.

Plots: Folder with large versions of the plots in Chapter 8.